A STUDY OF TWO INWARD CURRENTS AND THEIR INVOLVEMEMT

IN MEMBRANE POTENTIAL OSCILLATIONS

OF THALAMOCORTICAL CELLS IN VITRO

A thesis submitted for the degree of

Doctor of Philosophy in Science (Pharmacology)

at the University of London

by

Sean Lightowler BSc (Hons)

Department of Pharmacology

St. George's Hospital Medical School

Cranmer Terrace

London SW17 ORE

Department of Visual Science

Institute of Ophthalmology

Judd Street

London WC1H 9QS

ABSTRACT

In this study intracellular current clamp and single electrode voltage clamp experiments on single thalamocortical cells in brain slices of the cat dorsal lateral geniculate nucleus have revealed the presence of two voltage-dependent inward currents that are activated at relatively hyperpolarized membrane potentials. These currents have been isolated, characterized physiologically and pharmacologically, and their involvement in the generation of spontaneous membrane potential oscillations has been assessed.

The first current is a low-threshold, transient, inward calcium ion current. It is called low-threshold because it is activated at relatively hyperpolarized membrane potentials, upon depolarization. Since it is a transient conductance it has been termed I_T and indeed, throughout its development, has many kinetic characteristics in common with T-type calcium conductances found in other cells, but its pharmacology differs somewhat. It has been found that I_T is the generator of low-threshold calcium potentials i.e. of the large depolarizations seen in thalmocortical cells during membrane potential oscillations in vitro and in vivo.

The second current is a slowly developing, non-inactivating, inward, mixed sodium/potassium ion current. This is an inward rectifier current as it is responsible for causing an increase in membrane conductance upon hyperpolarization. Since it is activated when a cell is hyperpolarized it has

been termed I_h. Many of its kinetic properties and pharmacology are similar to those of mixed sodium/potassium ion inward rectifier currents found in other cells. I_h is responsible for depolarizing the cells membrane potential upon hyperpolarization and, like I_T, has been found to be essential for spontaneous membrane potential oscillations. Enhancing or inhibitng I_h, with noradrenaline or caesium ions respectively, can transform one kind of oscillation into another or, indeed, inhibit them altogether.

I would like to acknowledge the help of the following people, in carrying out some aspects of this work:-

- Dr. Chris Pollard, for his voltage clamp observations indicating the presence of a transient inward current (I_T) and a slowly developing, non-inactivating, inward current (I_h) in thalamocortical cells.

- Dr. Mario Pirchio for his help in carrying out some experiments to investigate the development of I_T, during which I taught him the discontinuous single electrode voltage clamp technique.

- Dr. Ivan Soltesz for his help in carrying out some experiments to investigate the effects of β-adrenoreceptor stimulation on I_h and the spontaneous membrane potential oscillations, during which I also taught him the discontinuous single electrode voltage clamp technique.

CONTENTS

LIST OF FIGURES AND ILLUSTRATIONS

ACKNOWLEDGEMENTS

I would like to thank Dr. Vincenzo Crunelli for being such a kind and supportive supervisor during the three years I have spent with him. Also, I would like to thank him for demonstrating the fine characteristics required for producing high quality scientific work.

I would also like to thank the other people I have worked with during this time, and who have helped me immeasurably, namely Drs. Chris Pollard, Ivan Soltesz and Mario Pirchio. Not only have these people taught me a lot and helped me with my work, but they have also made it a lot of fun.

Lastly, I would like to thank Penny for supporting me throughout, in more ways than one, and also my parents for their help and encouragement during my earlier years.

CHAPTER ONE

INTRODUCTION

1.1. Foreword

The thalamus, which has been called a sensory "gateway into the cortex" (Bremer, 1938; Adrian, 1941; Morison et al., 1943; Morison and Basset, 1945; Poggio and Mountcastle, 1963; Steriade and Deschenes, 1984; Hobson and Steriade, 1986; Steriade et al., 1986; Llinas and Geijo-Barrientos, 1988) is able to operate in two distinct modes: (1) a relay mode and (2) a burst-firing mode (Andersson et al., 1971; Jahnsen and Llinas, 1984a, b; Steriade and Deschenes, 1984; Steriade and Llinas, 1988). In (1) it operates to transmit sensory information to the cerebral cortex. In (2) its own excitability serves to control the level of excitability of the cerebral cortex and through this the level of arousal and consciousness. Indeed, the depressed responsiveness of the cerebral cortex, seen during slow wave sleep, occurs when thalamic neurones display rhythmic membrane potential oscillations (Bremer, 1938; Adrian, 1941; Morison et al., 1943; Morison and Basset, 1945).

The mechanism responsible for the oscillatory activities observed in thalamic neurones has mainly been regarded as involving the rhythmic recruitment of intra- and extra- thalamic synaptic inputs (Andersen and Andersson, 1968; Purpura, 1970; Steriade and Llinas, 1988). However, it has been shown that thalamocortical neurones possess intrinsic membrane conductances (Deschenes, et al., 1984; Jahnsen and Llinas, 1984a, b) that, it has been suggested, should make them capable of rhythmic electrical activity even in the absence of synaptic inputs (Jahnsen and Llinas, 1984b; Steriade and Llinas, 1988; Llinas, 1988). Indeed, recently it has been demonstrated

that individual thalamocortical neurones display spontaneous membrane potential oscillations, under certain conditions in vitro (Leresche et al, 1990, 1991).

One of the conductances responsible for this activity underlies a slow membrane depolarization (Deschenes et al., 1984; Jahnsen and Llinas 1984a, b) which, due to a Ca^{2+} dependence, has been termed a "low-threshold Ca potential", and is presumed to be responsible for the large amplitude depolarizations present during the membrane potential oscillations.

In addition, the in vitro low frequency oscillations seen in thalamocortical neurones (Leresche et al., 1990, 1991) bear a striking resemblance to cardiac pacemaker oscillations. In cardiac fibres an inwardly rectifying current (I_f) has been shown to contribute to the mechanism responsible for the generation of oscillations (Hauswirth et al, 1968; Brown et al., 1979a, b). Since intracellular recordings from thalamocortical neurones indicate the possible presence of an inwardly rectifying current in thalamocortical cells (Jahnsen and Llinas, 1984a, b; Crunelli et al., 1987c; McCormick and Pape, 1988), perhaps such a current also plays a role in thalamocortical cell membrane potential oscillations.

The aim of this thesis has been to characterize, physiologically and pharmacologically, the currents that underlie the low threshold Ca^{2+} potential and the inward rectification seen in thalamocortical neurones, and assess their roles in the generation of spontaneous membrane potential oscillations.

These two currents have been studied, using the single-electrode voltage-clamp technique, in thalamocortical cells of the cat dorsal lateral geniculate nucleus, in vitro.

2+

1.2. Anatomy of the thalamus

When describing the precise mechanisms of the thalamus relay and burst-firing functions it is necessary to look at thalamic cells and their synaptic interactions.

1.2.1. Cell types

There are three major types of neurone present within the thalamus

a. Thalamocortical (TC) neurones

The majority (85-90%) of these long axoned neurones have a soma area of 300 - 400 μm^2, radially arranged dendrites, and project to layers III, IV and VI of the cortex. The remainder of this cell type (10-15%) are half the size, have slender dendrites and project to layers I and II of the appropriate cortical area (Guillery, 1966; Leventhal, 1979; Stanford et al. 1981; Penny et al. 1982; Spreafico, 1983; Jones, 1985; Rausell and Avendano, 1985; Yen et al. 1985b; Tseng and Royce, 1986)

b. Interneurones

These neurones have short, localized axons, spherical somata with an area of approximately 200 μm^2 and dendrites with appendages (Szentagothai, 1963; Tombol, 1966; Morest, 1971; Ralston, 1971; Famiglietti and Peters,

1972). They are easily distinguished since they are glutamic acid decarboxylase (GAD) immunoreactive, and have, in the cat, been found to account for 20 - 30% of the total neuronal population in various thalamic nuclei (Levay and Ferster, 1979; Hendrikckson et al., 1983; Ohara et al., 1983; Penny et al., 1983; Spreafico, 1983). More recently direct evidence for GABA - immunopositive interneurones has been shown (Gabbot et al., 1985, 1986).

c. Reticular thalamic (RE) neurones

There is a third major type of thalamic neurone, which is present in the RE nucleus. RE neurones are characterized by a soma size of 300-400 μm^2 and by having several thick dendrites that give rise to secondary branches covered by long filamentous appendages (Scheibel and Scheibel, 1966; Steriade and Deschenes, 1984a; Yen et al., 1985a; Mulle et al., 1986). Instead of projecting to the cerebral cortex, it has been shown that RE cell axons terminate at various sites within the thalamus (Scheibel and Scheibel, 1966; Jones, 1975; Steriade et al., 1984b). Like interneurones, the RE neurones are GABAergic (Houser et al., 1980; Hendrickson et al., 1983; Gabbott et al., 1985; Yen et al., 1985a).

1.2.2. Synaptic connections

A schematic diagram of the synaptic connections within a nucleus (the lateral geniculate) of the thalamus is shown in Fig. 1.1. It is important to note that the part of RE innervating the lateral geniculate nucleus is termed the perigeniculate nucleus.

Within thalamic nuclei incoming sensory afferents synapse onto TC cells and interneurones releasing the excitatory amino acid neurotransmitters glutamate and/or aspartate (Kemp and Sillito, 1982; Sandberg and Lindstrom, 1983; Ottersen and Storm-Mathisen, 1984; Salt, 1986; Crunelli et al., 1987b). A common synaptic arrangement, characteristic of thalamic nuclei, is the glomerulus, consisting of synapic groups covered by a glial sheet (Harding and Powell, 1977). Within glomeruli, ascending sensory afferent fibres synapse onto the dendrites of both TC cells and GABAergic interneurones (Steriade and Llinas, 1988). Postsynaptic dendrites of the interneurones then synapse, releasing the inhibitory transmitter GABA, onto TC cell dendrites (Steriade and Llinas, 1988). This arrangement may form a "triad" synapse when a sensory afferent fibre synapses onto both the dendrites of a TC cell and the dendrites of a GABAergic interneurone which, in turn, synapse onto the TC cell dendrites, and mediates feed-forward inhibition.

As well as projecting to the cerebral cortex, TC cells possess axon collaterals which synapse onto cells within the RE nucleus (Friedlander et al., 1981; Jones, 1985).

In addition to the sensory synaptic input, thalamic nuclei receive cortical

(from the same area to which they project [Jacobson and Trojanowski, 1975]) and GABAergic RE synaptic inputs, which form extraglomerular contacts onto TC cells and interneurones (Ohara et al., 1980; Montero and Scott, 1981; Montero and Singer, 1985).

Within the RE nucleus the RE neurones receive synaptic contacts from axons that originate in the cerebral cortex, thalamic nuclei and the RE nucleus itself (Ide, 1982; Montero and Singer, 1984; Deschenes et al., 1985; Ohara and Lieberman, 1985; Yen et al., 1985a).

There are also major projections to thalamic nuclei from brain stem nuclei which send fibres containing acetylcholine, noradrenaline or serotonin to the thalamus (Jones, 1985).

The cholinergic pathway arises primarily from cells in the pedunculopontine and lateral dorsal tegmental nucleus (Mesulam et al., 1983), the noradrenergic pathway arises from the locus coeruleus and adjacent cells (Swanson and Hartman, 1975), and the serotoninergic pathway arises primarily from cells of the dorsal nucleus of the midbrain raphe (Cropper et al., 1984).

Fig. 1.1. Schematic diagram illustrating the relationship between the various inputs to TC cells (geniculate). The hatching highlights the inhibitory, GABAergic inputs to TC cells. Excitatory and inhibitory pathways are separately shown. The dashed line refers to the putative, long-lasting modulatory action of cholinergic, noradrenergic and serotonergic fibers from the brainstem reticular formation. Abbreviations: Ret - retina; LGN - lateral geniculate nucleus; VC - visual cortex; BRF - brain stem reticular formation (which includes midbrain and pontine components); PGN - perigeniculate nucleus; IV and VI - cortical layers IV and VI (from Sherman and Koch, 1986).

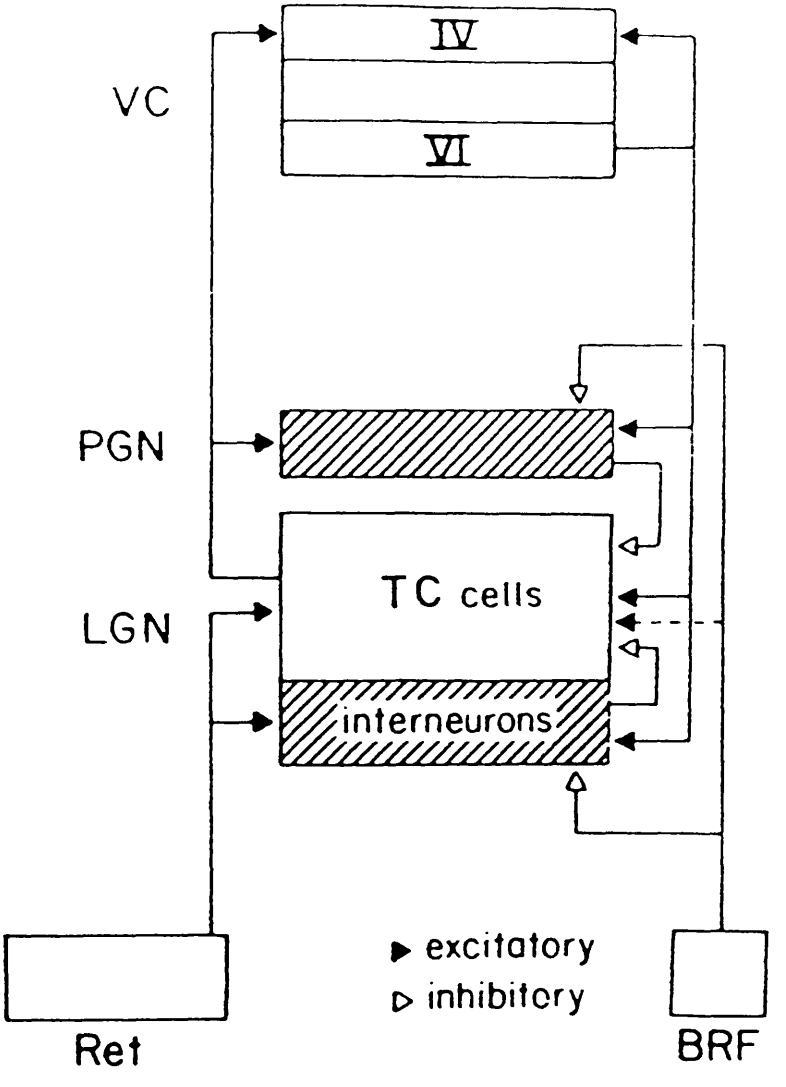
IV
VI
VC
PGN
TC cells
LGN
interneurons
excitatory
inhibitory
Ret
BRF

1.3. Role and activities of the thalamus

1.3.1. Relay Mode

The relay of sensory information through the thalamus can be best considered as its transfer via specific channels, or nuclei, to the cerebral cortex. Examples of such channels are the lateral geniculate nucleus (LGN), responsible for transferring visual sensory information from the retina to the visual cortex, and the ventrobasal (VB) complex, the principal nucleus responsible for transferring somatosensory information from the spinal cord to the somatosensory cortex.

The transmission of sensory information is characterized by a high safety factor, since cells are able to follow high-frequency peripheral stimulation (Poggio and Mountcastle, 1963). Electrical stimulation of the main excitatory sensory afferent pathways has been shown to evoke a characteristic sequence of synaptic potentials in TC neurones consisting of a monosynaptic EPSP, an early, short duration, $GABA_A$ receptor-mediated IPSP, and a late, long lasting $GABA_B$ receptor mediated IPSP (Eysel, 1976; Kelly et al. 1979; Kemp and Sillito, 1982; Crunelli et al., 1987a, b; Hirsch and Burnod, 1987; Soltesz et al., 1988, 1989b; c.f. Soltesz et al., 1989a).

1.3.2. Burst-Firing Mode

In contrast to the transmission performance of TC neurones when the thalamus is in the relay mode, in the burst-firing mode, such as during slow wave sleep, they, like RE neurones, are less easy to drive with natural stimuli, show an overall reduction in spontaneous activity, show less marked inhibitory and excitatory responses, and show reduced antidromic excitability (Steriade and Deschenes, 1984; Hobson and Steriade, 1986; Steriade et al., 1986).

In the burst-firing mode a periodic, synchronous rhythmic discharge from TC neurones leads to an oscillating electroencephalographic (EEG) pattern, the oscillation envelope of which may have a spindle shape. Oscillating rhythmic EEG recordings shown to possibly involve the thalamus include:-

(1) Slow wave sleep oscillations.

(2) Oscillations associated with pathological conditions.

(3) Drug-induced oscillations.

1.3.2.1. Slow wave sleep oscillations

The EEG pattern recorded in humans during slow wave sleep shows various distinct forms, examples of which are spindles and slow waves (delta activity).

Sleep spindles occur at the transitional period of drowsiness between waking and sleeping, and result in a periodically (0.1-0.3 Hz) oscillating EEG

with an intraspindle frequency of 7-14 Hz of over most of the cortical surface (Buser, 1987).

Following the confirmation that, in cats, the thalamus is the site of genesis of sleep spindles (Bremer, 1938; Adrian, 1941; Morison and Bassett, 1945), it was found that they are characterized by a TC cell membrane potential that waxes and wanes, and it was suggested that they depend upon sequential neuronal discharges in adjacent thalamic neuronal pools (Hanbery and Jasper, 1953; Jasper, 1960; Desiraju and Purpura, 1970; Purpura, 1970). Indeed more recently, it has been shown that they result from TC neurone membrane potential oscillations (see Fig. 1.2), that occurr in discrete periods and are generated by the RE (Steriade and Deschenes, 1984; Steride and Llinas, 1988; Hu et al., 1989a, b).

Slow waves, of which there are many types, display a low frequency (0.5 - 4 Hz) EEG synchronization and occur during the deep stages of sleep, those associated with the deepest stage having been termed delta waves. At present there is no information about the precise origin(s) of slow waves. Evidence suggesting that they may originate outside the thalamus is that, in cats, slow waves persist in cortical EEG after thalamectomy (Villablanca, 1974) or transections of thalamic connections (Kellaway et al., 1966; Steriade et al., 1987), although this doesn't rule out a role for the thalamus in their generation under normal conditions. Indeed TC cells have been shown to oscillate during deep sleep with a frequency coinciding with the delta rhythm (Fourment at al., 1985).

In between periods of slow wave synchronization, during deep sleep, there are periods of EEG desynchronization associated with rapid eye

movement (REM sleep). During REM sleep, as during wakefulness, cat TC neurones display a non-oscillating membrane potential and tonic firing, associated with secure synaptic transmission of oncoming signals (Steriade and Hobson, 1976; Hirsch et. al, 1983). The similarity between waking and REM sleep has led to the conclusion that during REM sleep the thalamocortical system is activated in such a way as to generate a form of conciousness that does not bear direct reference to reality (Jasper, 1981; Llinas and Geijo-Barrientos, 1988).

1.3.2.2. Oscillations associated with pathological conditions

There is evidence that rhythmic oscillations in the thalamocortical neuronal network play a role in generating the rhythmic EEG pattern characteristic of petit mal epilepsy and parkinsonian tremour (Buzsaki et al., 1990; Steriade, 1990; Williams, 1953). Petit mal is characterized by the occurrence of bilaterally symmetrical, high voltage spike and wave EEG discharges at 3-5 Hz, usually with some symmetrical clonic motor activity (Myslobodsky, 1976; Gloor, 1979; Kellaway, 1985). Resting tremour of parkinsonian patients also has a remarkably reproducible frequency of around 3-5 Hz (Findley and Gresty, 1981; Findley and Capildeo, 1984).

1.3.2.3. Drug-induced oscillations

Spindling oscillations have also been observed in cats during barbiturate-anaesthesia (Dempsey and Morrison, 1942; Andersen and Sears,

1964; Deschenes at al., 1984) (see Fig. 1.2). The TC neurones show an intraspindle oscillating frequency (7-14 Hz) very similar to the synchronized rhythms observed in the normal animal, and have, as a result, been used extensively as a model for sleep spindles (Andersen and Sears, 1964; Roy et al., 1984).

Furthermore, bilaterally synchronous, generalized spike and wave EEG patterns, of TC origin, can be induced in cats by parental application of large doses of penicillin (Prince and Farell, 1969; Kostopoulos et al., 1981; Gloor and Fariello, 1988), and are seen during periods of behavioural unresponsiveness similar to those seen in human petit mal attacks. For this reason penicillin induced convulsions have been used as a model for petit mal epilepsy (c.f. Buzsaki et al., 1990).

Fig. 1.2. Examples of recordings from oscillating thalamic cells in vivo. A shows an extracellular record of the start of a thalamic spindle in the postero-lateral ventral nucleus of a barbiturate anaesthetized cat (from Andersen and Sears, 1964). B shows an intracellular recording from an oscillating cell in the ventralis lateralis nucleus of a barbiturate anaesthetized cat (from Roy et al., 1984). C shows an intracellar recording from an oscillating cell in the LGN during slow wave sleep of a behaving cat (from Fourment et al., 1985).

A

B

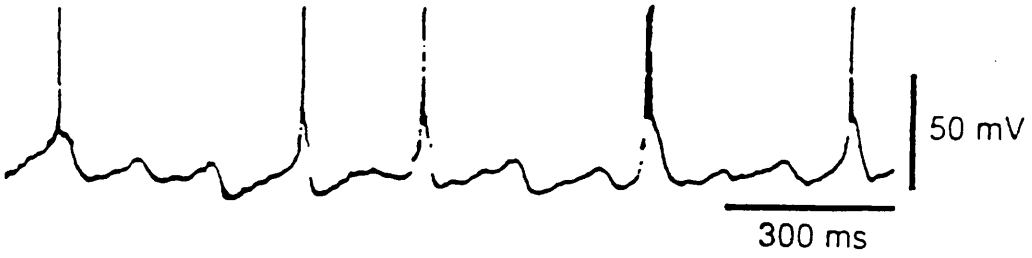

C

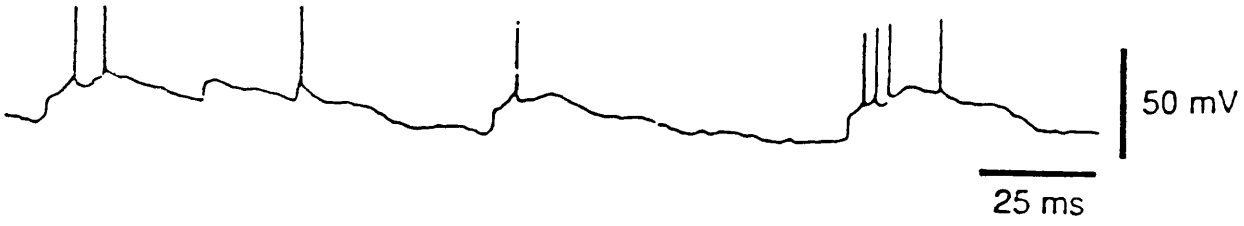

1.4. Cellular mechanisms underlying thalamocortical rhythms

Since it seems that the thalamus plays an essential role in the development of some of the above mentioned cortical rhythms the question arises: What cellular mechanisms are involved in TC rhythmic activities?

During the burst-firing mode TC neurones undergo rhythmic variations of their membrane potential (Benoit and Chateignier, 1973; Joffroy and Lamarre, 1974). These oscillations, examples of which are shown in Fig. 1.2, are typically composed of either isolated spikes or high frequency bursts (intra-burst frequency up to 300 Hz) interrupted by long hyperpolarizing phases lasting up to several hundreds of milliseconds.

The possible explanations, suggested to account for the overall genesis of such thalamic rhythms, can be designated as the "local circuit model", the "long-loop model", and the "auto-oscillation model". These possible explanations aren't exclusive, and the true mechanism could involve a part or all of each of the models.

1.4.1. The local circuit hypothesis

This model was originally proposed by Andersen and his coworkers (1964) and developed by Andersen and Andersson (1968). It was suggested that, following the excitation of TC neurones, they display a long lasting hyperpolarizing IPSP which is followed by a rebound depolarization and excitation. This excitation then leads, via axon collaterals, to the excitation of interneurones. The interneurones then synapse onto TC cells and cause a

second long lasting hyperpolarizing IPSP, and so on. Synchronization of this activity has been suggested to be due to fact that interneurones have branched axons and synapse onto a large number of TC neurones.

This model is supported by the findings that excitation of TC neurones is indeed followed by a long lasting IPSP, which is ideally suited for causing a rebound depolarization (Crunelli and Leresche, 1990). However, a second long lasting IPSP has never been seen following such a rebound depolarization in a brain slice preparation that contained a section of only one thalamic nucleus (Crunelli et al., 1988; Soltesz et al., 1989b). Furthermore, GABA-containing interneurones are present in a variety of nuclei, but absent in some others (such as the rat nucleus ventralis posterior). Therefore the recurrent local circuit, as hypothesized in its original form, is not valid (Szentagothai et al., 1966; Tombol, 1966; Morest, 1975; Buser, 1987)

1.4.2. The intrathalamic long-loop hypothesis

The hypothesis that some rhythmic thalamocortical activities are generated in a large thalamic network was initially proposed by Jasper and his coworkers (Jasper, 1954; Jasper et al., 1955) and later developed by Scheibel and his coworkers (Scheibel and Scheibel 1966, 1972; Scheibel et al., 1973). The model comprises of a long feedback loop, with a TC neurone activating a GABAergic RE neurone through its collaterals while traversing the RE nucleus and being in turn inhibited by the RE axon ending.

Perhaps the strongest evidence in support of a role for the RE nucleus

is that after its surgical disconnection, or after chemical RE lesion through ibotenic or kainic acid, TC cells display an abnormal firing pattern, with regular 1 to 2 Hz rhythmicity, quite distinct from the normal burst-hyperpolarization alternation observed in non-disconnected cells (Steriade and Deschenes, 1984). However the view that RE cells synapse directly onto the TC neurones, thus forming a disynaptic loop, is probably oversimplistic. Indeed, it is not common to find a group of TC neurones that undergo an hyperpolarization while RE neurones in the corresponding inhibitory zone are firing (Buser, 1987).

Moreover, the situation for this model is complicated by the finding that RE neurones are tonically activated when the thalamus is in the relay mode (i.e. in aroused animals) (Steriade and Deschenes, 1984). For the model to still hold RE neurones would have to act in a much more complex manner to impose rhythmic TC neuronal firing during the burst-firing mode - their action might be indirect, perhaps involving interneurones.

1.4.3. The auto-oscillation model

It was shown by Jahnsen and Llinas (1984a, b) and Deschenes and coworkers (Deschenes et al., 1984) that TC neurones possess intrinsic electrophysiological properties that should make them capable of displaying membrane potential oscillations in the absence of synaptic inputs, leading to the suggestion that this activity does not rely on synaptic inputs but is, instead, "automatic". Indeed, more recently, it has been demonstrated that individual TC neurones can display spontaneous rhythmic membrane

potential oscillations under certain conditions in vitro (Leresche, et al., 1990, 1991), an example of which is shown in Fig. 1.3. The activity illustrated in Fig. 1.3. is one of several observed in TC neurones in vitro (Leresche et al., 1990, 1991) and, because of its similarity to the cardiac pacemaker oscillations, has been termed "pacemaker". Another type of spontaneous TC neurone membrane potential oscillation observed in vitro and similar to the "pacemaker" oscillations, but occurring rhythmically in discrete periods, has been termed "spindle-like" because of some similarities to the sleep spindles (Leresche et al., 1990, 1991).

The in vitro observations that led to the suggestion that TC neurones possess a set of intrinsic membrane conductances suited for rhythmic electrical activity included the following:-

a. When the TC neurones are slightly depolarized (about - 55 mV) they show tonic firing, the frequency of which is generally proportional to the amount of injected current.

b. When TC neurones are slightly hyperpolarized (negative to about - 70 mV) a different kind of activity is seen. Low amplitude (10-25mV), long lasting (100-300ms) depolarizations (low threshold potentials) can be evoked. As the membrane potential is made more negative the low threshold potential amplitude also increases, until it eventually displays bursts of action potentials on its crest. While the fast spikes were found to be Na^+-dependent action potentials, suppressed by tetrodotoxin, low threshold potentials were shown to be due to a voltage dependent Ca^{2+} conductance increase, normally inactivated in depolarized cells, but de-inactivated, in a time dependent

manner, at hyperpolarized levels. Due to its Ca^{2+} dependence the low threshold potential has been termed a "low threshold Ca^{2+} potential" (LTCP) (Crunelli et al., 1987c).

Depending on the polarization level of the cell, two types of oscillation could thus be elicited by current injection into the cell.

The tonic firing, achieved at more depolarized levels, is a well suited response for the faithful transfer of sensory information, as seen when the thalamus is in the relay mode. Conversely the activation of LTCPs, achieved at more hyperpolarized potentials, is well suited for the generation of low frequency membrane potential oscillations in TC neurones, as seen during the burst-firing mode. Evidence in support for the importance of this point comes from the finding that during spindling, in vivo, the membrane potential of TC cells is indeed hyperpolarized, in comparison to the levels seen when the thalamus is in the relay mode (Hirsch et al., 1983).

However, there is no experimental evidence for a time-locking of the individual oscillations, in vitro. It could well be that in vivo a synchronization mechanism involves a structure lying outside the population of oscillating neurones, possibly via a long loop through the RE nucleus. In this capacity the RE nucleus would be acting purely as a synchronizing process, and not as part of the circuitry for the oscillatory behaviour itself.

Another property of TC neurones that could contribute to autorhythmicity is a voltage dependent inwardly rectifying conductance. An inwardly rectifying conductance (I_f) has been shown to contribute to the mechanism responsible for the generation of cardiac pacemaker oscillations

seen in Purkinje and possibly sino-atrial fibres (Hauswirth et al, 1968; Brown et al., 1979a, b), and which bear a striking resemblance to the low frequency oscillations seen in TC neurones (Leresche et al., 1990), particularly the "pacemaker" type (Fig. 1.3). In cardiac pacemaker oscillations the inwardly rectifying current acts to depolarize the membrane potential when it reaches its most hyperpolarized level (the diastolic potential) (Hauswirth et al., 1968; Brown et al., 1979a, b). This is comparible to the slowly developing depolarizing sag of the TC neurone electrotonic potential, seen when they are hyperpolarized in current clamp by a relatively large, square, hyperpolarizing current pulse (Jahnsen and Llinas, 1984a, b; Crunelli et al., 1987c; McCormick and Pape, 1988).

Therefore, when considering the auto-oscillation model, two voltage dependent conductances seem of particular interest for the generation of the burst-firing mode by TC neurones:-

a. A voltage dependent Ca^{2+} conductance, responsible for generating the LTCP.

b. An inwardly rectifying conductance, responsible for depolarizing the cells membrane potential upon hyperpolarization.

Fig. 1.3. An example of membrane potential oscillations that occur in TC cells in vitro. These intracellular voltage recordings, from a cat LGN TC neurone, show that the "pacemaker" oscillations were observed only when the membrane potential was moved (by steady dc current injection) to between -57 and -73 mV. At potentials more positive than -45 mV the activity of the cell was characterized by continuous firing that showed no accommodation (from Leresche et al., 1991).

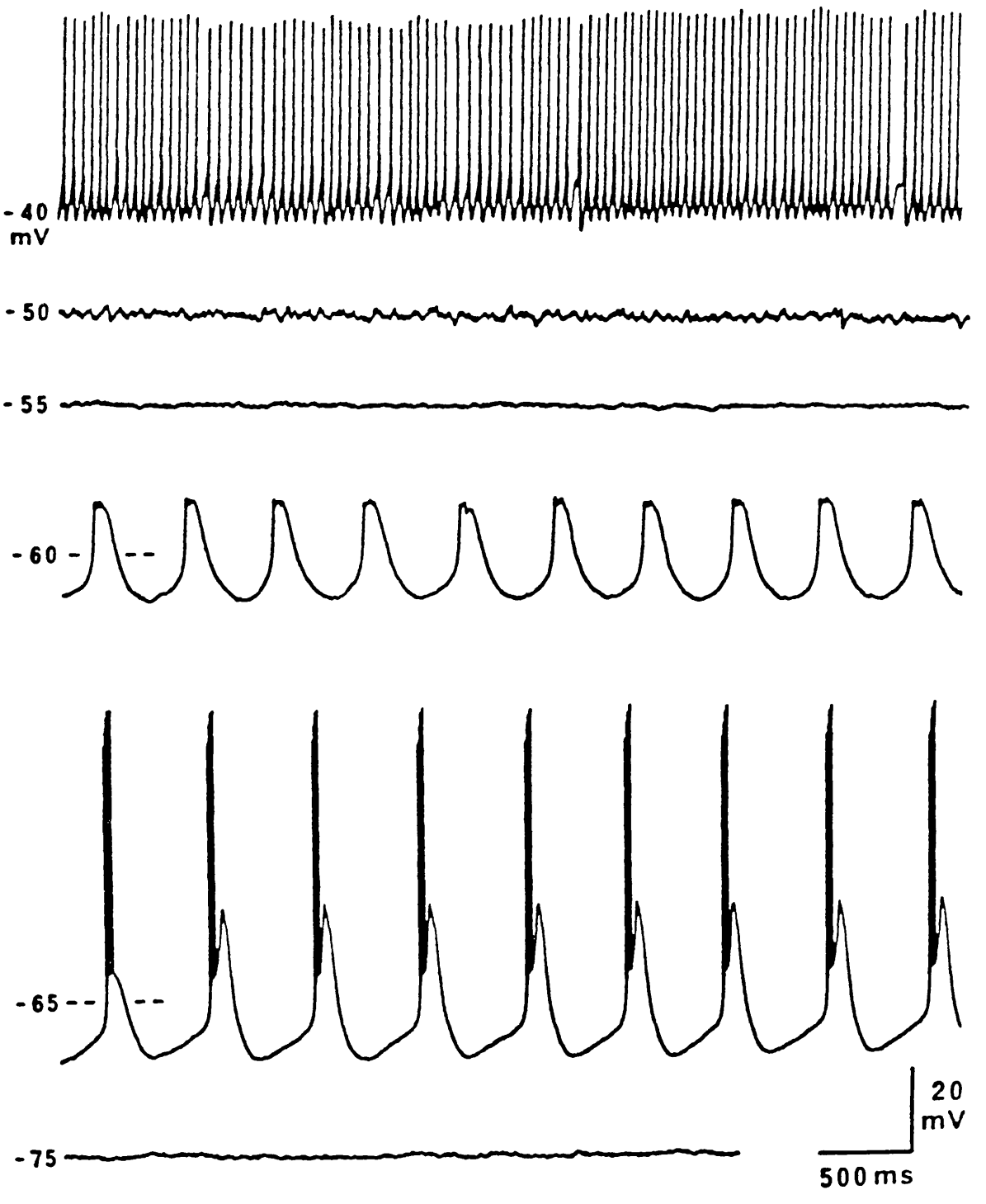
-40
mV
-50
-55
-60
-65
-75
20
mV
500 ms

1.5 Voltage dependent Ca^{2+} channels (VDCC's)

1.5.1 Multiple types of VDCC

Multiple types of VDCC have been shown to co-exist within a given type of non-neuronal cell such as invertebrate eggs (Hagiwara et al., 1975), ciliates (Deitmer, 1984) and heart cells (Bean, 1985). In mammalian CNS neurones the first clear demonstration of two classes of VDCC ("low threshold" and "high threshold" channels) came from experiments performed by Carbone and Lux (1984a) on chick dorsal root ganglion (DRG) neurones. Further recordings in chick DRG neurones confirmed the distinctness of low voltage activated (LVA) Ca^{2+} channels, designated T-type, because of their transient nature, and also distinguished between two kinds of high voltage activated (HVA) Ca^{2+} channels, called N- and L- type, giving a total of three types (Carbone and Lux, 1984b, 1987a; Nowycky et al., 1985; Fox et al., 1987a, b). A summary of some of the electrical properties of these three types of VDCC is shown in the table overleaf.

TABLE 1.1. Some of the electrical properties of the three types of Ca^{2+} channels in chick DRG neurones (Tsien et al., 1988)

Channel type	T	N	L
Activation range	Positve to -70 mV	Positive to -20 mV	Positive to -10 mV
Inactivation range	-100 to -60 mV	-120 to -30 mV	-60 to -10 mV
Inactivation rate	Rapid (τ 20-50 ms)	Moderate (τ 50-80ms)	Very slow (τ >500ms)

VDCC's with similar properties to the T-, N- and L-type channels of chick sensory neurones have been found in many vertebrate cells, such as: hippocampal neurones, which possess all three types of channel (Takahashi et al., 1989; Thompson and Wong, 1989); sympathetic neurones, which possess N- and L- type channels (Marchetti et al., 1986; Hirning et al., 1988); adrenal chromaffin cells, which possess the L-type channel only (Fenwick et al., 1982; Hoshi and Smith, 1987); fibroblasts and glial cells, which possess T- and L-type channels (Tsien et al., 1988). However, VDCCs within the classes of T-, N- and L-type are similar but not identical from one preparation to another. For example, a somewhat variable aspect of T-type channels is their voltage-dependence of activation, which can become

significant as negative as - 65 mV in sensory neurones (Carbone and Lux, 1984a, b; Nowycky et al., 1985; Fox et al., 1987a) but only near -50 mV in heart cells (Bean, 1985; Mitra and Morad, 1986; Hagiwara et al., 1988)

More recently, a fourth type of VDCC, the P channel, has been identified in Purkinje cells, which is activated at -50 mV and differs pharmacologically to L- and N-type VDCCs (Llinas et al., 1989a). Additional VDCC's, that cannot be classified as T, L, N or P, have been found in a number of vertebrate cells such as skeletal muscle fibres (Garcia and Stefani, 1987) and BC3H1 cells (Caffrey at al., 1987), and it has been suggested that a wealth of VDCC's await further explorations in the vertebrate CNS (Llinas et al., 1989b).

It has been suggested that VDCC's are important during ontogeny, and, as a result, several studies have investigated their properties in different neuronal and muscle cell types during pre- and postnatal development. Since it has been shown that I_T contributes to oscillations in dorsal raphe neurones (Burlhis and Aghajanian, 1988), and it seems that membrane potential oscillations play a key role during neuronal development (Llinas, 1988; Walton and Llinas, 1986), the development of T- type VDCCs is an important factor to be considered. There seems to be general agreement that the T-type Ca^{2+} current decreases in amplitude and in some cases even disappears during embryogenesis in chick limb motoneurones (McCobb et al., 1989), or during the first weeks of postnatal life in rat hippocampal pyramidal neurones (Thompson and Wong, 1989), in rat dorsal root ganglion

neurones (Kostyuk et al., 1986; Kostyuk, 1989) and in rat (Beam and Knudson, 1988) and mouse (Gonoi and Hasegawa, 1988) skeletal muscle. Thus, most neuronal cell types that have been studied so far are characterized by a weak, or even absent, I_T in adulthood and, in addition, the analysis of its properties has often been carried out during in vitro development which might not necessarily be similar to the in vivo development.

Since the Ca^{2+} conductance underlyng the LTCP in TC neurones is activated at a membrane potential of around -70 mV (Jahnsen and Llinas 1984a, b) it would seem to most closely correlate, at first sight, with the T-type Ca^{2+} current of the VDCCs already identified in other cells. Furthermore, it has been shown that T-type Ca^{2+} channels do, indeed, contribute to the generation of pacemaker depolarizations in other cell types such as heart cells (Hagiwara et al., 1988) and dorsal raphe neurones (Burlhis and Aghajanian, 1988).

1.5.2. The pharmacology of VDCC's

Agents that selectively block different VDCC types have been useful therapeutically (Overweg et al., 1984) and also as "tools" when investigating VDCC's (Thompson and Wong, 1989; Scott et al., 1990). Several classes of compounds have been shown to interact with VDCCs (Triggle, 1981), and perhaps the most extensively investigated are the dihydropyridines (DHP's), many of which inhibit the L-type VDCC (Tsien et al., 1988). Some of these

VDCC "antagonists" relax smooth muscle preparations, and have, as a result, been used in the treatment of angina pectoris and hypertension. Small structural changes in the antagonist DHP molecule yield novel compounds that keep VDCC's open for increased periods of time, allowing a larger influx of Ca^{2+} into the cell (Hess et al., 1984). An example of this is the DHP BAY K 8644, which acts as a VDCC "agonist", although its optical enantiomer 202-791 acts as an antagonist.

The VDCCs have also been shown to differ in their sensitivity to inorganic ion block. While N- and L-type VDCC's are more sensitive to blockade by Cd^{2+} than by Ni^{2+} ions, the reverse is true for the T-type VDCC.

The peptide toxin, Ω-conotoxin GVIA, acts almost irreversibly to reduce the N-type current selectively, although there are reports that it also reduces the L-type current (McCleskey et al., 1987).

Of the various compounds reported to potently and selectively block the low voltage-activated, transient (T- type) calcium current amiloride and 1-octanol have appeared promising (Tsien et al, 1988; Kostyuk, 1989). Amiloride was originally shown to selectively block T-type calcium currents in neuroblastoma cells and dorsal root ganglion cells (Tang et al., 1988), and 1-octanol was reported to have the same effect in inferior olive cells (Llinas and Yarom, 1986). On the basis of these results, they have been used as pharmacological "tools" to help identify T-type calcium currents (Thompson and Wong, 1989; Scott et al., 1990), and to investigate their contribution to different physiological and pathological processes both in vitro and in vivo (Kamiya, 1989; Seabrook and Adams, 1989; Sinton et al., 1989).

1.6. Voltage dependent inward rectifier channels

Inward rectifier channels permeable to K^+ ions only were the first to be discovered, in K^+ depolarized muscle, by Katz (1949) who used the term "anomalous rectification" to contrast the properties from those of "normal" delayed rectification. The anomaly was a conductance that increases under hyperpolarization and decreases under depolarization. Two newer terms, inward rectifier and inward-going rectifier, describe this tendency to act as a valve or diode, permitting entry of cations (or exit of anions) and inward current under hyperpolarization, but not exit under depolarization.

Inward rectifier channels have since been observed in many different cell types, including neurones, and, as well as being selectively permeable to K^+ ions in some cells (Adrian, 1969; Hagiwara and Takahashi, 1974; Gay and Stanfield, 1977; Hille and Scwharz, 1978; Constanti and Galvan, 1983; Osmanovic and Shefner, 1987; Edwards et al., 1988) may, instead, be selectively permeable to Cl^- ions (White and Miller, 1979; Chesnoy-Marchais, 1982, 1983; Selyanko, 1984; Madison et al., 1986), or be permeable to both Na^+ and K^+ ions (Brown and DiFrancesco, 1980; DiFrancesco and Ojeda, 1980; DiFrancesco, 1981a, b; Halliwell and Adams, 1982; Mayer and Westbrook, 1983; Bader and Bertrand, 1984; Crepel and Penit-Soria, 1986; Benham et al., 1987; Edman et al., 1987; Spain et al., 1987; Lacey and North, 1988).

1.6.1. Inward rectifier channels permeable to K^+ ions only

The characteristic features of inward rectifier currents carried by K^+ ions only are as follows:-

a) The activation curve of the current depends on V - E_K rather than on voltage alone, provided the potassium equilibrium potential (E_K) is altered by changing the external K^+ concentration (Hagiwara and Yoshii, 1979; Leech and Stanfield, 1981).

b) The conductance develops with a kinetics which is immeasurably fast or which has both fast and slow components (Nakamura et al., 1965; Hagiwara et al., 1976; Leech and Stanfield, 1981).

c) The current is affected by caesium, barium, or rubidium in a voltage-dependent manner (Nakamura et al. 1965; Hagiwara and Takahashi, 1974; Hagiwara et al., 1976, 1978; Gay and Stanfield, 1977; Standen and Stanfield, 1978, 1980).

In some cell types, such as egg, muscle and cortical cells, inward rectifer currents carried by K^+ ions appear to inactivate (Almers, 1972; Constanti and Galvan, 1983; Ohmori, 1978; Standen and Stanfield, 1979). Although in frog muscle and calf Purkinje fibres this has been shown to be due to the external depletion of K^+ (Adrian and Freyang, 1962; Adrian et al., 1970; DiFrancesco, 1981a), in cortical and locus coeruleus neurons it has been shown to be a genuine inactivation of the current (Constanti and Galvan, 1983; Inoue et al., 1988).

Various functions for pure K^+ inward rectifiers have been suggested, such as:-

a) By closing upon depolarization, they may provide a form of economy preventing the dissipation of ionic gradients in cells that spend a lot of time in a depolarized state, such as ventricular and egg cells (Weidmann, 1951; Hagiwara and Jaffe, 1979; Hille, 1984).

b) In some cell types, such as frog muscle and rat cerebral arterioles (Hestrin, 1981; Leech and Stanfield, 1981; Edwards et al., 1988), it seems that the current contributes to the resting conductance.

However, in other cell types, such as cortical neurons (Constanti and Galvan, 1983), the K^+ inward rectifier is activated only at very negative potentials, probably not reached during normal activities, making it difficult to hypothesize a physiological function.

1.6.2. Inward rectifier channels permeable to Cl^- ions only

Hippocampal pyramidal cells contain a voltage-dependent, slowly developing, non-inactivating Cl^- conductance which is active at the resting membrane potential, is turned off by membrane depolarization (Madison et al., 1986) and which resembles, in many respects, Cl^- currents described in peripheral and invertebrate systems (White and Miller, 1979; Chesnoy-Marchais, 1982, 1983; Selyanko, 1984).

Although it is not dependent on Ca^{2+} influx, the Cl^- inward rectifier, in hippocampal pyramidal and superior cervical ganglion cells, is blocked by

Cd^{2+} (Madison et al., 1986; Selyanko, 1984).

The current is progressively activated over the range from -20 to -90mV and, although a physiological role for it remains to be demonstrated, since it is activated at the resting membrane potential it should contribute substantially to the resting conductance (Madison et al., 1986).

1.6.3. Inward rectifier channels permeable to Na^+ and K^+ ions

An inward rectifer current carried by both Na^+ and K^+ ions was first discovered in spontaneously active rabbit sino-atrial (SA) node fibres. Brown and coworkers (1979a, b) found that this current (termed I_f because of its "funny" behaviour) was important in pacemaking and also that it mediated the acceleratory effect of noradrenaline in the SA node. The same current was also reported at the same time by Yanagihara and Irisawa (1980) who termed it I_h (hyperpolarization-activated current). Later a similar current was found to also be present in calf Purkinje fibres (DiFrancesco, 1981a, b).

I_f is a slowly developing, non-inactivating current and is progressively activated over the membrane potential range from -60 mV to -95 mV (DiFrancesco, 1985). Evidence for the fact that I_f is carried by both Na^+ and K^+ ions came from the finding that the reversal potential of this current (E_f - around -20 to - 30 mV in normal Tyrode) is dependent upon both the external Na^+ and K^+ concentrations (DiFrancesco, 1981b).

Although Ba^{2+} is known to block the pure K^+ inward rectifier in skeletal

muscle (Standen and Stanfield, 1978) and egg cells (Hagiwara et al., 1978), it has been shown to have little effect on I_f (Yanagihara and Irisawa, 1980). This therefore allows for a pharmacological distinction of the two currents. Cs^+, however, has been shown to block both of these types of inward rectifiers (Gay and Stanfield, 1977; DiFrancesco, 1981c).

The proposed physiological role of I_f in cardiac fibres is that it is activated during the hyperpolarized portion of the pacemaker potential (the diastolic phase) and acts to depolarize the cells membrane potential, thereby activating another pacemaker cycle (DiFrancesco, 1985). For this reason I_f is also known as the "pacemaker current". I_f is crucial for pacemaking activity in Purkinje fibres and its modulation mediates the cardiac accelerating effects of adrenaline (Hauswirth et al., 1968; DiFranscesco, 1985). However, although Brown and coworkers (1979a, b) showed that adrenaline also reversibly increases the size of I_f, in SA fibres, pacemaker activity can be recorded in the SA node even when I_f is fully inhibited by Cs^+ (Kreitner, 1981; Brown et al., 1981), indicating that, in these cells, it is not essential for this activity.

Experiments where SA node preparations are voltage clamped at various times during pacemaker activity (Brown et al., 1984) have shown that as well as I_f a decaying outward K^+ current also contributes to the diastolic depolarization, but this does not exclude the importance of I_f in pacemaker depolarizations.

Time and voltage dependent currents like I_f have been reported in

several non-cardiac tissues. Bader and coworkers (Bader et al., 1982; Bader and Bertrand, 1984) have discovered a similar current in salamander photoreceptors, termed I_h. It is activated below -50 mV, and, it has been suggested, may act to limit the hyperpolarized level reached by the membrane after light stimulation. A similar "safety mechanism" role has been suggested by Mayer and Westbrook (1983) for the I_f (also termed I_h) like component found in mouse spinal sensory ganglion neurones. The current described by Mayer and Westbrook depends on Na^+ and K^+ in a way similar to I_f, is activated in much the same voltage range (negative to -60 mV) and is blocked by low concentrations of Cs^+. A hyperpolarizing activated inward current, like I_f, has also been reported in guinea-pig hippocampal cells (Halliwell and Adams, 1982), and has been termed I_Q (for "queer"). Although I_Q is activated slightly more negative to I_f, it is blocked by Cs^+ but not by Ba^{2+}, and is sensitive to changes in external Na^+ and K^+. It has been suggested that I_Q may contribute to the spontaneous firing of hippocampal cells. Since mixed Na^+/K^+ inward rectifiers, like I_f, are found in some cells, such as cat sensorimotor cortex (Spain et al., 1987) and lobster stretch receptor neurones (Edman et al., 1987), in which they are activated at the resting potential it has been suggested that they contribute to the resting conductance.

1.7. Aims and objectives

The aims and objectives of this thesis are to isolate and characterize the physiological and pharmacological properties of:-

a) The voltage dependent current responsible for generating low threshold Ca^{2+} potentials in TC neurones.

b) The inward rectifier current, responsible for depolarizing TC cell membrane potential upon hyperpolarization.

In addition, the possible involvement of these currents in generating the spontaneous membrane potential oscillations of TC cells, in vitro, is to be investigated.

The in vitro slice preparation of the cat dorsal lateral geniculate nucleus was used to carry out these studies because:-

1) Stable, long-lasting, intracellular recordings can be made from individual cells (Kerkut and Wheal, 1981; Dingledine, 1984).

2) Drugs can be applied at known concentrations.

3) The basic membrane properties of TC cells in this nucleus are known to be characteristic of TC cells in general (Crunelli et al., 1987d).

4) TC cells within this nucleus have been shown to display spontaneous membrane potential oscillations in vitro (Leresche et al., 1990, 1991).

CHAPTER 2

MATERIALS AND METHODS

2.1. Brain Slice Preparation

Slices of cat LGN were prepared according to the method described by Crunelli et al. (1987a).

Cats (1-3.2Kg) were anaesthetized with halothane (1.2%) and a mixture of N_2O and O_2 (1:2), and the muscles around the skull were removed gently. The skull was then removed from the lambda to the bregma to expose the whole brain and the meninges were carefully dissected. The most rostral part of the brain was then lifted up with the help of two spatulas and the optic nerves cut. A coronal cut was then made at the level of the inferior colliculi to free the brain from the spinal cord and the brain was transferred into a cold (4-10°C) standard artificial cerebrospinal fluid of composition (mM): NaCl, 134; KCl, 5; KH_2PO_4, 1.25; $MgSO_4$, 2; $CaCl_2$, 2; $NaHCO_3$, 16; and glucose, 10 (pH 7.4). A sagittal cut was then made, and the cortex was removed. The brain was then turned ventral portion up so that the optic chiasm and tract were clearly visible. Two other cuts were made parallel to the optic tract: the first about 2-4mm rostral and the second about 5mm caudal to the optic tract itself. Using a Vibroslice (Campden Instrument) slices of the LGN (250-400μM thick) were then cut in such a way that the most lateral part of the LGN was closest to the blade.

The slices were transferred to a recording chamber (Fig. 2.1) and perfused with a warmed (35±1°C), continuously oxygenated (95% O_2 - 5%CO_2) standard artificial cerebrospinal fluid.

Fig. 2.1. A diagram of the recording chamber. (1) - brain slice; (2) - lid of perfusion chamber; (3) - water bath; (4) - thermostat; (5) - heater; (6) - 95%O_2 / 5%CO_2 gas mixture; (7) - polythene tubing; (8) - prechamber; arrows indicate flow of gas mixture.

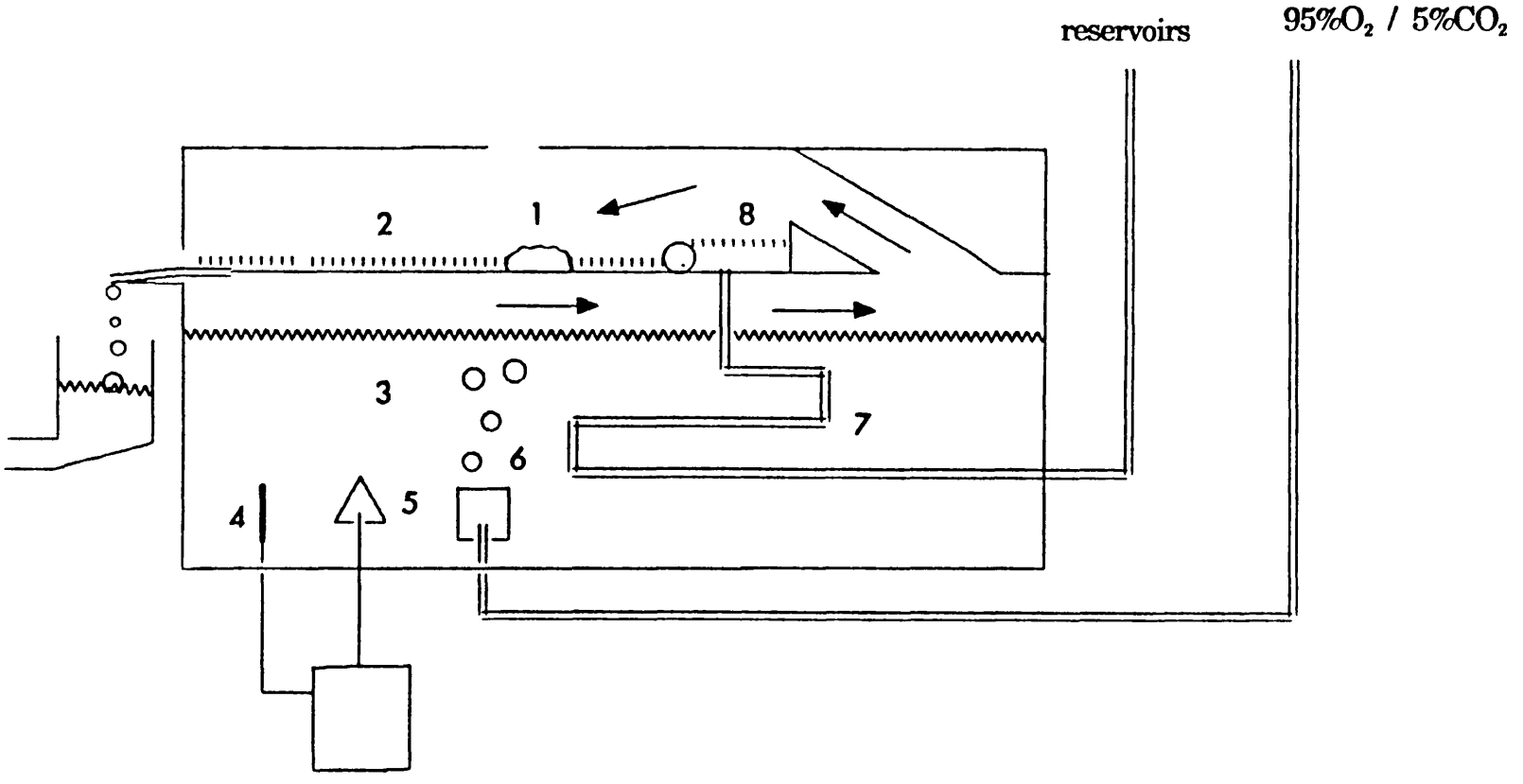
reservoirs
95%O2 / 5%CO2
1
2
3
4
5
6
7
8

2.2. Brain slice maintenance

The technique used for maintaining brain slices in this study was based on the method first described by Yamamoto and McIlwain (1966) and later modified by Haas and coworkers (1979).

The brain slice (1) was placed onto the lid (2) of a perfusion chamber (Fig.2.1) which is made from plexiglass and sits on the top of a rectangular water bath (3) maintained at 35±1°C by a thermostatically controlled (4) heater (5) and bubbled with a 95%O_2 / 5%CO_2 gas mixture (6). Perfusion fluids, stored in reservoirs, were also continuously bubbled with the 95%O_2 / 5%CO_2 gas mixture and flowed through the perfusion chamber by gravity. A three-way tap selected the required fluid and the flow rate was regulated by a disposable precision valve (Venisystems Dial-A-Flow). Fine polythene tubing (I.D. 0.76mm) carried the fluid through the water bath (7) to a prechamber (8) which made a bubble-trap chamber unnecessary. Fluid was transported from the prechamber by capillarity along a nylon mesh (cut from pantihose) through the recording chamber (2) and out over a projecting ledge of the lid where a piece of lens paper absorbed it and drained it away to a collection beaker.

One modification of the perfusion chamber from the Haas et al. (1979) design was that an adjustment in the flow rate by the precision valve also led to an alteration of the depth of the fluid in the slice chamber. The flow rate was experimentally ideal when the depth in the chamber was such that there was only a thin film of fluid over the brain slice and was invariably achieved at a rate in the order of 1-2 ml/min. Since there was a dead space

of approximately 1.9 ml between the three-way tap and the slice chamber a fluid exchange time course of less than 5 mins resulted.

After the slices had been in the recording chamber for 1 hour (recovery period) the standard medium was changed to one modified (experimental media) so that either I_T or I_h could be observed in isolation, or so that spontaneous low frequency membrane potential oscillations could be induced (see sections 3.1, 4.1 and 3.5.2., respectively). At least 30 minutes was allowed for the appropriate experimental artificial cerebrospinal fluid to reach the brain slice before intracellular electrophysiological recordings were made from single cells.

2.3. Electrophysiological recording

Intracellular recordings were made using glass microelectrodes (GC 120, Clark Electrical Instruments), prepared by a horizontal microelectrode puller (Narishige Instruments), filled with 1M-potassium acetate (DC resistance, 45-65 MΩ) and coupled to a current-voltage clamp preamplifier (Axoclamp-2A). Recordings were made in current clamp and single electrode voltage clamp modes (SEVC).

When recording in bridge mode the operational amplifier techniques were based on the Wheatstone bridge circuit (Fig. 2.2) so that microelectrode voltages could be monitored continuously, and continuous currents could be injected down the microelectrode. The bridge balance control, on the Axoclamp, was used to balance out the voltage drop across the microelectrode, due to the product of current flow and the microelectrode

resistance, so that only the membrane potential was recorded. This was achieved by advancing the bridge balance control until the fast voltage steps, seen at the start and finish of an externally triggered current pulse, were just eliminated. A residual transient was seen at the start and finish of the current step and was due to the finite response speed of the microelectrode.

When voltage clamping a cell, the preamplifier was switched from current clamp to discontinuous SEVC mode using the procedure described by Finkel and Redman (1984). This involved the optimal adjustment of the capacitance neutralization, phase, gain and sampling rate controls commensurate with complete settling of the continuously monitored input voltage and voltage-step settling times of < 3 ms. Sampling rates were in the range of 4-7.5 kHz and the gain was typically around 1 nA/mV. The basic circuitary of the discontinuous single electrode voltage clamp is shown in Fig. 2.3.

After recording on a RACAL FM 4D or a Biologic DAT recorder, membrane currents and voltages were digitized, stored on floppy disks and analysed using a 502 analog-to-digital interface (Cambridge Electronic Design) linked to a PDP11/23 computer or a 1401 analog-to-digital interface (Cambridge Electronic Design) linked to a Tandon microcomputer. Current data obtained from voltage clamp recordings were low pass filtered at 1KHz (Barr and Stroud) and all membrane currents are reproduced in the figures as the average of three consecutive records. Results in the text are expressed as mean±S.E.M.

Fig. 2.2. An example of the Wheatstone bridge circuit. A shows the relation of the resistors to the current source and the potential difference indicator (PDI). B shows the experimental arrangement for the utilization of a bridge circuit in order to record potential and to apply current across a cell membrane with a single electrode (Hubbard et al., 1969).

The Wheatstone bridge ciruit shown in Fig. 2.2A is arranged in such a manner that the zero potential differences between two terminals, during the application of a current between the other two terminals, indicates that a precise relation exists between the electrical parameters of the resistances in the bridge,

i.e.

$$\frac{R_1}{R_3} = \frac{R_2}{R_4}$$

When no potential difference is recorded between points c and d of the bridge, the device is said to be "balanced". Given this dynamic condition, if the resistive value of one of the arms is altered it is possible to calculate the magnitude of the change by rebalancing the bridge to a null reading in the potential difference indicator (PDI).

Fig. 2.2B shows an arrangement which allows the use of the circuit to measure the input resistance and capacitance of a given cell. R_1 and R_2 are fixed resistors. R_2 is the current limiting resistor. The values for R_1 and R_3 are selected depending on the resistance of the electrodes to be utilized and the input resistance of the cell to be studied. R_4 is shown separately in the lower part of Fig. 2.2B and is calculated as two resistances in series, that of the microelectrode - R_E and that of the cell - R_M. The capacity in parallel with R_M represents the capacitance of the cell.

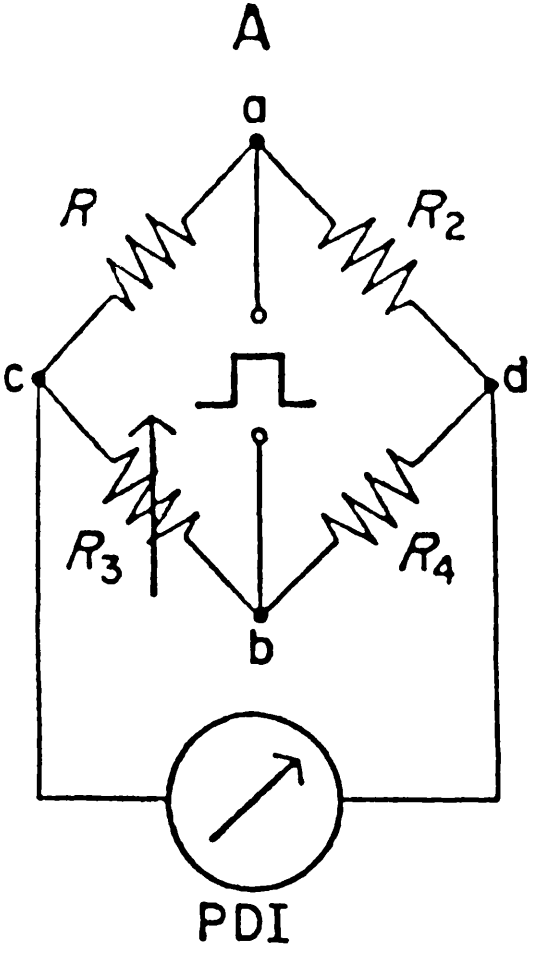
A
a
R
R2
c
d
R3
R4
b
PDI

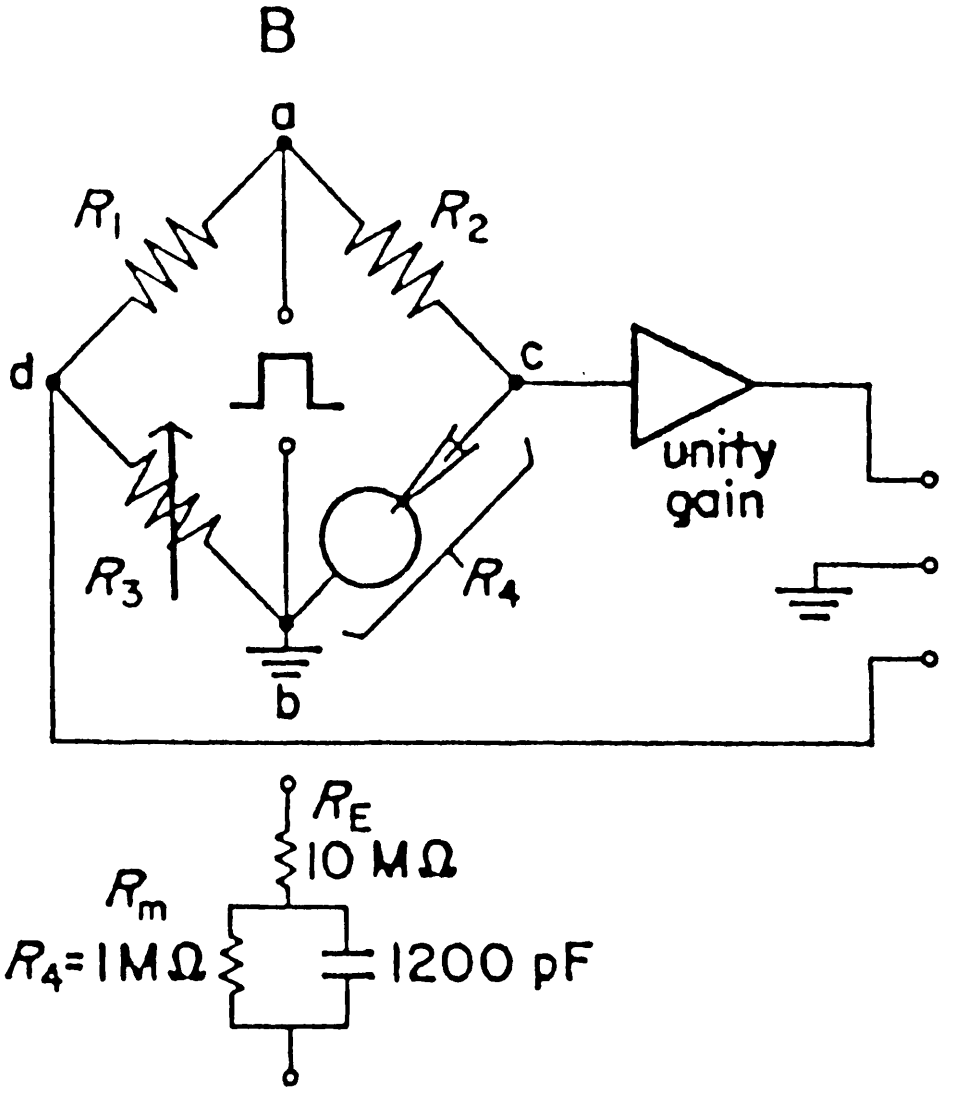
B
a
R1
R2
d
c
unity
gain
R3
R4
b
RE
10 MΩ
Rm
R4=1MΩ
1200 pF

Fig. 2.3. The discontinuous single-electrode voltage clamp circuitary. ME1 - a single microelectrode; V_m - membrane potential; V_1 - voltage recorded; A1 - unity gain headstage; SH1 - sample-and-hold circuit; V_c - command voltage; A2 - differential amplifier; E_1 - steady-state error (difference between V_m and V_c because G_T is finite); CCS - controlled current source; G_T - gain of CCS; I_o - current injected into the microelectrode. (from Finkel and Redman, 1984)

The discontinuous single electrode voltage clamp circuitary illustrated in Fig. 2.3 is arranged in such a manner that allows the tasks of voltage-recording and current-passing to be allocated to the same electrode. Time-sharing techniques are used to prevent interactions between the two tasks.

Following the penetration of a cell its membrane potential (V_m) is recorded so that it can be sampled and held by a sample-and-hold circuit (SH1) for the rest of the cycle. This sampled potential is compared with a command voltage (V_c) in a differential amplifier (A_2). The output of this amplifier becomes the input of a controlled-current-source (CCS) if the switch S1 is in the current passing position, which injects a current into the microelectrode that is proportional to its input, irrespective of the microelectrode resistance. S1 then switches to the voltage recording position so that a new sample of V_m can be taken and a new cycle begins.

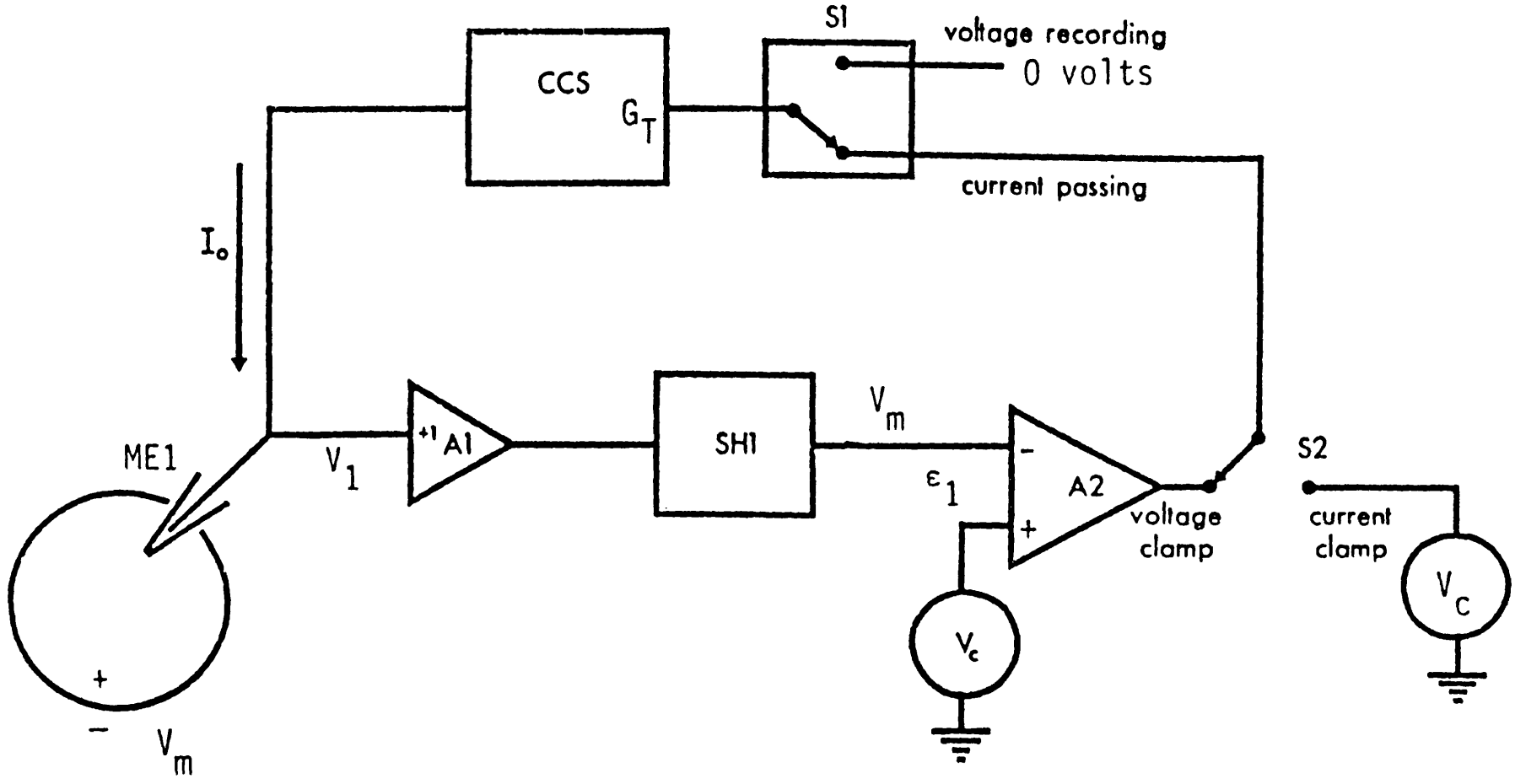
S1
voltage recording
0 volts
CCS
G_T
current passing
I_o
ME1
V_1
+1 A1
SH1
V_m
ε_1
A2
voltage clamp
S2
current clamp
V_c
V_c
+
−
V_m

2.4 Data analysis

The time course of membrane current development or decay was fitted by the mathematical function:

$$I = ae^{(bt)} + c, \qquad (1)$$

where I = membrane current, b = the rate constant, t = time (ms), c = a constant and a = a constant. The time constant of the current decay (in ms) was therefore given by the reciprocal of b. The fitting of data points to this equation was achieved using either a recursive method of minimizing the squares of the deviations about the mathematical function, as described by Benham and coworkers (1987), or by the single exponential curve fitting procedure present in the voltage clamp analysis module of the Patch and Voltage Clamp Software (Cambridge Electronic Design).

Data points from current activation and inactivation studies were fitted by an equation of the form:

$$I/I_{max} = \frac{1}{1 + \exp\left(\frac{V - V_o}{k}\right)} \qquad (2)$$

where I = current amplitude, V = membrane voltage, V_o = membrane voltage at half-maximal activation/inactivaion and k = the steepness coefficient. The fitting of data points to this equation was achieved by using the non-linear regression program of the Graphpad Software (Institute for Scientific Information [R], Version 2).

Lines were fitted to instantaneous and steady-state current-voltage relationships, using linear regression analysis, so that they could then be extrapolated. This was also done using the Graphpad Software.

2.5 Space clamp considerations

A critical consideration in voltage clamp studies is the question of whether the area of membrane being investigated is under good voltage control. Since previous studies of cat LGN cells have shown them to be electrotonically compact (Bloomfield et al., 1987; Crunelli et al., 1987d), the somatic area and a good portion of the proximal dendritic area of a TC cell membrane can be considered to be under good voltage control. In addition, the finding that the rate and voltage dependence of activation of the membrane conductances considered in this study were smooth and continuous functions of the membrane potential, suggests that sufficient clamp was obtained in order to avoid serious errors.

2.6. Drugs

The following drugs were used during the course of this study:

Tetrodotoxin (Sigma), a Na^+ channel blocker.

Amiloride hydrochloride (Sigma), a K^+-sparing diuretic.

Noradrenaline (Sigma), an adrenoreceptor agonist.

Isoprenaline hydrochloride (Sigma), a β-specific adrenoreceptor agonist.

Yohimbine hydrochloride (Sigma), an α_2-specific adrenoreceptor antagonist.

Prazosin hydrochloride (Sigma), an α_1-specific adrenoreceptor antagonist.

1-Octanol (Sigma).

Nifedipine (Bayer), a dihydropine Ca^{2+} channel blocker.

All of the above drugs, except nifedipine, were dissolved directly into the experimental medium at the required concentration.

Nifedipine was dissolved in absolute alcohol and added to the experimental medium to give a final alcohol content of 0.075%. A similar alcohol concentration was present in the control solution during these experiments and extreme care was taken to avoid exposure of the nifedipine solution to light.

CHAPTER THREE

THE Ca^{2+} CURRENT UNDERLYING LOW-THRESHOLD Ca^{2+} POTENTIALS

3.1. Isolating and quantifying the Ca^{2+} current

In order to isolate the Ca^{2+} current, the artificial cerebrospinal fluid was modified by the addition of 0.5 μM tetrodotoxin (TTX, Sigma), 3-5 mM CsCl and the adjustment of divalent cation concentrations to 1 mM Ca^{2+} and 3 mM Mg^{2+}. At the same time the chamber heater was turned off allowing the perfusion medium to cool to room temperature (25±1°C). The relatively low temperature and the 3:1 Mg^{2+}:Ca^{2+} ratio both assisted in routinely achieving good control of the membrane voltage during activation of the Ca^{2+} current, while CsCl abolished the inward rectifier current I_h (see chapter 4), whose "off" tail would otherwise have contaminated its development. In experiments where $CdCl_2$ or $BaCl_2$ were ultimately to be added to the experimental medium, KH_2PO_4 was ommitted and $MgSO_4$ was replaced with $MgCl_2$.

On some occasions however, a temperature of 35±1°C was maintained and divalent cation concentrations were changed to 1.5 mM Ca^{2+} and 1 mM Mg^{2+}, in an attempt to match physiological conditions.

It was not necessary to block outward voltage-dependent K^+ currents (i.e. I_A, delayed rectifier) since both had activation thresholds positive to -50 mV, which is outside the range of membrane potentials used to test the Ca^{2+} current under study.

The Ca^{2+} current was activated by depolarizing voltage steps from relatively hyperpolarized membrane potentials. This resulted in an inward Ca^{2+} current superimposed on an outward "leak" current. While the size of the inward Ca^{2+} current could have been quantified using a "leak" subtraction procedure (Fig. 3.1), this approach was not routinely used since

the "leak" subtraction process inevitably led to increased noise levels on current records and occupied precious experimental time. Instead, the size of the Ca^{2+} current was measured by taking the difference in current level between the peak of the Ca^{2+} current and the level of the outward "leak" current 500 ms after this peak. This measuring procedure makes the assumption that the outward "leak" current activates rapidly with respect to the Ca^{2+} current, an assumption which is supported by the fact that the time course and the amplitude of I_T are the same whether measured from "leak"-subtracted or non-subtracted records (Fig. 3.1). This similarity in time course and amplitude between "leak"-subtracted and non-subtracted Ca^{2+} currents applied over the full activation range.

The results of this part of the study are based on the recordings from 133 cat TC cells located in laminae A, A1 and C of the LGN from which stable recordings were made. Their passive membrane properties were similar to those described in previous studies (Crunelli et al., 1987b), but their active properties were altered by the blocking agents used in the medium.

Fig. 3.1. Leak subtraction of the transient, inward Ca^{2+} current. A shows the membrane current response to a depolarizing voltage step to -55 mV following a 2 s hyperpolarizing pre-pulse to -95 mV. The resulting current response takes the form of a transient inward current superimposed on the outward "leak" current. B illustrates the outward "leak" current resulting from an identical depolarizing step after a relatively brief (50 ms) hyperpolarizing pre-pulse. The "leak" current appears in isolation since no inward Ca^{2+} current is generated after such a short period of hyperpolarization (see Fig. 3.3.2.). C is the result of subtracting the trace in B from that in A and therefore represents only the transient inward Ca^{2+} current.

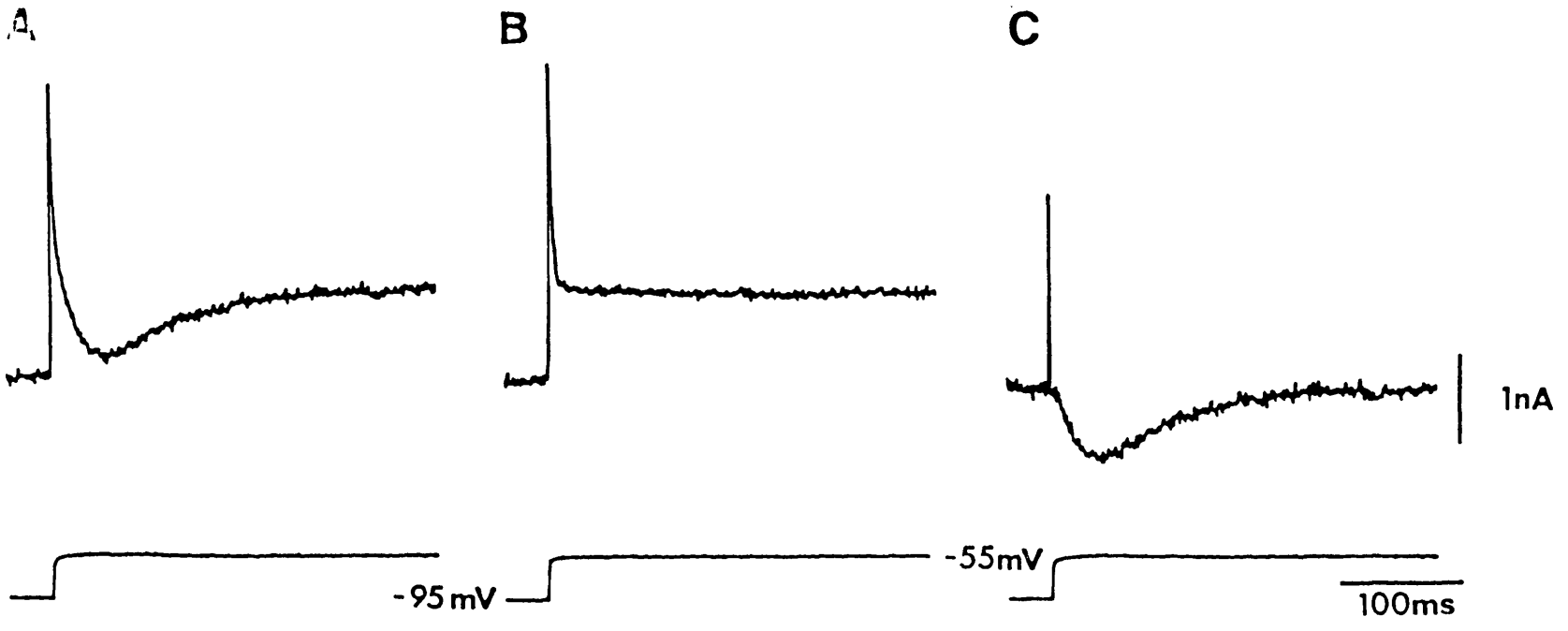
A
B
C
1nA
-55mV
-95 mV
100ms

3.2. Preliminary observations

In current-clamp recordings, depolarizing current pulses from membrane potentials negative to -75 mV invariably evoked a robust LTCP which was significantly reduced or abolished when the Ca^{2+} concentration of the perfusing medium was decreased from 1 to 0.1 mM (n=4) (Fig. 3.2). Immediately after each of the current-clamp recordings shown in Fig. 3.2A, the preamplifier was switched to SEVC mode. In standard medium, a depolarizing voltage step to -55 mV from a holding potential of -95 mV evoked a transient inward current, with respect to the leak current, which was virtually abolished when the external Ca^{2+} concentration was lowered to 0.1 mM (Fig. 3.2B). Taken together these observations indicate that Ca^{2+} ions are the charge carriers for the transient inward current and that this current is the generator of the LTCPs observed in current clamp recordings. As outlined in Chapter 1 low voltage activated Ca^{2+} currents have been observed in other cell types, and, because of their transient nature, have been termed T-type Ca^{2+} currents. For this reason the Ca^{2+} current underlying low-threshold Ca^{2+} potentials has been termed I_T.

Fig. 3.2. The Ca^{2+} dependence of low-threshold Ca^{2+} potentials and I_T. A shows two current-clamp records from the same cell which was hyperpolarized by steady inward current and briefly depolarized using an outward current pulse. With an external Ca^{2+} concentratin of 1 mM (left) depolarizations from -85 mV evoked a robust low-threshold Ca^{2+} potential, but, after a 50 min perfusion with a solution containing 0.1 mM Ca^{2+} (right), a larger depolarization from -90 mV generated only a passive electrotonic potential. B shows voltage-clamp data from the same cell recorded immediately following those directly above in A. With an external Ca^{2+} concentration of 1 mM (left), a step depolarization to -55 mV, following a 2 s hyperpolarizing prepulse to -95 mV, evoked a transient inward current (I_T) which was virtually abolished in the solution containing 0.1 mM Ca^{2+} (right).

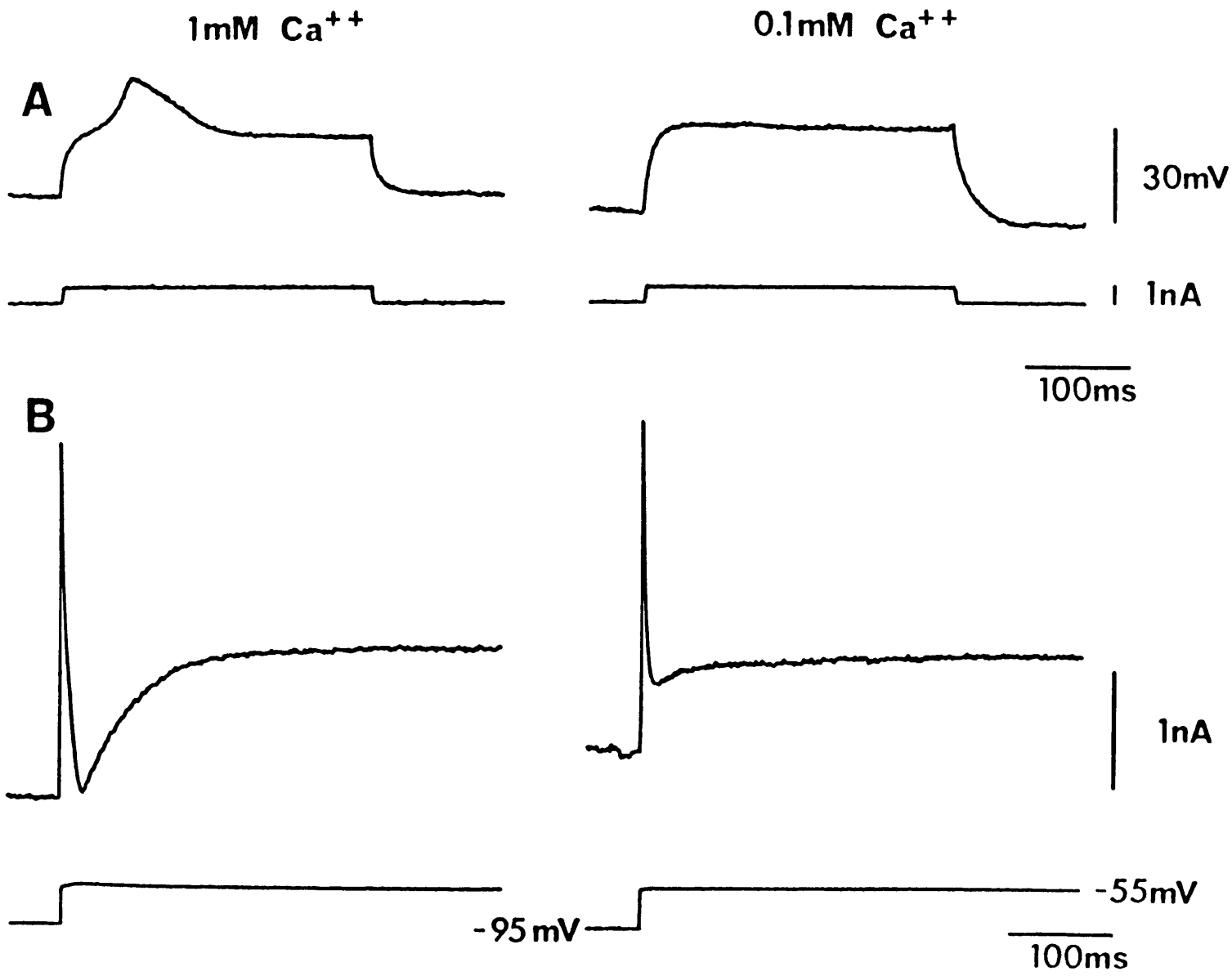
1mM Ca++
0.1mM Ca++
A
30mV
1nA
100ms
B
1nA
-55mV
-95 mV
100ms

3.3. Basic properties of I_T

3.3.1. I_T activation and inactivation

The activation of I_T was studied using depolarizing voltage steps of increasing amplitude after a 2 s hyperpolarizing prepulse to -95 mV (Fig. 3.3A_2). Once the I_T threshold of approximately -70 mV had been reached, its size was found to be extremely voltage sensitive, with 10-90% activation occurring over a 6-10 mV range (Fig. 3.3B). After fitting the experimental data points, from 4 cells, with equation (2), the mean membrane voltage at half-maximal activation (V_o) was found to be -61±2 mV and the mean steepness coefficient (k) was found to be 2.3±0.2 mV. To observe the inactivation characteristics of I_T, 2 s hyperpolarizing pre-pulses of increasing amplitude were imposed before a depolarizing voltage step to around -50 mV (Fig. 3.3A_1). The inactivation curves generated showed that I_T was largely inactivated at membrane potentials positive to -65 mV. This inactivation was gradually removed as the membrane potential was made more negative, and was totally removed at a level of around -100 mV (Fig. 3.3B). After fitting the inactivation experimental data points, obtained from 4 cells, with equation (2) the curve was found to have a mean V_o of -80±3 mV and a mean k of 3.8±0.2 mV.

As can be seen from Fig. 3.3B there was a small overlap of the activation and inactivation curves, and this implies that over a narrow range of membrane potentials (-70 to -65 mV) there may be a steady inward Ca^{2+} current. However, the precise form of the fitted activation and inactivation

curves for small amplitude currents has overestimated the size of I_T when compared to the actual currents recorded, therefore exaggerating the overlap between curves.

The increase in membrane conductance due to I_T activation was estimated by measuring the instantaneous inward current resulting from a step hyperpolarization from -55 mV to -90 mV, and subtracting this value from the instantaneous current generated by an identical step at the peak of I_T. In 7 cells the difference in current flow indicated a mean peak conductance increase of 8.4±0.9 nS.

3.3.2. Time dependency of removal of inactivation

The removal of inactivation was time as well as voltage dependent. If, from a holding potential of -55 mV, hyperpolarizing voltage steps to -95 mV were maintained for increasing lengths of time (up to 1 s), the amplitude of I_T was increased (Fig. 3.4). In the standard medium at 25°C, 800-1000 ms were needed for complete removal of inactivation.

Considering the temperature and divalent cation concentrations of the standard perfusion medium, it was felt necessary to perform some experiments at 35°C in a medium with divalent cation concentrations closer to those likely to prevail in vivo (1.5 mM Ca^{2+}, 1 mM Mg^{2+}). Under such conditions complete removal of inactivation was obtained after 500-600 ms.

3.3.3. I_T decay

The decay phase of I_T could be fitted with a single-exponential curve, using equation (1), the time constant of which was voltage dependent and decreased as the membrane potential at which I_T was evoked became more positive (Fig. 3.5). The data in Fig. 3.5B illustrate that the time constant of decay is extremely voltage sensitive over the range -70 to -60 mV, decreasing from 100 to 25 ms, although it remains fairly constant at more depolarized levels.

Fig. 3.3. I_T activation and inactivation characteristics. A shows membrane currents generated in the same cell by the voltage steps indicated in order to examine the inactivation (A_1) and activation (A_2) of I_T. B shows activation (closed squares) and inactivation (closed triangles) curves fitted using equation (2) to the data points generated by the experiment illustrated in A. The peak amplitude of each Ca^{2+} current is plotted relative to the maximum current obtained. The parameters of the fitted curve are: inactivation k = 3.7 mV, V_o = -77 mV; activation k = 2.2 mV, V_o = -61 mV. These activation and inactivation curves were not corrected for changes in the driving force for Ca^{2+} at different membrane potentials.

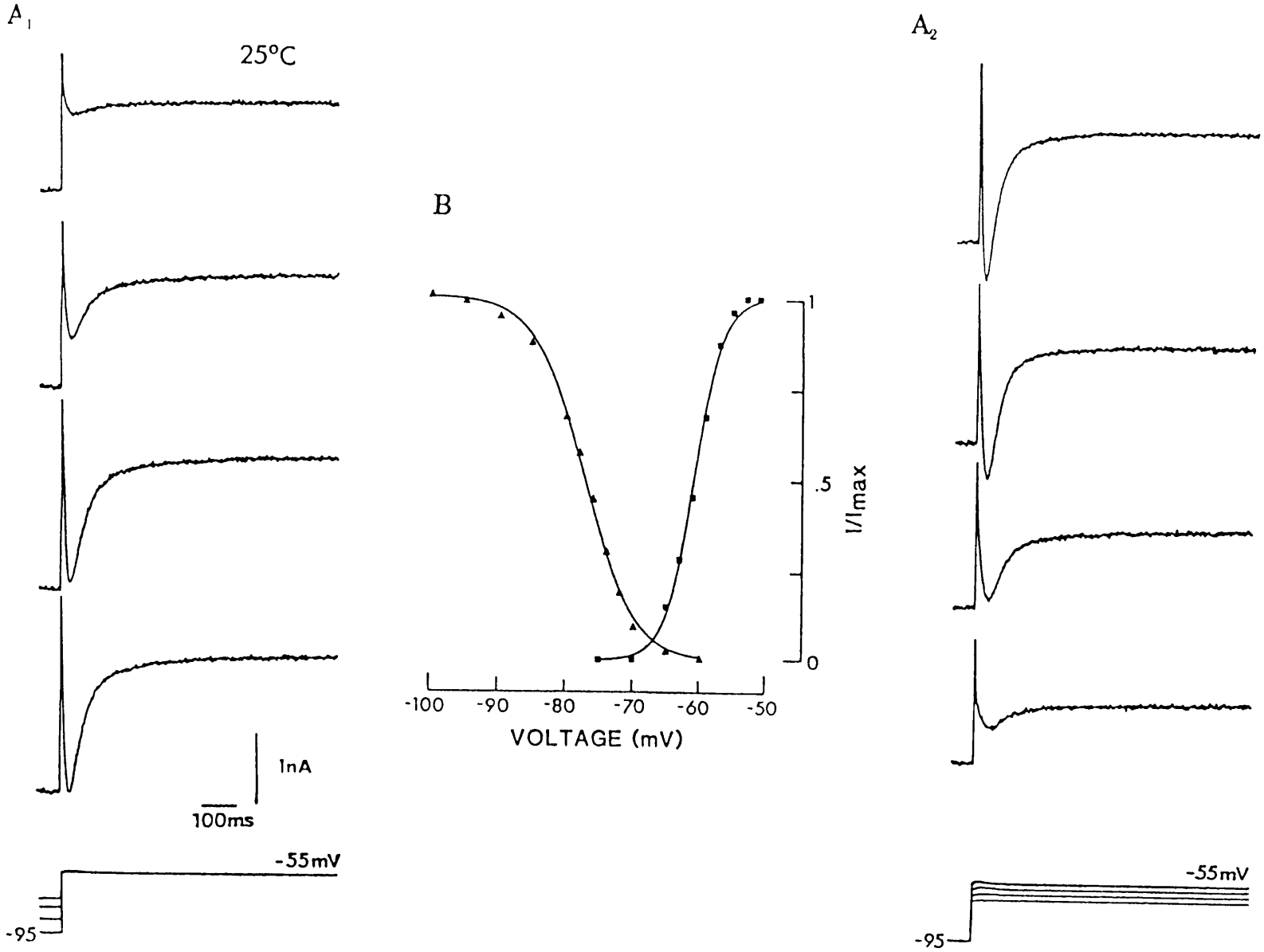
A1
25°C
1nA
100ms
-55mV
-95
B
1
.5
0
I/Imax
-100
-90
-80
-70
-60
-50
VOLTAGE (mV)
A2
-55mV
-95

Fig. 3.4. Removal of I_T inactivation. A shows the membrane currents generated by voltage steps to -95 mV of increasing duration from a holding potential of -55 mV. Note the absence of any active currents during membrane hyperpolarization. B represents two graphs produced by plotting the size (relative to the I_T amplitude evoked following a 2 s hyperpolarization) of a particular I_T against the duration of the hyperpolarization which preceded it. The graph labelled 25°C was produced using the data shown in A and illustrates that a 800-1000 ms period of hyperpolarization was needed to totally remove inactivation. This is markedly longer than the 500-600 ms necessary for a corresponding removal of inactivation in a different cell at 35°C (1.5 mM Ca^{2+}, 1 mM Mg^{2+}).

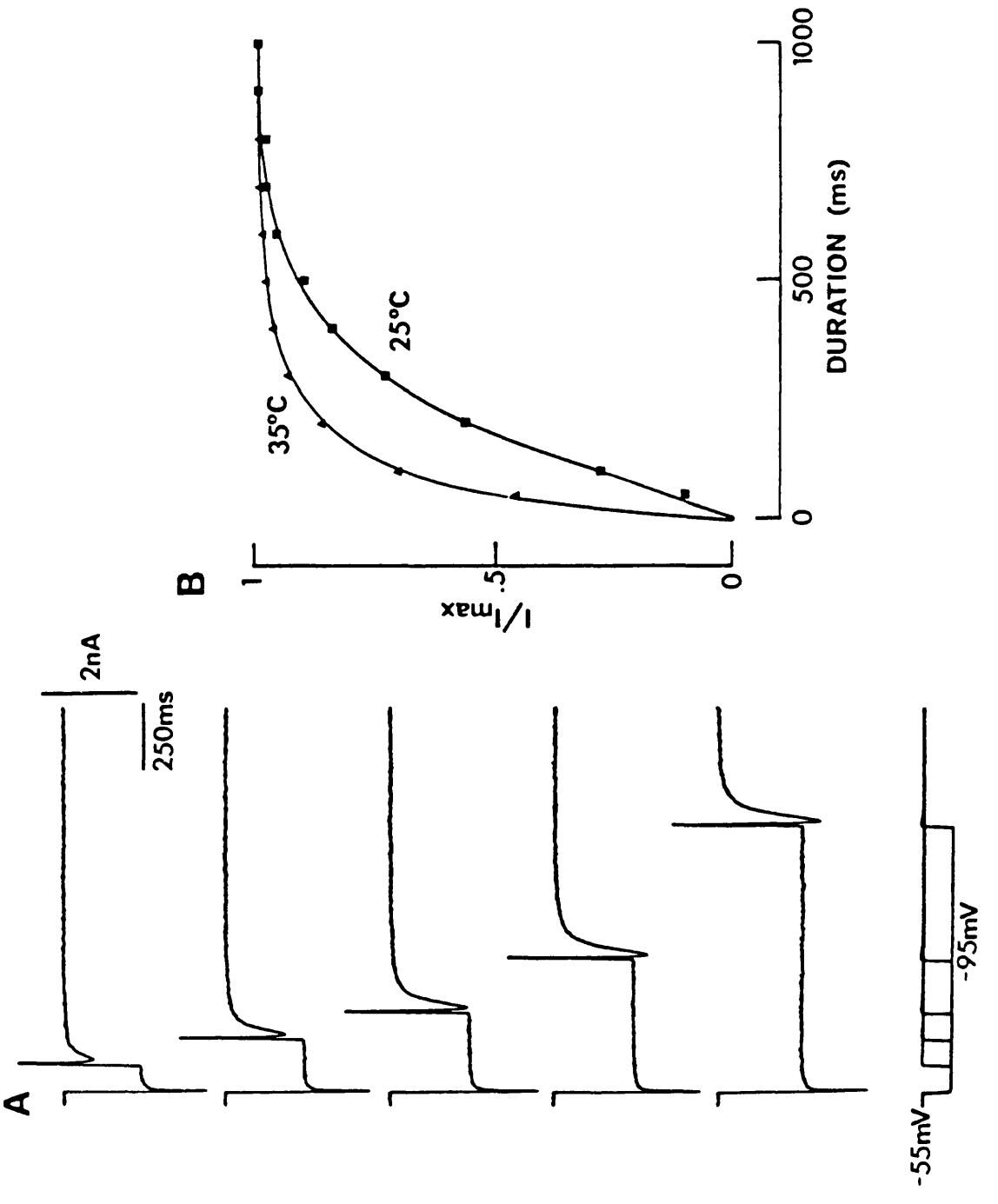
A
2nA
250ms
-55mV
-95mV
B
35°C
25°C
I/Imax
1
.5
0
0
500
1000
DURATION (ms)

Fig. 3.5. The decay of I_T follows a single-exponential time course. A shows four single membrane current records evoked by voltage steps to the membrane potential indicated to the right of each trace after a 2 s hyperpolarizing pre-pulse to -90 mV. The decay phase of each current has been fitted with a single exponential curve, formed by equation (1). The data from the cell shown in A has been used to produce the graph in B. The time constant of decay of a particular I_T is plotted against the membrane voltage at which it was evoked, illustrating the voltage dependency of the rate of I_T decay.

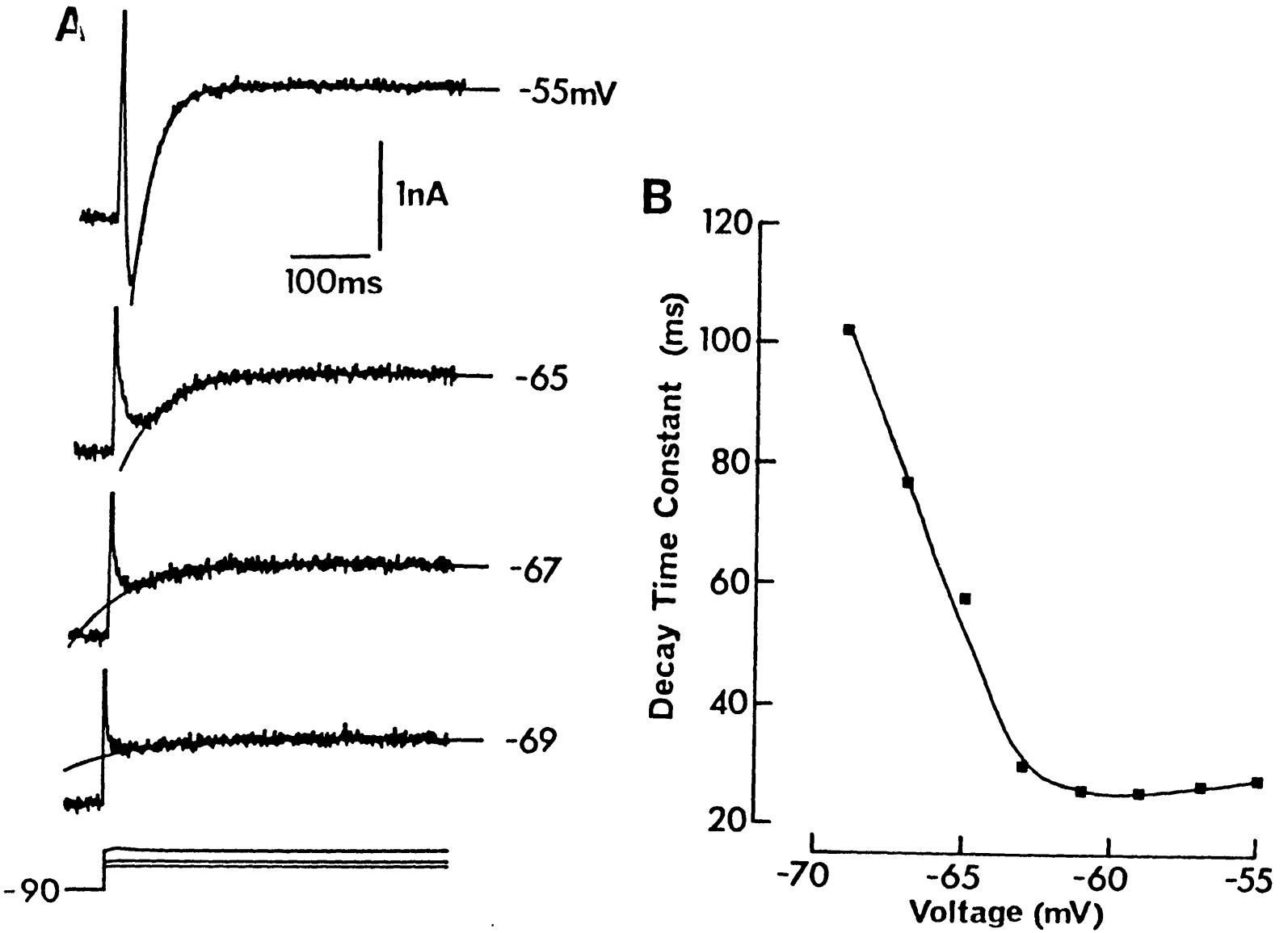
A
-55mV
1nA
100ms
-65
-67
-69
-90
B
Decay Time Constant (ms)
120
100
80
60
40
20
-70
-65
-60
-55
Voltage (mV)

3.4. Pharmacology of I_T

The classical Ca^{2+} channel blocker Cd^{2+} was relatively ineffective as an I_T antagonist, even at a concentration of 500 μM. However the current was signifantly more sensitive to Ni^{2+} at equivalent concentrations. In 5 cells 500 μM Ni^{2+} decreased I_T by 99±1%, while, in 4 cells, 500 μM Cd^{2+} reduced I_T by 40±5%. This difference in sensitivity is highlighted in Fig. 3.6A which shows that a 30 min perfusion with 500 μM Ni^{2+} abolished I_T, while a 45 min perfusion with 500 μM Cd^{2+} produced only a 44% decrease of I_T in the same cell.

The dihydropyridine Ca^{2+} channel blocker, nifedipine (25 μM), had no effect on I_T (n=4).

Thus, the pharmacology of I_T, as well as its kinetic properties, support its classification as a T-type Ca^{2+} current.

Since recent studies have suggested that amiloride and 1-octanol (Tsien et al, 1988; Kostyuk, 1989) selectively block T-type Ca^{2+} currents the effects of these two compounds on I_T were also investigated. At a concentration of 250 μM, amiloride decreased the maximum amplitude of I_T, by 35±6% (n=3). This was the maximum reduction observed since concentrations of 500 μM and 1 mM only reduced the size of I_T by 27±3% (n=4) and 29±3% (n=3), respectively. Typical examples of this effect are illustrated in Fig. 3.7 which shows that 250 μM amiloride reduced I_T by 32% while 1 mM amiloride produced a reduction of 22%. Over the concentration range used, amiloride had no consistent effect on the holding and "leak" current.

As shown in Fig. 3.8, 1-octanol, which is fully soluble at the

concentrations used in this study (Bell, 1973), reversibly decreased the maximum amplitude of I_T. For the data illustrated, 100 μM 1-octanol inhibited I_T by 13% while at a concentration of 600 μM 1-octanol reduced I_T amplitude by 67%. The dose-dependence of the inhibition of I_T by 1-octanol is illustrated by the log dose-response curve shown in Fig. 3.9 which indicates an IC_{50} of 430 μM and a full block of the current at a concentration of 2 mM. Over the concentration range used 1-octanol had no effect on the holding current nor the potential at which the maximum current was evoked.

However, it is apparent from the records shown in Fig. 3.9 that 1-octanol reversibly increased the "leak" current. This effect was also evident from the decrease in amplitude of the electrotonic potentials evoked in current clamp mode by a negative current pulse, indicating a reduction in cell input resistance. The increase in "leak" current was independent of the concentration used, since 0.1 mM to 2 mM 1-octanol caused a similar increase (200%) in the "leak" current.

Fig. 3.6. The effects of Cd^{2+} and Ni^{2+} on I_T of TC cells. The cell was voltage clamped at a holding potential of -55 mV and hyperpolarized to -95 mV for 2 s, of which the last 10 ms are shown. Four voltage-clamp records from a single LGN cell are shown during the experimental conditions indicated. After a 30 min perfusion with 500 μM Ni^{2+} had abolished I_T, a 2 h wash-out period restored I_T to 70% of its control amplitude. Despite a 45 min perfusion with 500 μM Cd^{2+} only a 44% inhibition was seen relative to I_T after the wash-out period. Each example of I_T represents the largest current that it was possible to evoke, indicating that the membrane voltage for maximal I_T activation of -55 mV was unchanged by Cd^{2+} or Ni^{2+}. It is apparent that in the presence of 500 μM Ni^{2+} there was a significant rise in "leak" conductance. This is probably due to a temporary deterioration in the quality of electrode impalement since 500 μM Ni^{2+} did not usually have this effect.

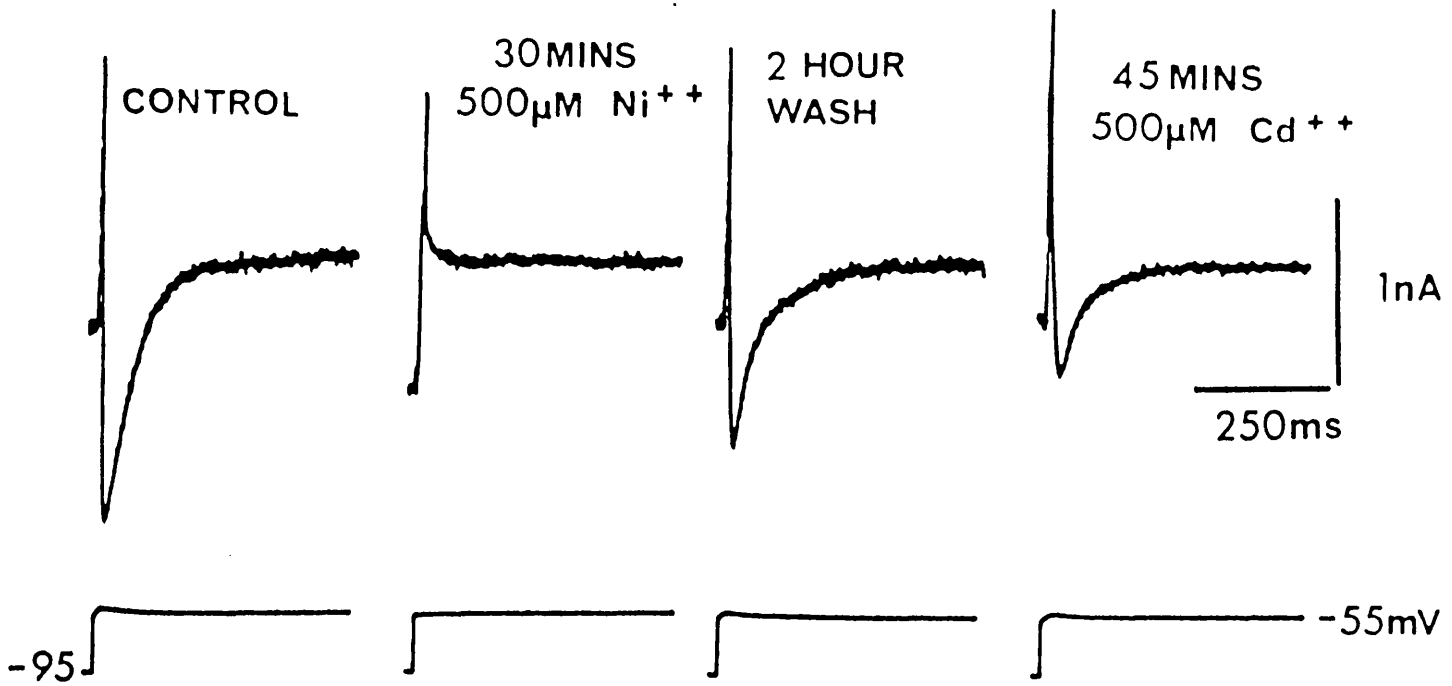
CONTROL
30MINS
500μM Ni++
2 HOUR
WASH
45MINS
500μM Cd++
1nA
250ms
-95
-55mV

Fig. 3.7. The effect of amiloride on I_T of TC cells. The figure shows membrane currents (upper traces in A and B) evoked by a step depolarization to -55 mV following a 2 s hyperpolarizing pre-pulse to -95 mV (lower traces) of which the last 25 ms are shown. In A, application of 250 μM amiloride decreases the maximum amplitude of I_T by 32% (from 1.7 to 1.2 nA). B: in a different cell, 1 mM amiloride reduces I_T by 22% (from 1.2 to 0.9 nA). Note that amiloride did not change the membrane voltage at which the maximum amplitude of I_T was evoked and that the change in "leak" current in A was not a consistent finding.

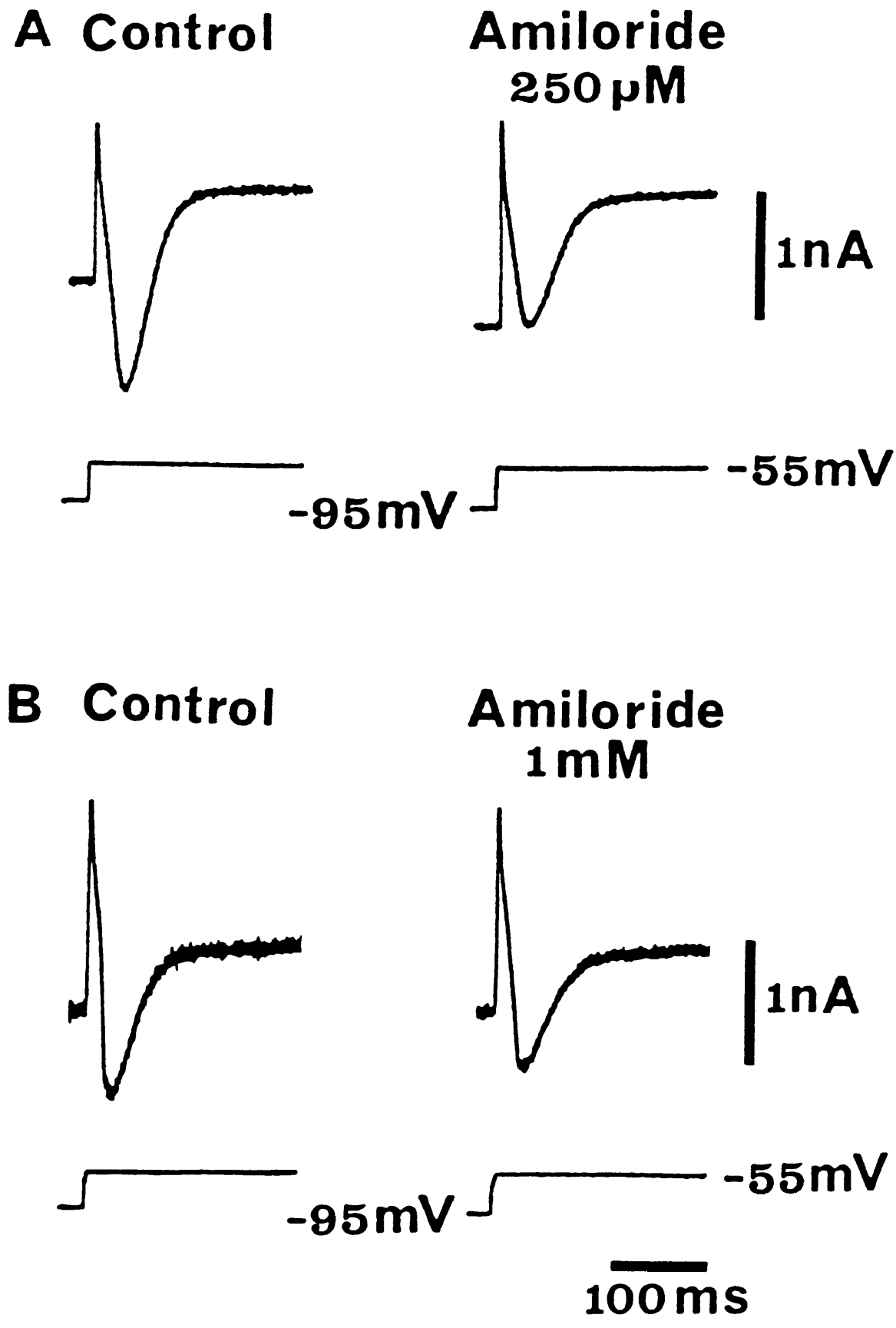
A Control
Amiloride
250 µM
1nA
-95mV
-55mV
B Control
Amiloride
1mM
1nA
-95mV
-55mV
100ms

Fig. 3.8. The effect of 1-octanol on I_T of TC cells. Voltage clamp records (A_1) show that 100 μM 1-octanol reduces I_T by 13% (from 2.0 to 1.8 nA) with recovery. It is also apparent that this concentration of 1-octanol increases the "leak" current by 200%. The current clamp records in A_2 show that the amplitude of the electrotonic potentials (upper traces) evoked, in the same cell, by a constant pulse of current (lower traces) is decreased during perfusion of the slice with 1-octanol. In B, voltage (B_1) and current (B_2) clamp records show the effect of 600 μM 1-octanol in a different cell. The maximal amplitude of I_T is reduced by 67% (from 1.2 to 0.4 nA) while the "leak" current is increased by more than 200%, an effect which is also evident from the smaller amplitude of the electrotonic potentials shown in the upper traces in B_2.

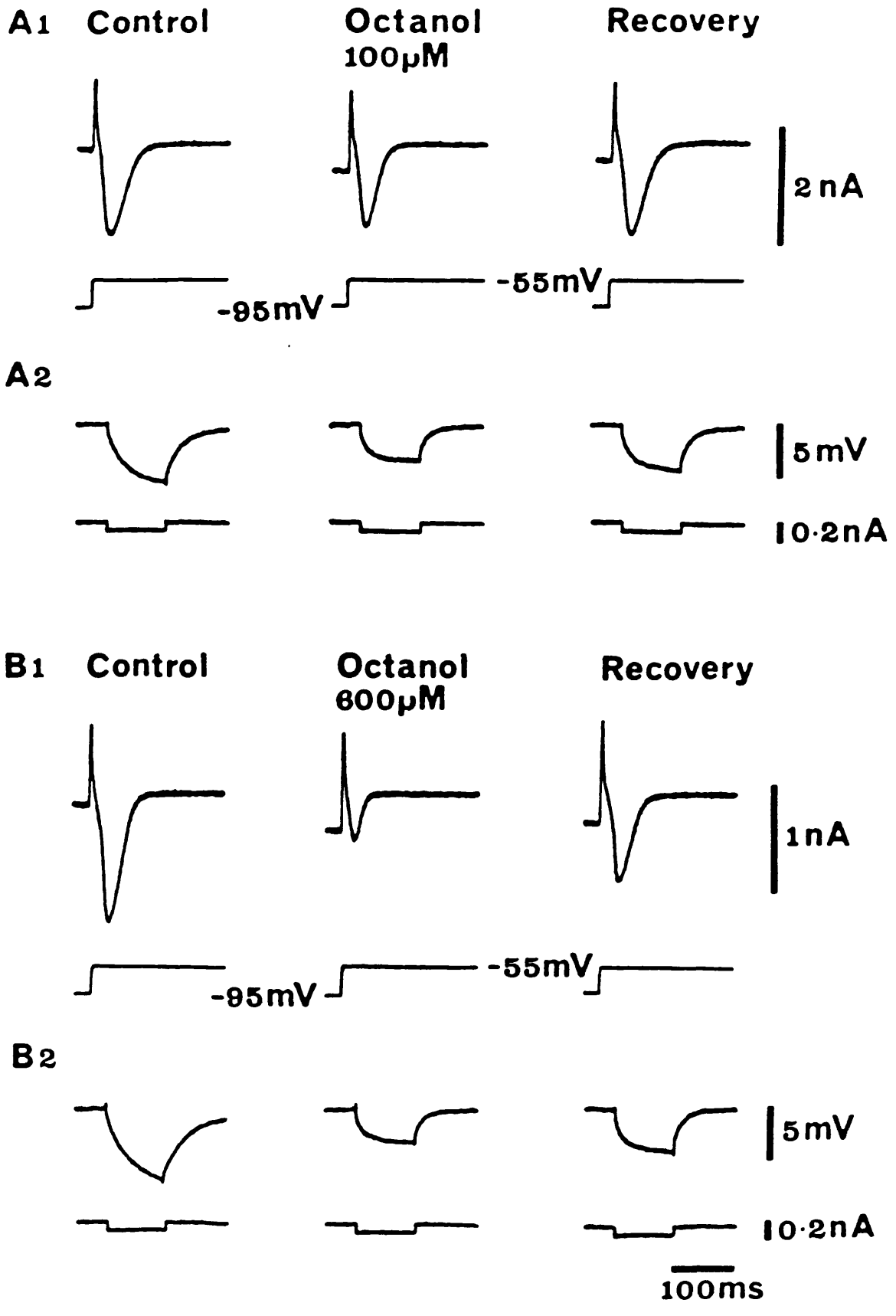
A1
Control
Octanol
100μM
Recovery
2nA
-95mV
-55mV
A2
5mV
0·2nA
B1
Control
Octanol
600μM
Recovery
1nA
-95mV
-55mV
B2
5mV
0·2nA
100ms

Fig. 3.9. Log dose-response curve of the effect of 1-octanol (abscissa scale) on I_T amplitude (ordinate scale). The number beside the points indicates the number of cells tested at each concentration. Vertical lines represent the S.E.M.. I_T was generated by voltage steps to −55mV from a holding potential of −95mV.

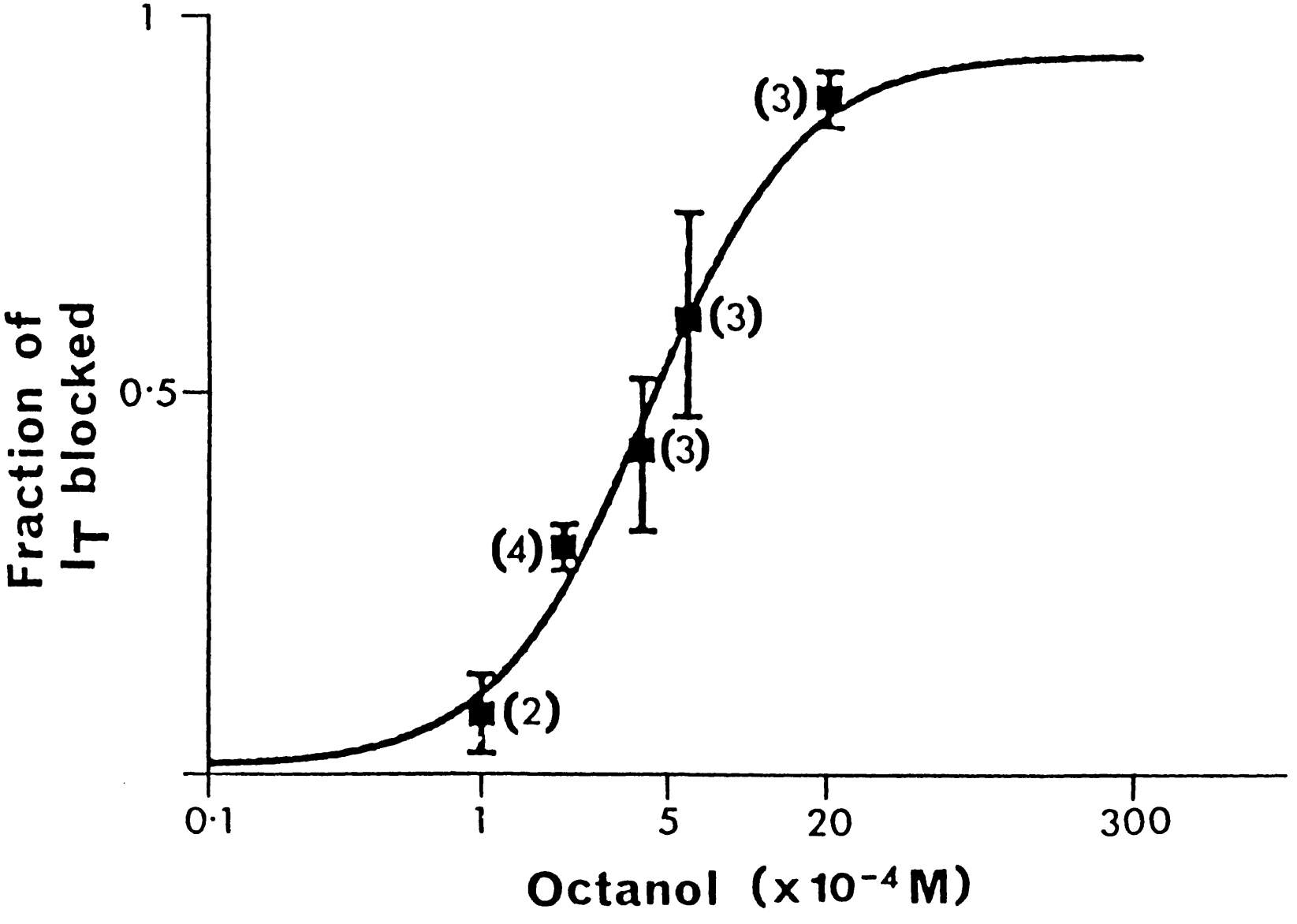
1
0·5
Fraction of I_T blocked
(3)
(3)
(3)
(4)
(2)
0·1
1
5
20
300
Octanol (x 10^{-4} M)

3.5. Contribution of I_T to oscillatory activities

3.5.1. I_T activation using voltage ramps

During membrane potential oscillations of TC cells in vivo and in vitro, LTCPs are preceded by a gradual, linear depolarization (Andersen and Sears, 1964; Roy et al., 1984; Leresche et al, 1990, 1991) (see Figs. 1.2 and 1.3). With this in mind, voltage ramps were used to activate I_T rather than the abrupt voltage steps necessary to study its basic properties. Linear membrane depolarizations of different rates were imposed after a 2 s hyperpolarization greater than 40 mV had removed current inactivation. As illustrated in Fig. 3.10, the size of I_T increased along with the rate of depolarization. In four cells recorded at 35°C (1.5 mM Ca^{2+}, 1 mM Mg^{2+}), the threshold rate of depolarization required for the activation of I_T was 30±2 mV/s. This is very similar to the rate of depolarization that occurs during the spontaneous membrane potential oscillations observed in TC cells in vitro, illustrating that I_T may be activated during such activities.

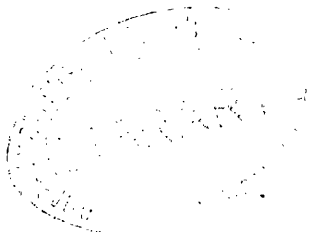

3.5.2. The effect of I_T blockade on the "pacemaker" oscillations

In experiments where it was desirable to study the spontaneous membrane potential oscillations the following experimental medium was used (mM): NaCl, 134; KCl, 2; KH_2PO_4, 1.25; $MgSO_4$, 0.5-0.8; $CaCl_2$, 3-4; and glucose 10 (pH 7.4).

In order to confirm that the large depolarizations, present during in vitro oscillations (see chapter 1.4.3) are generated by I_T activation, the effect of Ni^{2+} on the "pacemaker" oscillations was investigated. As shown in Fig. 3.11, 500 μM Ni^{2+} was found to abolish the "pacemaker" oscillations reversibly, indicating that the large depolarizations present in these oscillatory activities are indeed LTCPs.

Fig. 3.10. Activation of I_T with ramp depolarizations. Following a 2 s hyperpolarizing pre-pulse to -90 mv, the cell was depolarized to -55 mV using voltage ramps of increasing depolarization rate. The rates of depolarization are (mV/s): a = 20, b = 29, c = 58, d = 150, e = 530 and f = 1600. I_T first becomes evident in c. Cell recorded at 35°C (1.5 mM Ca^{2+}, 1 mM Mg^{2+}).

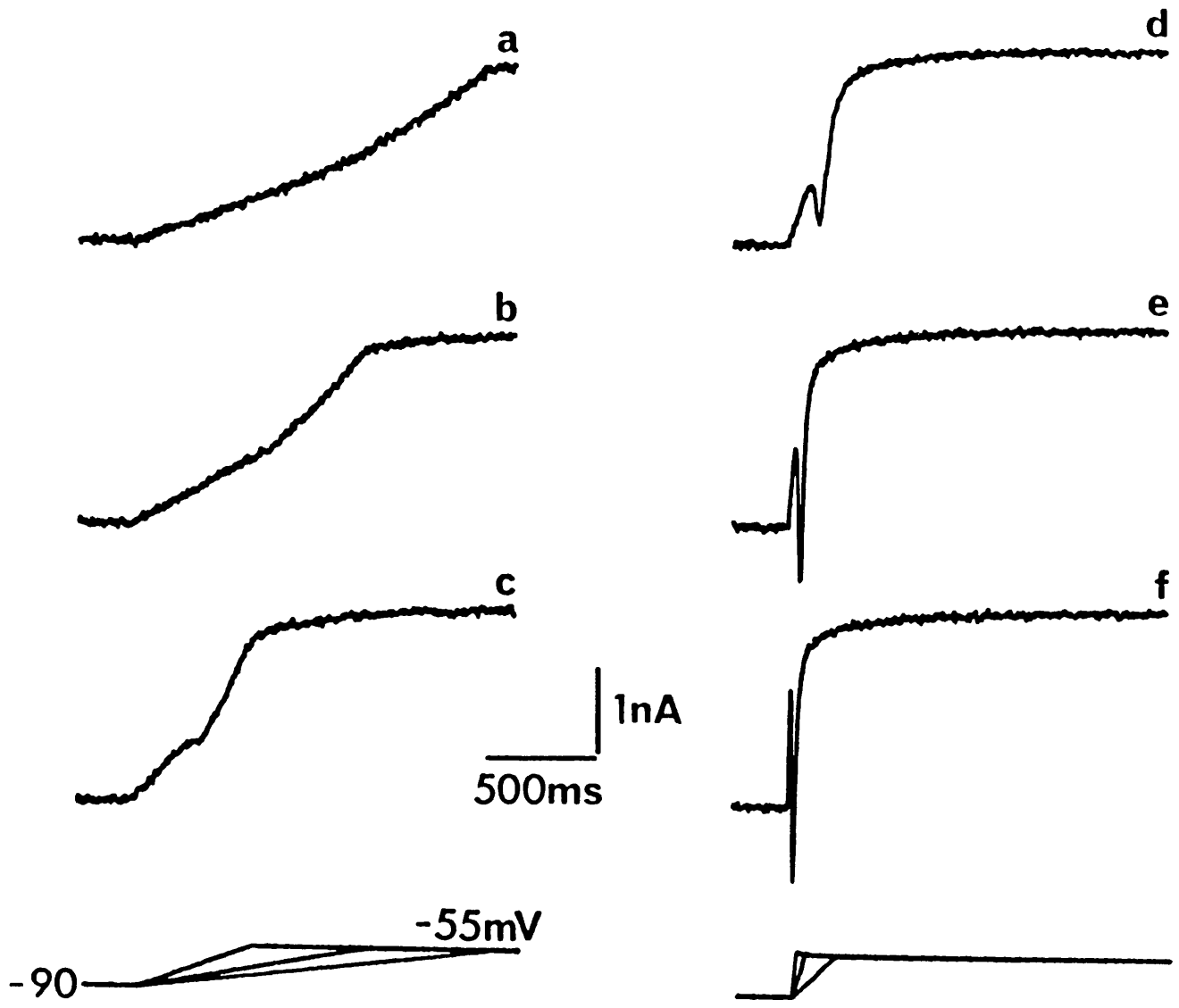
a
b
c
d
e
f
1nA
500ms
-55mV
-90

Fig. 3.11. Blockade of the "pacemaker" oscilations by Ni^{2+}. Intracellular voltage records from a dLGN cell show the block by Ni^{2+} (0.5 mM) of the "pacemaker" oscillations, 11 min after its addition to the perfusion medium. The recovery was obtained 45 min after removing Ni^{2+} from the medium. The membrane potential in nickel and at the peak of the hyperpolarization in control and recovery was -75 mV.

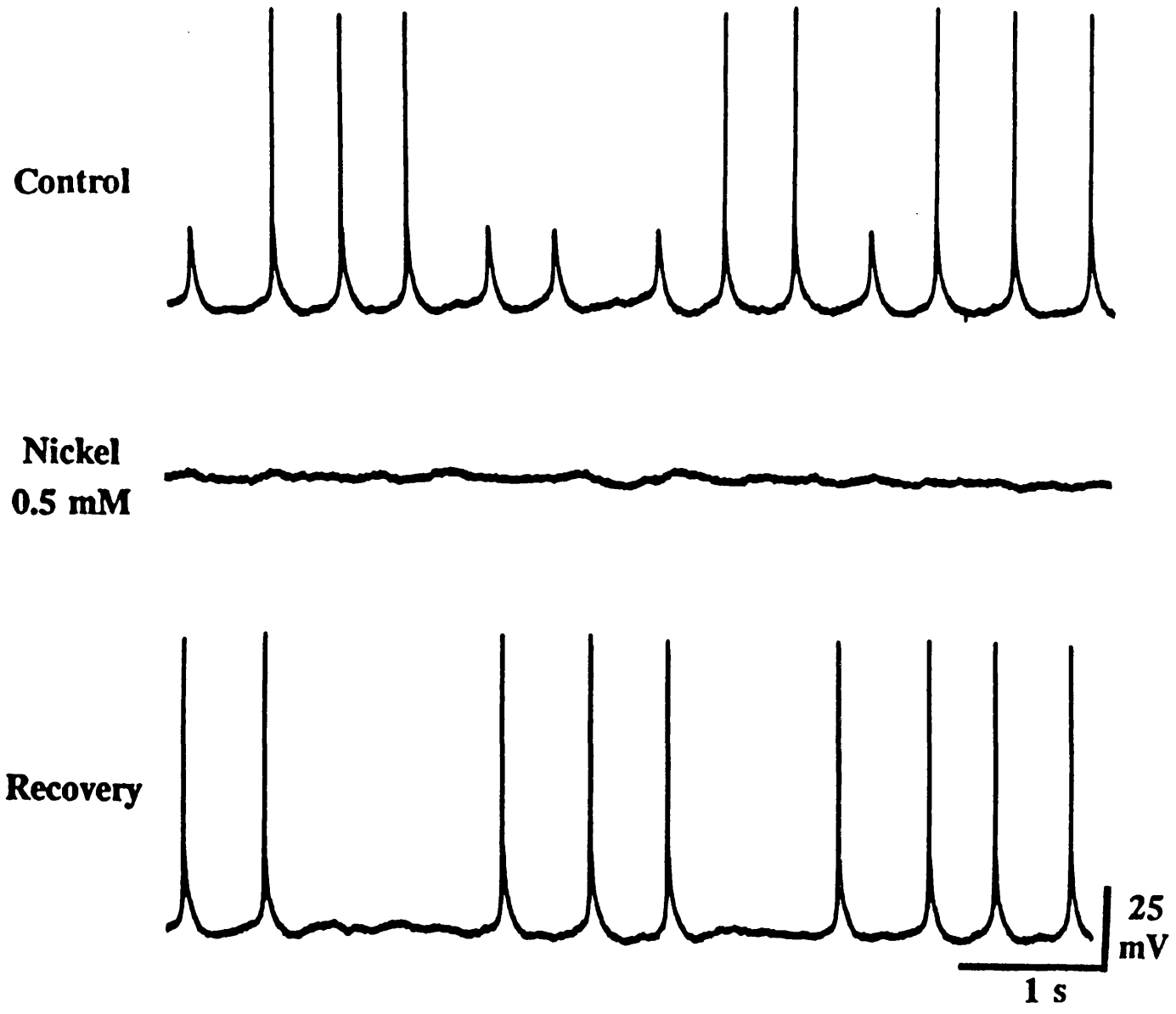
Control
Nickel
0.5 mM
Recovery
25
mV
1 s

3.6. Postnatal development of I_T

3.6.1. Development of maximum I_T amplitude

Since, as outlined in chapter 1.5.1., it seems that membrane potential oscillations play a key role during neuronal development (Llinas, 1988; Walton and Llinas, 1986) the development of I_T has been investigated. Typical records of the maximum I_T obtainable in neurones from young and adult cats are shown in Fig. 3.12A. It can be seen that the maximum amplitude I_T was larger in neurones from the adult animal than from the 13-day old animal. Statistical analysis (Student's t-test for independent samples) of results from 7 adult and 11 young neurones showed that the mean amplitude of I_T for the adult (1.7±0.2 nA) is significantly larger ($p<0.001$) than for the young neurones (0.7±0.1 nA).

As expected from the increase in soma size during postnatal development (Elgeti et al., 1976; Garey et al., 1973; Hickey, 1980; Kalil, 1978; Mason, 1983), the "leak" conductance increased with age, from 29±4 nS (n=12) to 46±6 nS (n=5). It is important to note that the increase in amplitude of I_T with age did not result in major changes in the properties of the LTCPs. As shown in Fig. 3.12B, for instance, the maximum amplitude of the LTCPs was indeed similar in young and adult cats.

3.6.2. Development of I_T activation and inactivation

The activation and inactivation curves of I_T from a neurone of a

five-day-old cat are shown in Fig. 3.13A. As found in the adult, the inactivation curve (continuous line) shows that I_T was largely inactivated at membrane potentials positive to -70 mV and that this inactivation was progressively removed as the membrane potential approached -100 mV. The removal of inactivation was thus voltage dependent. The activation curve (dashed line) shows that, as with the adult (chapter 3.3.1.), once the I_T activation threshold of approximately -70 mV had been reached, the size of I_T became voltage sensitive, with 10 to 90% activation occurring over a 10 mV range. The similarity of these curves to those found in the adult (Fig. 3.3) is also supported by the similarity of V_o and k (see legend of Fig. 3.13), though a slight decrease was observed in the k of inactivation compared with the adult cat.

3.6.3. Development of time dependency of removal of inactivation

As shown in Fig. 3.4 the removal of inactivation of I_T is time as well as voltage dependent in adult neurones. To measure the time dependency of inactivation removal in a neurone from a young cat, I_T responses were evoked by a depolarizing voltage step to -50 mV following hyperpolarizing pre-pulses of different durations (50-2000 ms). The results from a neurone of a 13-day-old cat are shown in Fig. 3.13B. The amplitude of I_T increased with increasing duration of the hyperpolarizing prepulse and reached a maximum at about 1100 ms (n=3), a value not dissimilar to that in the adult (see chapter 3.3.2.).

Fig. 3.12. I_T and low threshold Ca^{2+} potentials in TC cells from young and adult cats. A, voltage clamp records show the maximum I_T that could could be typically obtained, in LGN neurones from a 13-day and a 90-day old cat, with a step depolarization following a 2 s hyperpolarizing pre-pulse of which only the last 50 ms are shown. It is clear that the amplitude of I_T increases with age. The increase in the "leak" conductance is likely to be related to an increase in soma size with age. B, current clamp records show the maximum amplitude of the low threshold Ca^{2+} potential in TC neurones from a 13-day and a 90-day-old cat following a 2 s hyperpolarizing electrotonic potential of which only the last 60 ms are shown. Note the difference in input resistance of the two cells, which is a reflection of the increases in "leak" conductance with age.

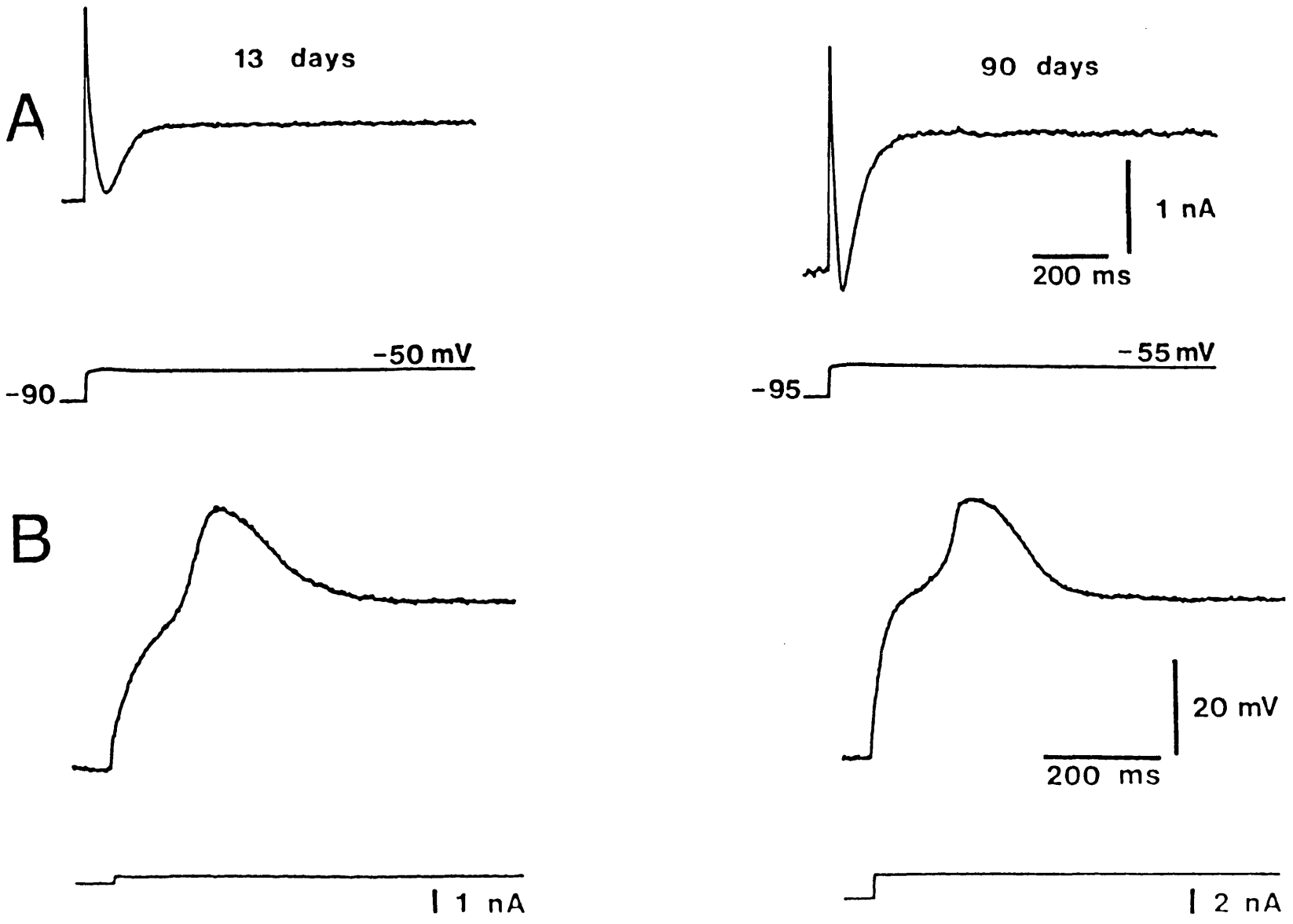
A
13 days
-50 mV
-90
90 days
1 nA
200 ms
-55 mV
-95
B
1 nA
20 mV
200 ms
2 nA

Fig. 3.13. Activation, inactivation and removal of inactivation characteristics of I_T in TC cells from a young cat. A, inactivation (squares, solid line) and activation (triangles, dashed line) curves of I_T in a TC neurone from a 5-day-old cat. The curves were fitted to the experimental points using equation (2), as described in chapter 2.4, and then normalized to the maximum current obtained. The parameters of the fitted curves are: inactivation k = 3.2 mV, V_0 = -82 mV; activation k =2.7 mV, V_0 = -55 mV. The activation curve was not corrected for changes in the driving force for Ca^{2+} at different membrane potentials. B, removal of inactivation of I_T in a TC neurone a 13-day-old cat. The plot shows the relative amplitude of a particular I_T against the duration of the hyperpolarizing pre-pulse. Each value is normalized relative to the size of the I_T obtained after a 2 s long pre-pulse and the curve was fitted to the points by eye. In this cell complete removal of inactivation was achieved after 1.2 s.

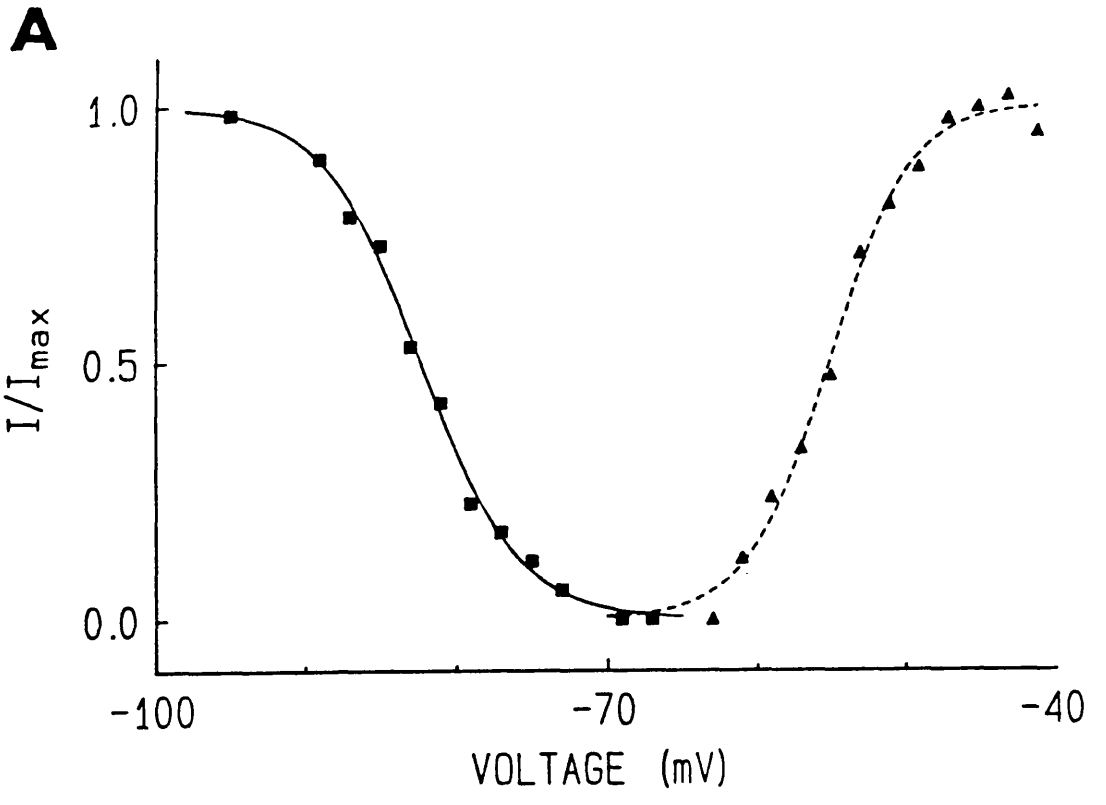
A
1.0
0.5
0.0
I/I max
-100
-70
-40
VOLTAGE (mV)

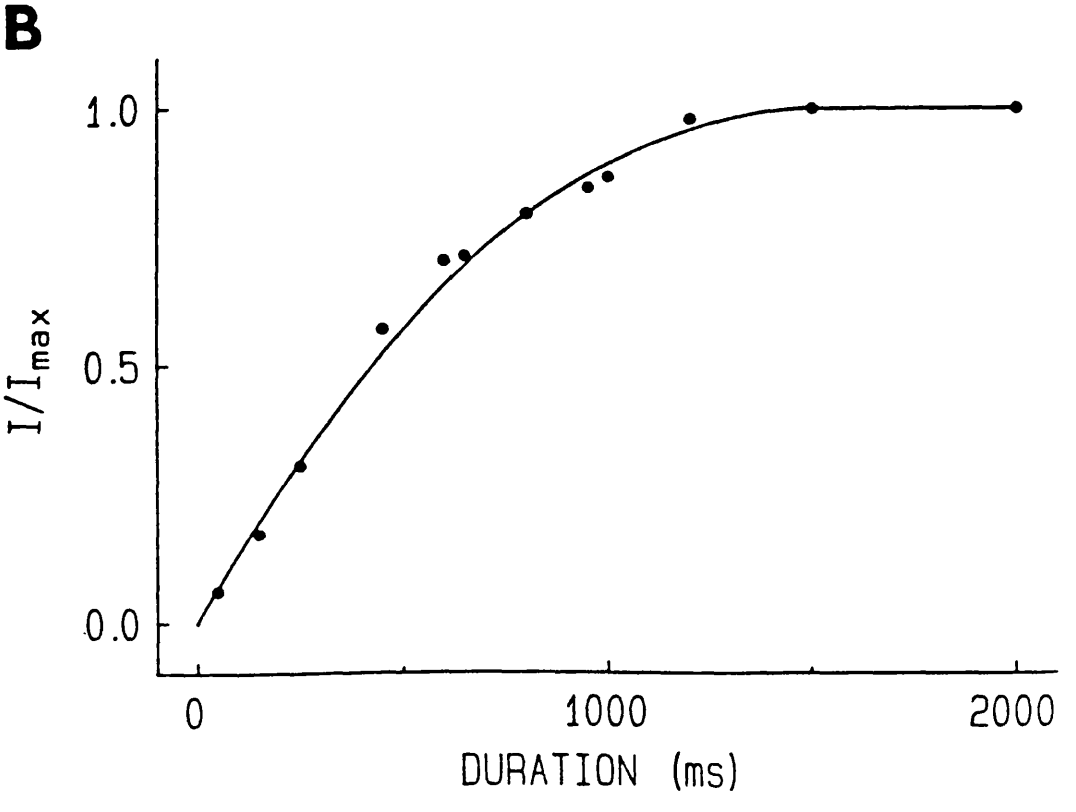
B
1.0
0.5
0.0
I/I max
0
1000
2000
DURATION (ms)

CHAPTER FOUR

THE INWARD RECTIFIER CURRENT RESPONSIBLE FOR DEPOLARIZING THE MEMBRANE POTENTIAL UPON HYPERPOLARIZATION

4.1. Isolating the inward rectifier current (I_h) and its "off" tail

The results of this part of the study are based on the recordings from 126 cat TC cells located in laminae A, A1 and C of the LGN from which stable recordings were made. Their passive membrane properties were also similar to those described in previous studies (Crunelli et al., 1987b), but their active properties were again altered by the blocking agents used in the experimental medium.

When isolating the inward rectifier current the standard medium was changed to one modified by the addition of 0.5 μM TTX, 1 mM $NiCl_2$ and the adjustment of divalent cation concentrations to 0.5 mM Ca^{2+} and 3 mM Mg^{2+}, after the brain slices had been in the recording chamber for 1 hour recovery. The Ni^{2+} and the divalent cation concentration adjustment abolished I_T, which would otherwise have obscured I_h tail current decay. When the extracellular Na^+ and Cl^- concentrations were varied equimolar amounts of choline chloride or sodium isethionate were substituted for NaCl, respectively.

The inwardly rectifying current was activated by hyperpolarizing voltage steps from holding membrane potentials in the range -50 mV to -60 mV. This resulted in a slowly developing, inwardly rectifying current superimposed on an inward "leak" current. By fitting the development of the rectifying current with a single exponential function, and extrapolating it to time zero of the voltage step, the amount of inward "leak" current could be determined. The size of I_h was calculated by subtracting the "leak" current from the total inward current caused by the hyperpolarizing step.

A "leak" subtraction procedure, similar in principle to the one illustrated

for the Ca^{2+} current (Fig. 3.1), could theoretically have been used to quantify I_h. This would have involved summing the I_h development, superimposed on an evoked inward "leak" current, with a pure outward "leak" current evoked by an equal and opposite step command. However, this was not routinely done since it increased "noise" levels and wasted valuable experimental time.

4.2. Preliminary observations

In current clamp recordings, current pulses that took the membrane potential negative to a level of approximately -60 mV produced electrotonic potentials with a slowly developing, depolarizing sag (Fig. 4.1). This sag, as shown in Fig. 4.1A, became more obvious at more hyperpolarized potentials.

In SEVC, voltage steps from a similar holding potential evoked a slow, non-inactivating, inward relaxation (I_h), superimposed on an instantaneous inward "leak" current, over the same membrane potential range as that producing sags in hyperpolarizing electrotonic potentials (Fig. 4.1B). Upon repolarization to the holding potential outward tail relaxations were evoked (4.2A), as I_h deactivated.

The instantaneous conductance measured from the current recorded upon stepping from -50 to -100 mV was 36±2 nS (n=15), while the instantaneous conductance measured upon stepping from -100 to -50 mV was 46±2 nS. The difference between these two values represents an increased conductance, indicating that the inward relaxation is indeed an activating inward current as opposed to a de-activating outward current.

Fig. 4.1. A slowly developing, non-inactivating, inward relaxation is responsible for the depolarizing "sag" of the membrane potential when TC cells are hyperpolarized. A, shows current clamp records from a cell that was depolarized by constant outward current before being hyperpolarized by a constant inward current pulse. As can be seen, a slowly developing sag in the cells electrotonic potential developed when the cell was hyperpolarized to a potential more negative than -60 mV, an effect which was larger at more negative levels. B, shows voltage clamp records from the same cell recorded following those in A. A step hyperpolarization, from a holding potential of -50 mV, to around -60 mV, evoked a small, slowly developing, non-inactivating inward relaxation, while at -80 mV a larger and faster developing relaxation was evoked.

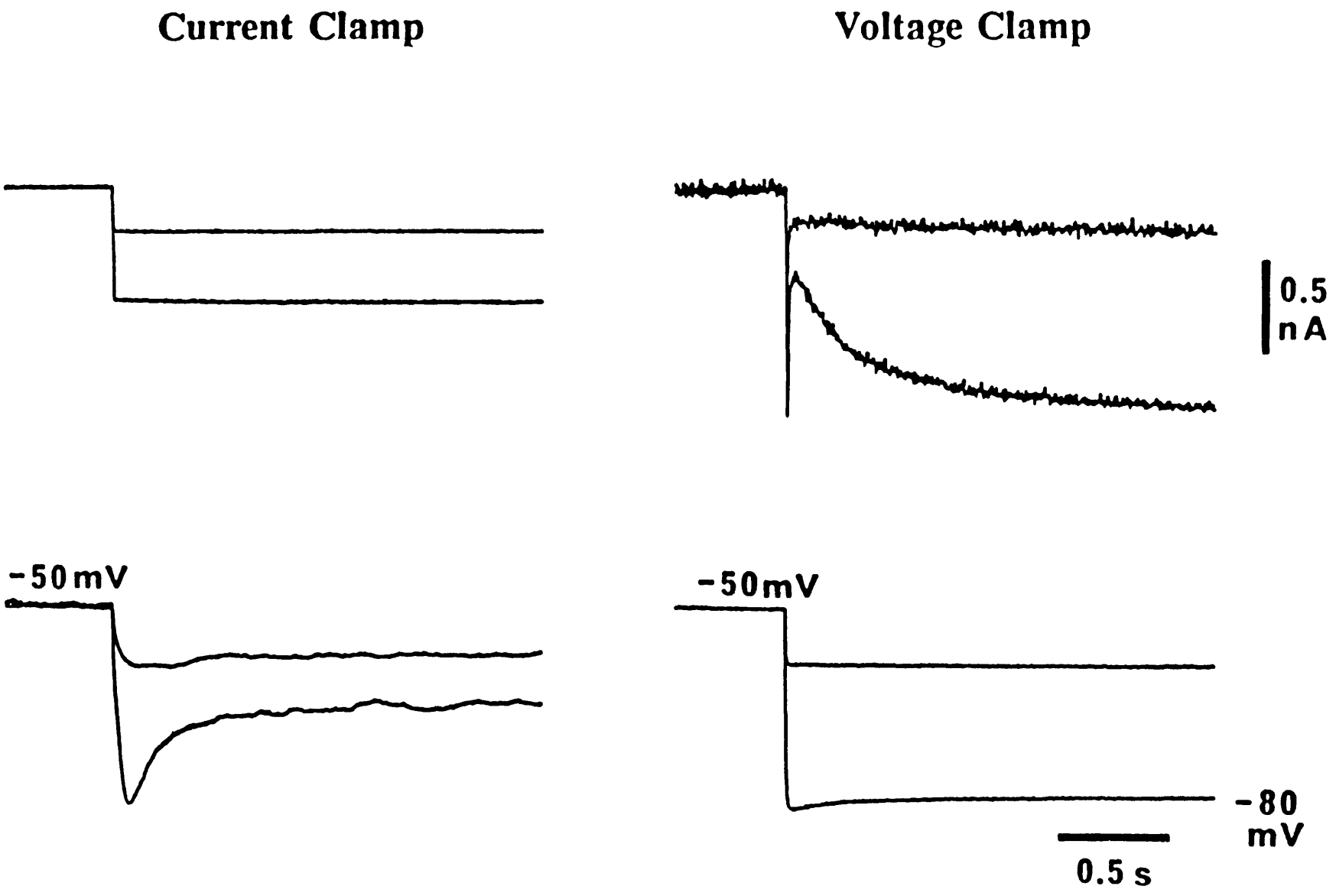
Current Clamp
Voltage Clamp
0.5
nA
-50mV
-50mV
-80
mV
0.5 s

4.3. Basic properties of I_h

4.3.1. Reversal potential of I_h

Under normal conditions the tail currents of I_h could not be studied because they were obscured by I_T. However by incorporating 1mM Ni^{2+} into the medium and adjusting the divalent cation concentration to 0.5 mM Ca^{2+} and 3 mM Mg^{2+} I_T was blocked, enabling the I_h tail currents to be studied in isolation, at least up to -45 mV. Above this level, however, other contaminating currents are activated. Consequently the reversal potential of I_h (E_h) could not be measured directly. Instead, E_h was determined by extrapolation (c.f. Mayer and Westbrook, 1983), as explained below.

The instantaneous current flowing at the start of hyperpolarizing steps from a membrane potential of -50 mV (ie. where I_h is not activated) (Fig.4.2A) was determined, and also at the start of depolarizing steps from a membrane potential of -90 mV (ie. where I_h is activated) (Fig. 4.2B). The instantaneous current-voltage plots, formed from each holding potential, were usually linear (Fig. 4.2C) and the intersection of the extrapolated lines indicated a reversal potential for I_h at -27 mV, for the cell shown in Fig. 4.2C. In 10 similar experiments the mean value of E_h was -33.0±1.2 mV (Table 1). Sometimes the instantaneous current-voltage relationship, following hyperpolarizing steps from around -50 mV, inwardly rectified below -80 mV. This may represent inward rectification of individual I_h channels, if some were open at the holding potential, or may indicate the presence of a very fast activating, pure K^+, inwardly rectifying current, in some cells.

The steady-state current (measured 6 secs after stepping to each potential in Fig. 4.2A) voltage plot (Fig. 4.2C) shows a marked inward rectification, due to I_h activation, taking effect below -60 mV. The increase in inward current, due to I_h activation and indicated by the difference between the instantaneous and steady-state current following hyperpolarizing steps from -50 mV, demonstrates that I_h, in the cell shown in Fig. 4.2C, begins to activate at potentials negative to around -55 mV.

4.3.2. Effects of varying the external Na^+, K^+ and Cl^- concentrations on E_h

The mean E_h is around 35 mV positive to the value expected for a pure K^+ conductance which suggests that other ions such as Na^+ may contribute to the charge flow responsible for G_h. As outlined in chapter 1.6.2. Cl^- ions are responsible for carrying inwardly rectifying currents in some cell types, and may, indeed, also contribute to G_h. In order to investigate a possible contribution by these ions to G_h, experiments were performed in which the effects of varying their external concentration on E_h (measured using the method described above) were determined.

When the external Na^+ concentration was reduced from 150 to 54 mM by replacement with choline, E_h (n=3) was shifted to a significantly more hyperpolarized potential ($p<0.01$, Students t-test for independent samples, table 4.1). Similarly, when the external K^+ concentration was increased from 6.3 to 18.9 mM, E_h (n=3) was moved to a significantly more depolarized potential ($p<0.05$, table 4.1). The levels to which E_h were shifted in each of

these cases indicate a 32 and 29 mV/decade shift for Na^+ and K^+, respectively.

Table 4.1. E_h in media with different Na^+ and K^+ concentrations

conc.	150 mM $[Na^+]_o$	150 mM $[Na^+]_o$	**54 mM $[Na^+]_o$**
conc.	6.3 mM $[K^+]_o$	**18.9 mM $[K^+]_o$**	6.3 mM $[K^+]_o$
E_h	-33.0 ± 1.2	-24.3 ± 3.7*	-42.1 ± 1.0***
n	(10)	(3)	(3)

* $p<0.05$ *** $p<0.01$

When the Cl^- equilibrium potential was altered either by decreasing the external Cl^- concentration from 143 to 28 mM, by replacement with isethionate ions (n=3), or measuring I_h with microelectrodes that contained 1 M KCl (n=3) a reversal potential not significantly different from the one seen in control conditions was determined (33.8±6).

It is important to note that the reversal potential of $GABA_A$ receptor mediated, Cl^--dependent IPSPs measured in TC cells, in standard artificial cerebrospinal fluid, in response to electrical stimulation of the optic fibres, using microelectrodes that contained 1 M KCl, was significantly more positive than the value (-67 mV) obtained using microelectrodes that were filled with 1 M potassium acetate (Crunelli et al., 1988).

4.3.3. Activation of I_h

The size of the instantaneous "off" tail current of I_h, measured by extrapolating its decay to time zero and subtracting this value from the resting leak current at the same level, gives an indication of G_h at each voltage level. With this in mind the activation curve of I_h was formed by measuring the amplitude of the instantaneous tail current following depolarizing steps from different hyperpolarized potentials to a common level (around -50 mV), as illustrated in Fig. 4.3A, and expressing it as a percentage of the maximum tail current that could be obtained (usually from a level of about -95 mV), as illustrated in Fig. 4.3B. Once plotted against voltage the curve formed by the instantaneous tail current amplitudes (Fig. 4.3B), was fitted with equation (2) (see chapter 2.4).

The curve shows that the activation of I_h begins below a level of -60 mV and is fully activated at around -95 mV. Similar curves were obtained from 3 additional cells with a V_o of -78.5±4.2 mV and a k of 5.8±0.8.

4.3.4. Rate of I_h development

Large hyperpolarizing voltage step commands resulted in a larger and quicker developing I_h. The development of I_h could be fitted with a single exponential curve ($r>0.98$) formed by equation (1) (see chapter 2.4), and, as shown in Fig. 4, the time constant of activation (tau) of I_h was found to be voltage dependent. In 4 cells the mean tau ranged from greater than 11 s at membrane potentials just past threshold (i.e. -60 mV) to an average of 500

ms (±115 ms) at -100 mV.

4.3.5. Time dependence of I_h de-activation

Experiments were performed to investigate how long a cell has to remain depolarized before I_h can be activated upon hyperpolarization. After I_h had been activated, at a holding potential of -90 mV, it was found that a cell had to be depolarized to a level of -50 mV for more than 1 s before, upon re-hyperpolarization, a maximum activation of I_h could again be achieved (Fig. 4.5). It is important to note that, following a depolarization of 80-350 ms (i.e. the duration of LTCPs present in the "pacemaker" oscillations of TC cells, cf. Leresche et al., 1990, 1991), I_h was partially de-activated (20-60%) and, as a result, upon re-hyperpolarization to the holding potential, the instantaneous current was outward with respect to the steady-state current at the onset of the depolarizing step (Fig. 4.5A).

Fig. 4.2. The instantaneous and steady-state current-voltage relationship of TC cells. A shows the development of I_h at a number of membrane potentials following hyperpolarizing steps from a holding level of -50 mV. B, shows the de-activation of I_h (tail currents) at a number of potentials following depolarizing steps from a holding level of -90 mV, which had been maintained for 7 s prior to the depolarization. The instantaneous currents following the hyperpolarizing steps from -50 mV (open triangles) and depolarizing steps from -90 mV (open squares) have been measured, from a different cell, and plotted against voltage in C. The intersection of the extrapolated linear instantaneous current plots gives an indication of the reversal potential of I_h (-27.4 mV in this cell). The steady-state current, measured 7 s after stepping to each level in A, forms an inwardly rectifying relationship with voltage as clearly shown in C (closed triangles).

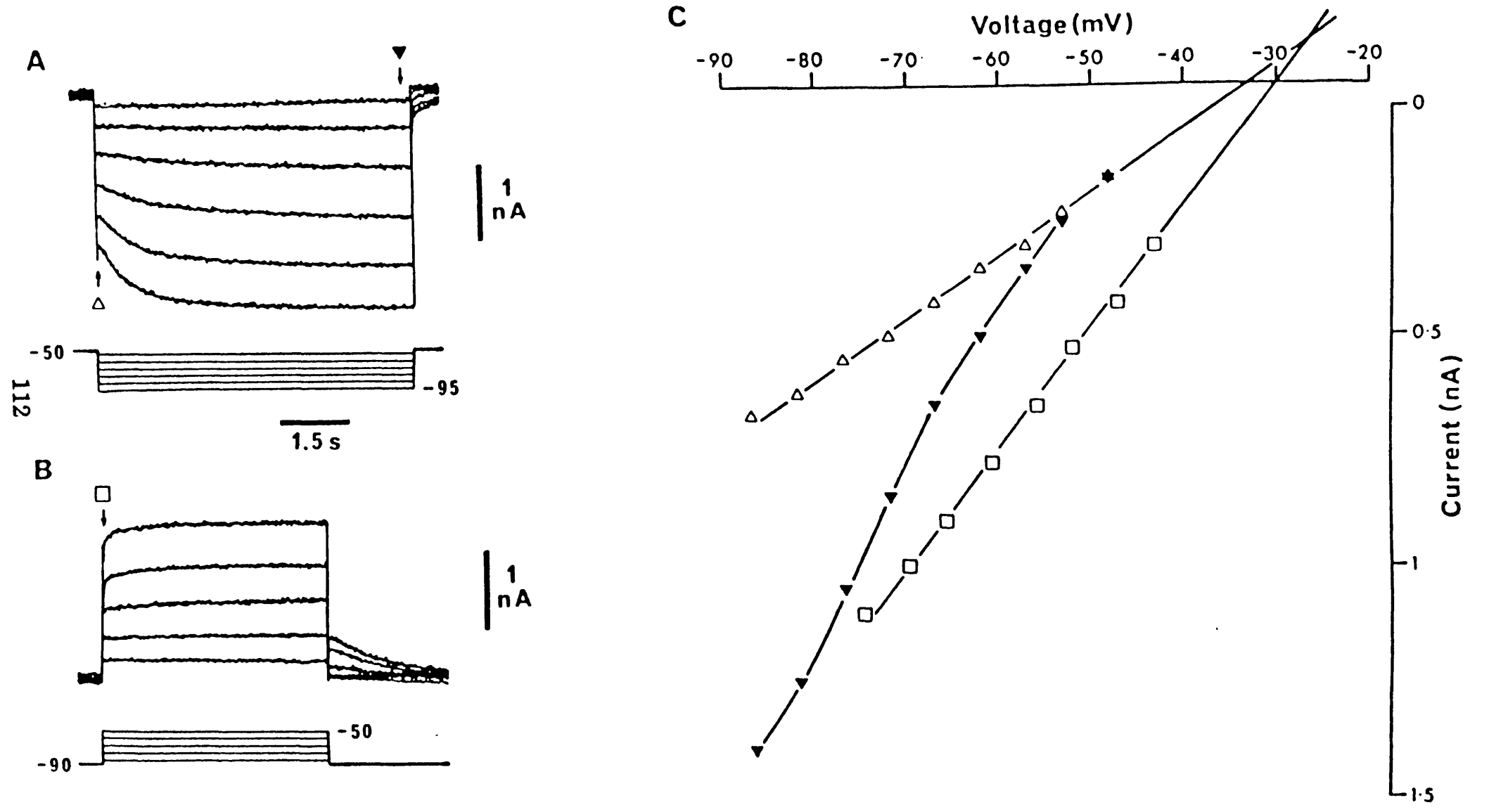
A
1
nA
-50
-95
1.5 s
112
B
1
nA
-50
-90
C
Voltage (mV)
-90
-80
-70
-60
-50
-40
-30
-20
0
0·5
1
1·5
Current (nA)

Fig. 4.3. I_h activation characteristics. A shows superimposed tail currents upon returning to a level of -50 mV following hyperpolarizing step commands (7 s) to different potentials. B shows the steady-state activation curve of I_h, determined by measuring the size of the evoked tail currents, from a different cell, and plotting them relative to the maximum tail current obtained. The curve was fitted to the points using equation (2) and gave a V_o of -76.0 mV and a k of 4.2 mV.

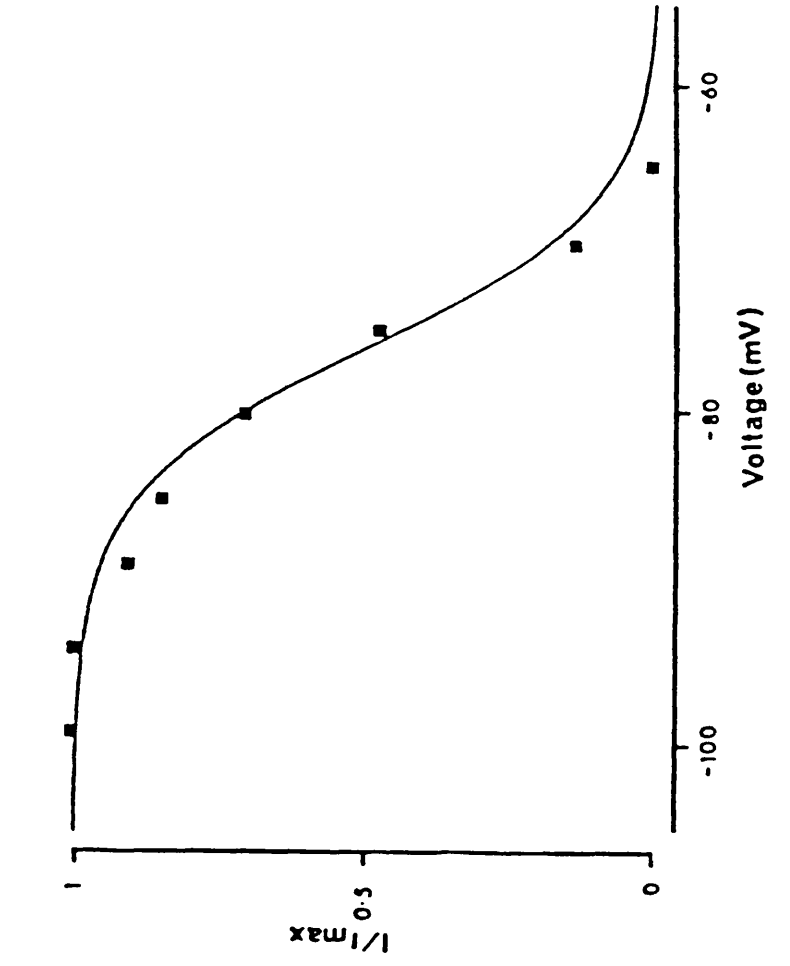
B
I/Imax
1
0.5
0
-100
-80
-60
Voltage (mV)

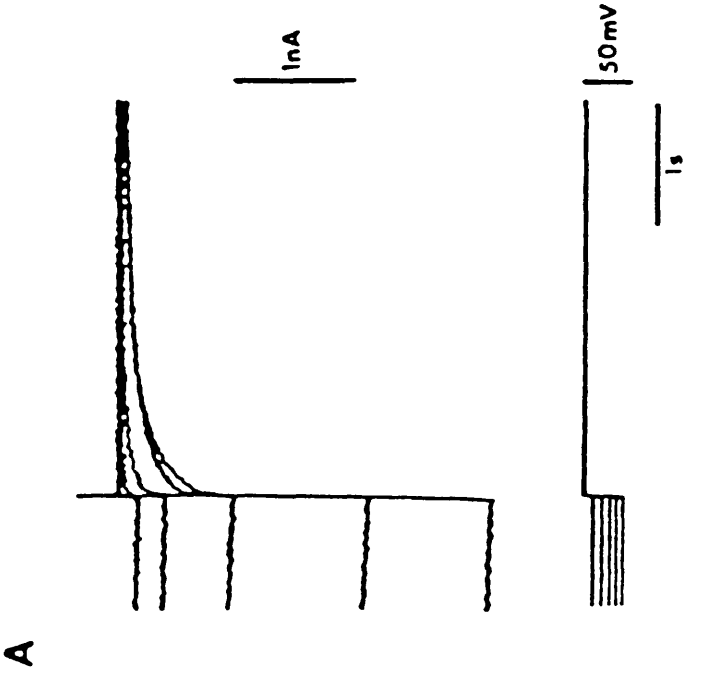
A
1nA
50mV
1s

Fig. 4.4. The effect of potential on the activation of I_h. After fitting the onset of I_h with a single exponential curve (equation 1) at five different membrane potentials the mean (n=4) time constant of its onset (tau) has been plotted against voltage, illustrating the voltage dependency of the rate of I_h onset.

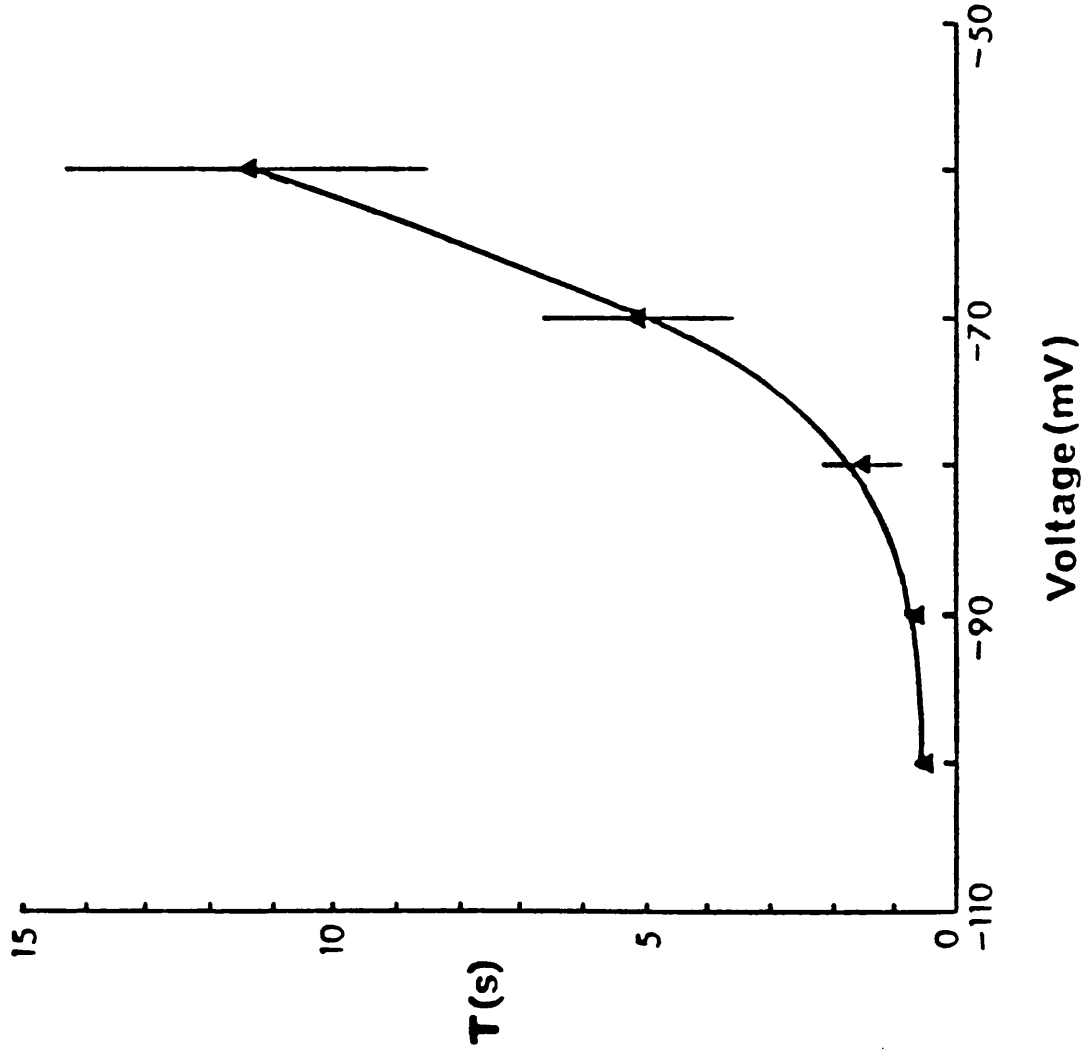
15
10
5
0
T(s)
-50
-70
-90
-110
Voltage (mV)

Fig. 4.5. The de-activation kinetics of I_h. A shows the activation of I_h, at -90 mV, following depolarizations to -55 mV of increasing duration from a holding potential of -90 mV, which had been maintained for 7 s (allowing full development of I_h). B shows a graph produced by plotting the size of I_h that develops as a fraction of the maximum that could be activated (expressed as the fraction of I_h de-activated during the depolarization) against the duration of the depolarization, for the cell shown in A. It illustrates that a depolarization lasting approximately 1300 ms was needed to totally de-activate I_h.

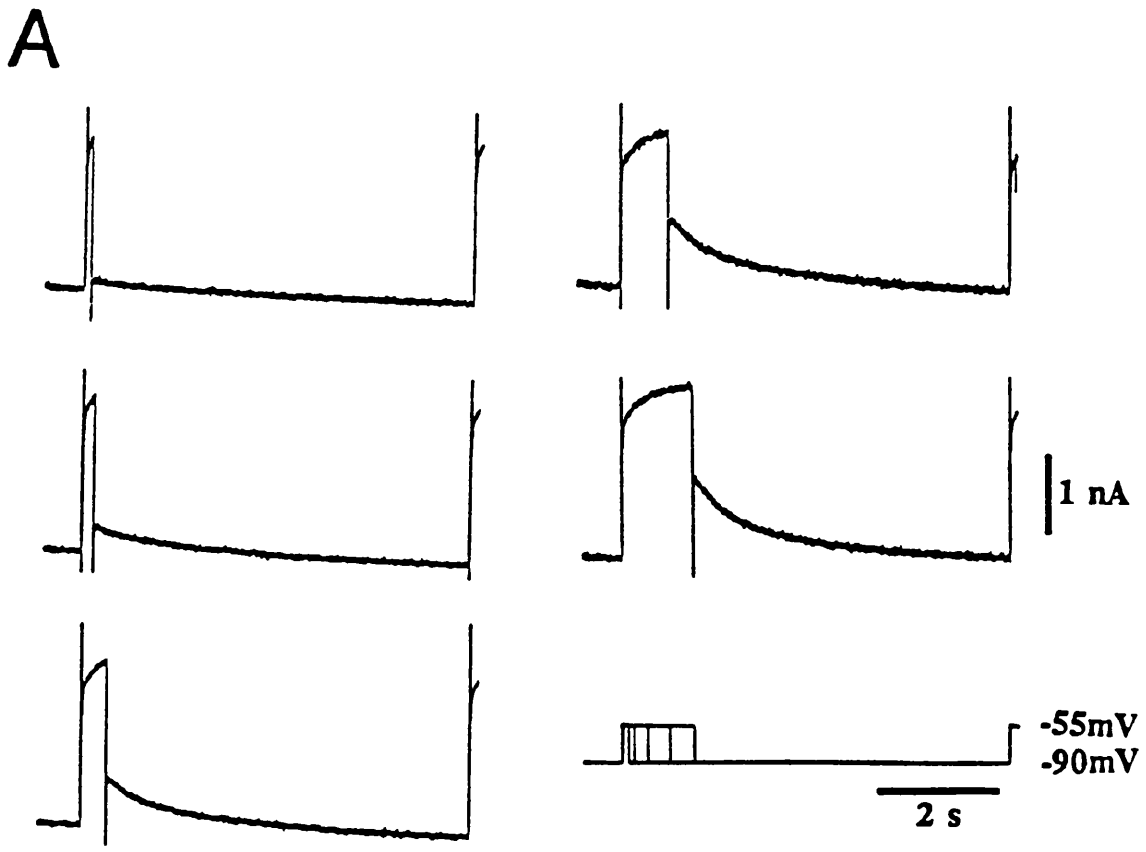
A
1 nA
-55mV
-90mV
2 s

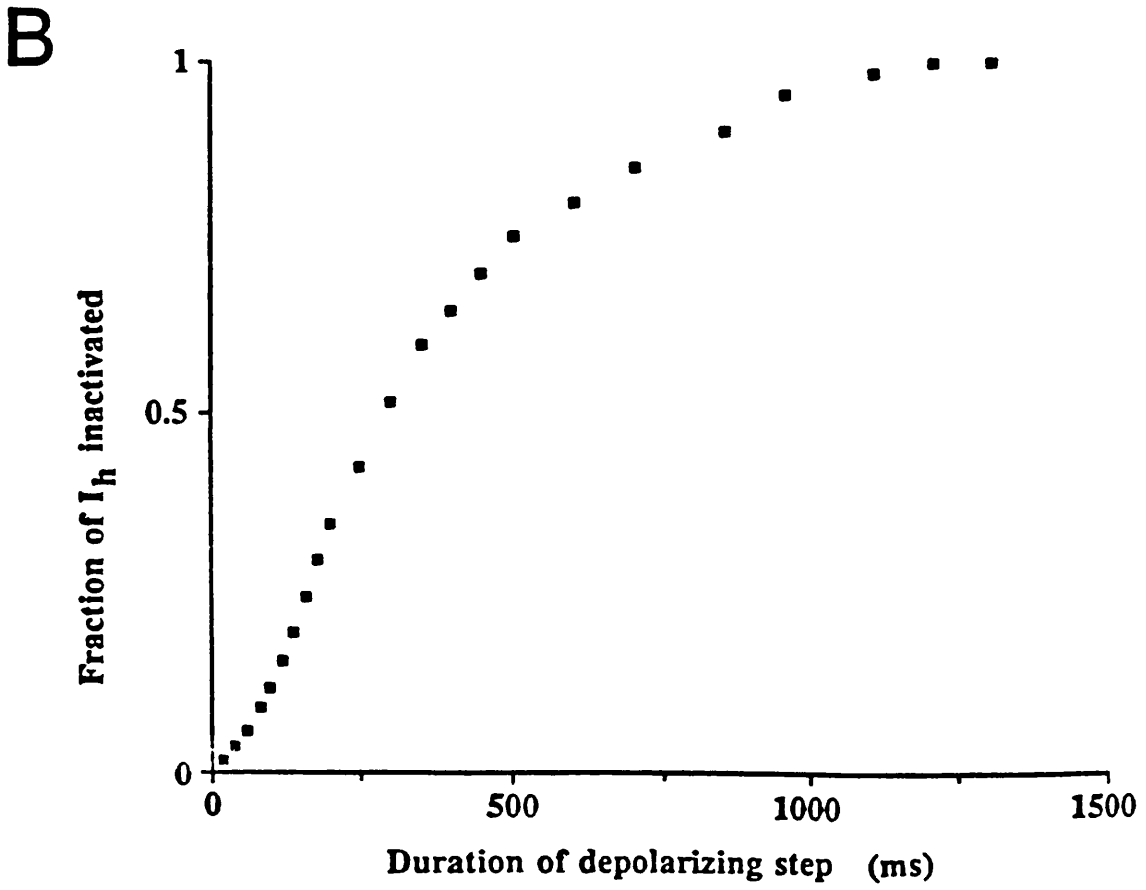
B
1
0.5
0
Fraction of I_h inactivated
0
500
1000
1500
Duration of depolarizing step (ms)

4.4. Pharmacology of I_h

As outlined in chapter 1.6, Ba^{2+} has been shown to block pure K^+ inward rectifier currents in various cell types (at concentrations lower than 1 mM) (Standen and Stanfield, 1978; Hagiwara et al., 1978), but to be ineffective at blocking mixed Na^+/K^+ inwardly rectifying currents (Yanagihara and Irisawa, 1980). Therefore it is a useful "tool" for distinguishing between these two types of current. As shown in Fig. 4.6A 4 mM barium chloride had only a small effect on I_h, and, in 3 cells reduced it by an average of 8.7±7%.

Also, 20 mM TEA had a negligable effect on I_h (Fig. 4.6B), in the 3 cells that were tested, at a time when, judging from observations made in current clamp, it did block pure outward K^+ conductances. This latter effect was demonstrated, in current clamp, by the occurrence of maintained depolarizations, presumably due to the block of a pure K^+, delayed rectifier current.

Experiments that were performed when I_h was evoked in the presence and absence of 0.5-1 μM TTX (Fig. 4.5B) demonstrated that it, also, had a negligible effect on the current (n=3), at a time when action potentials were blocked.

As previously stated, when studying I_h the artificial cerebrospinal fluid routinely contained 1 mM Ni^{2+}. In experiments that were carried out in the absence of Ni^{2+} ions there seemed to be no obvious alteration in the development of I_h (n=43). It has recently been reported that, in rabbit sino-atrial node cells, 2 mM Ni^{2+} alters the voltage dependence of activation of a

current similar to I_h (Brown et al., 1989). However, because no off tail current analysis could occur in the absence of Ni^{2+} (due to contamination by I_T) any effect that it may have on the activation and reversal potential of I_h could not be assessed.

Cs^+ has been found to block mixed Na^+/K^+ inward rectifier currents in various cell types. As shown in Fig. 4.7A 1-3 mM Cs^+ reversibly blocked I_h. This is also demonstrated in Fig. 4.7B which shows that an inwardly rectifying, steady-state current-voltage relationship of the cell is changed to a linear one by 3 mM Cs^+. At the concentrations used in this study Cs^+ ions also reduced the instantaneous current particularly at levels negative to -70 mV, which is in keeping with results from previous studies (Halliwell and Adams, 1982; Constanti and Galvan, 1983), and probably represents a voltage-dependent block of a "leak" conductance.

Fig. 4.6. I_h is not blocked by TTX or TEA. A shows the currents evoked by various hyperpolarizing step commands from a holding potential of -50 mV in control and during bath application of both 0.5 μM TTX and 0.5 μM TTX together with 20 mM TEA. They each had only very little effect on I_h.

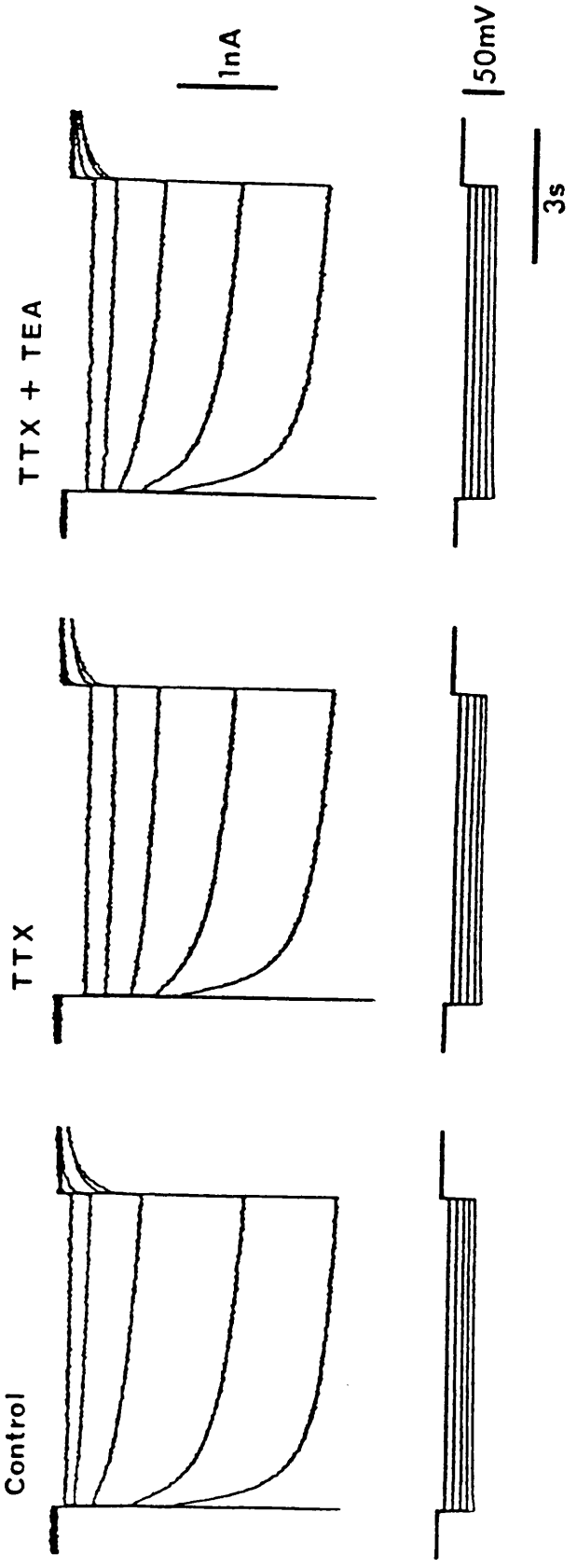
1nA
50mV
3s
TTX + TEA
TTX
Control

Fig. 4.7. The effects of Cs^+ and Ba^{2+} on I_h. A shows the development of I_h at a number of potentials following hyperpolarizing steps from a holding level of -50 mV in control medium, its bock by 4 mM Cs^+ and its recovery, following a 60 min washout. The data in A has been used to produce the graph in B. The steady-state current-voltage relationship, measured 7 s after stepping to each potential, has been plotted against voltage before (closed triangles) and after (open circles) the addition of Cs^+, clearly demonstrating the block of inward rectification, due to I_h activation. It is also interesting to note the reduction in instantaneous current by Cs^+ in (A), particularly at more hyperpolarized potentials, indicating a possible voltage-dependent block of the "leak" current. C shows the development of I_h at a number of potentials, in a different cell, following hyperpolarizing step commands from a holding level of -50 mV in control and following the addition of 4 mM Ba^{2+}. As can clearly be seen, although Ba^{2+} has blocked the leak current it has left the size of I_h unchanged.

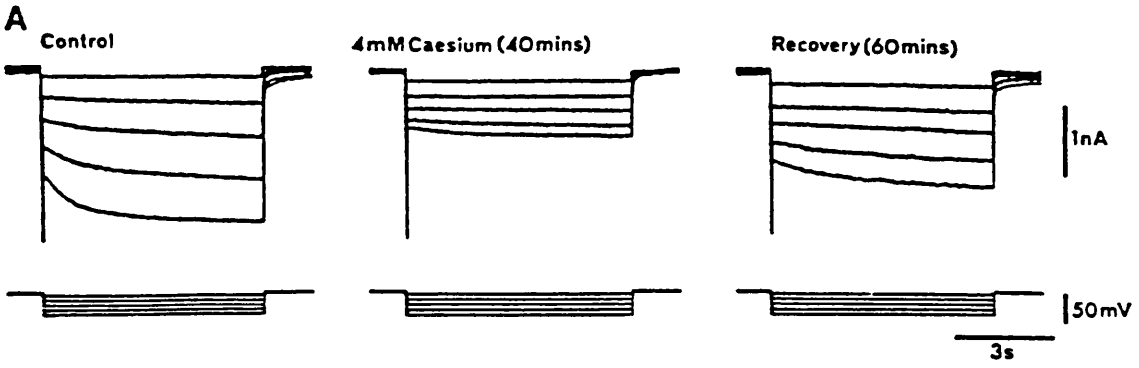
A
Control
4mM Caesium (40mins)
Recovery (60mins)
1nA
50mV
3s

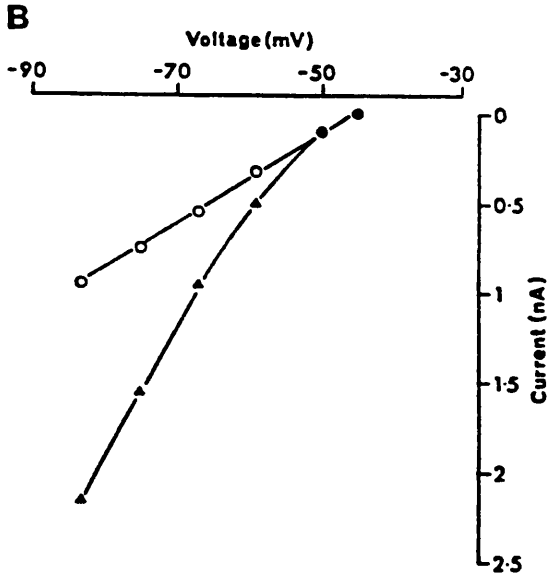
B
Voltage (mV)
-90
-70
-50
-30
0
0·5
1
1·5
2
2·5
Current (nA)

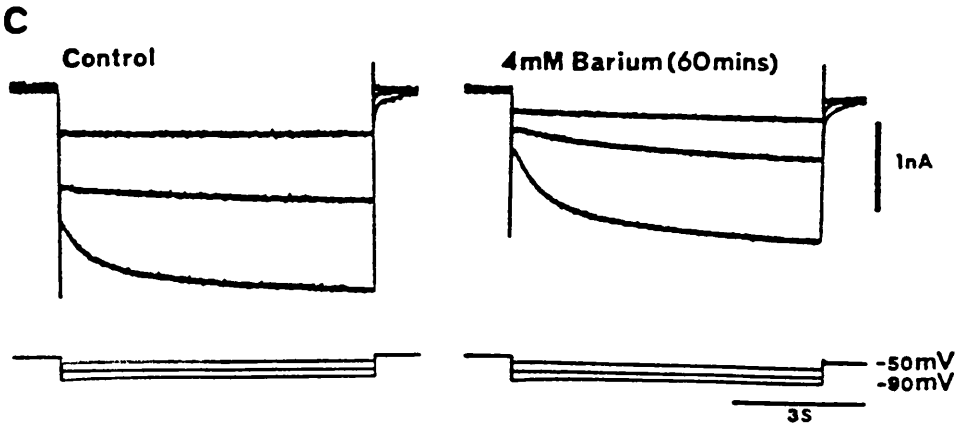
C
Control
4mM Barium (60mins)
1nA
-50mV
-90mV
3s

4.5. Contribution of I_h to oscillatory activities

4.5.1. Effect of I_h blockade on the "pacemaker" oscillations

The "pacemaker" type of oscillations appear similar to the cardiac pacemaker oscillations seen in sino-atrial and purkinje fibres. As outlined in chapter 1.6.3., in some of these cardiac muscle cells a current similar to I_h (I_f) seems to play a role in depolarizing the cells membrane potential when it reaches its diastolic level (Hauswirth, Noble and Tsien, 1968; Brown, DiFrancesco and Noble 1979a, b). In order to investigate a possible contribution of I_h to the oscillatory process, 3 mM CsCl was added to a freely oscillating cell maintained in the medium described in chapter 3.5.2.. Cs^+ produced a 3-8 mV hyperpolarization and, for the cell shown in Fig. 4.8, its effect on the oscillations was to initially slow their rate from 1.5 to 0.75 Hz before totally abolishing them, with recovery. This is a result similar to that found in other cells, although in some cases the oscillations were not totally abolished. The voltage clamp records shown in Fig. 4.8B show that CsCl did, indeed, block I_h, with recovery, in the same cell. Since external Cs^+ blocks only inward K^+ currents (Hagiwara et al., 1976; Gay and Stanfield, 1977; Adelman and French, 1978; Storm, 1989) its inhibition of the oscillations can be considered to be due to a specific block of I_h.

4.5.2. Effect of I_h enhancement (through β-adrenoreceptor activation) on the "pacemaker" oscillations

It has recently been shown that noradrenaline (NA) increases the amplitude of I_h in TC cells by activating β-adrenoreceptors (McCormick and Pape, 1989). Consequently, it has been suggested that the increased I_h should depolarize the membrane potential and thus block oscillatory activities of TC cells that involve LTCPs. This hypothesis was therefore tested directly by looking at the action of NA (1-50 μM), in the presence of 5 μM yohimbine and 10 μM prazosin, two α-adrenoreceptor antagonists (n=7) (Fig. 4.9) or isoprenaline (a selective β-adrenoreceptor agonist)(n=3) (Fig. 4.10) on the "pacemaker" oscillations. As shown in Fig. 4.9, the first effect of NA was to transform the "pacemaker" into a type of spontaneous membrane potential activity that is similar to the "pacemaker" oscillations, but which occurs rhythmically in discrete periods and, as stated in chapter 1.4.3, is termed "spindle-like" (Leresche et al., 1990, 1991). These "spindle-like" oscillations persisted for a variable period of time (5-15 mins, depending on the flow rate of the perfusion medium). Later, in the continuous presence of NA, the "spindle-like" oscillations were blocked and no other spontaneous activity could be evoked at the control or at any other depolarized or hyperpolarized level of membrane potential (achieved by steady dc current injection). However, as shown in Fig. 4.10, even in the presence of a continuous β-adrenoreceptor stimulation, the cell had not completely lost the ability to evoke some repetitive LTCPs during the initial portion of large hyperpolarizing electrotonic potentials.

The selective β-adrenoreceptor stimulations described above were accompanied by a 2-6 mV depolarization and a progressive increase in the amplitude of I_h (Figs. 4.9 and 4.10) and were reversible.

4.5.3. Effect of I_h blockade on non-oscillating cells

Not all cells oscillate under the appropriate conditions in vitro. Since we have shown that NA, by enhancing I_h, inhibits the "pacemaker" type of oscillations, it may be the case that those cells not displaying spontaneous activity possess an I_h which is already "enhanced". In order to investigate this possibility, 3 mM CsCl was added to cells that did not display any spontaneous rhythmic potential oscillations, and a typical example of the results obtained in 4 cells is shown in Fig. 4.11. The effect of the CsCl was to initially cause the cells to oscillate, not continuously, however, but in discrete periods, giving rise to the "spindle-like" oscillations. These lasted for about 3-11 mins, before being transformed into the "pacemaker" oscillations. Finally in the continuous presence of Cs^+ and after a variable period of time (4-8 mins), the "pacemaker" oscillations were completely abolished. These effects of Cs^+ were accompanied by a progressive decrease and block of I_h and were reversible.

4.5.4. Activation of I_h during spontaneous membrane potential oscillations

Since I_h blockade has been shown to inhibit the pacemaker oscillations experiments have been carried out to assess I_h activation at the most hyperpolarized potential reached during a "pacemaker" oscillation cycle. As shown in Fig. 4.12, a TC cell was allowed to oscillate in current clamp and, when its membrane potential reached the most negative level of an oscillation cycle (-75 mV), the preamplifier was switched into voltage clamp (arrow in Fig. 4.12A). For comparison, the amplitude and time course of I_h development was also measured by holding the same cell at -55 mV (where all I_h channels are inactivated) and stepping to the same, most hyperpolarized potential reached during the pacemaker oscillations (i.e. -75 mV) (Fig. 4.12B). As shown in the current trace of Fig. 4.12A, from the oscillating cell an inward relaxation was observed whose time course differed from that of I_h (bottom trace in Fig. 4.12B), since it was faster and decayed partially. In addition, the subtraction of I_h from this inward relaxation showed a current that peaked at about 1 sec and then slowly, and partially, decayed reaching a steady level after 7 sec (Fig. 4.12C) (n=4). This difference in time course cannot be due to I_T inactivation, since at the most hyperpolarized level of a pacemaker oscillation cycle, I_T should be almost fully decayed (as shown in chapter 3.3.3. the time constant of I_T decay is 25-100 msec in the range -55 to -70 mV at 25°C).

Fig. 4.8. The effects of Cs^+ on the "pacemaker" oscillations. A, intracellular voltage traces show the reversible blockade, by 3 mM Cs^+ of the "pacemaker" oscillations in a TC cell of the cat LGN recorded in the presence of 1 μM TTX. The voltage clamp records in B show the concomitant reversible blockade by Cs^+ of I_h in the same cell and were taken immediately after the traces shown in A. The transient inward current evoked at the end of the hyperpolarizing voltage step is I_T that was however poorly clamped because of the unfavourable divalent cation concentration ratio.

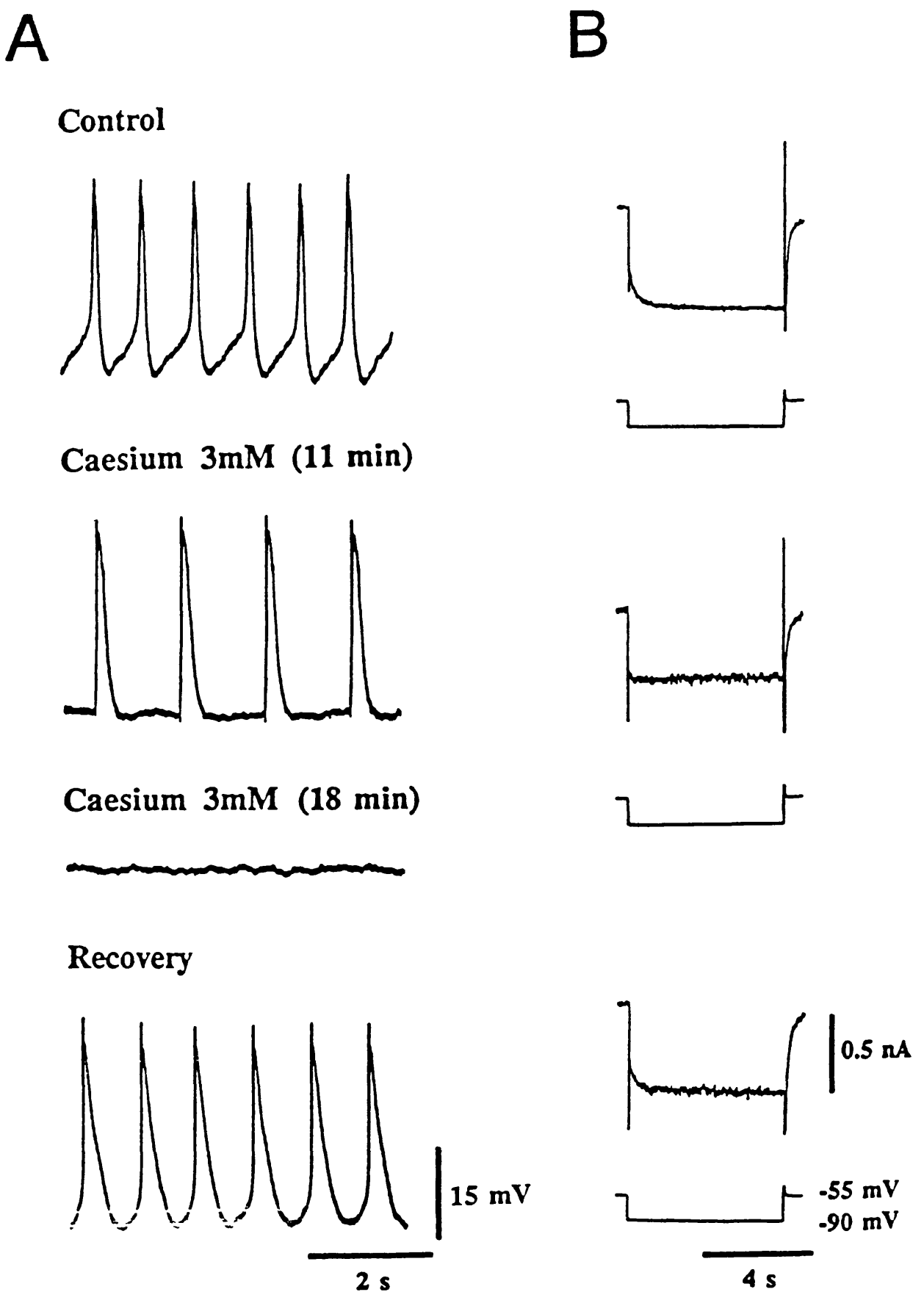
A
B
Control
Caesium 3mM (11 min)
Caesium 3mM (18 min)
Recovery
15 mV
2 s
0.5 nA
-55 mV
-90 mV
4 s

Fig. 4.9. Effect of β-adrenoreceptor stimulation, by noradrenaline, on the "pacemaker" oscillations. A, intracellular voltage records show the effect of 50 μM NA in the presence of the α-adrenoreceptor antagonists yohimbine (5 μM) and prazosin (10 μM) on an LGN TC cell displaying "pacemaker" oscillations. 5 mins after the introduction of NA the "pacemaker" oscillations were transformed into "spindle-like" oscillations that persisted for about 6 mins. After 13 mins all spontaneous activity ceased. The trace shown in Wash was obtained 20 mins after removing NA from the perfusion medium. B, voltage clamp records show the concomitant progressive increase in the amplitude of I_h following selective activation of β-adrenoreceptors by noradrenaline and were recorded 10-30 s after the corresponding current clamp trace in A. The transient inward current present at the end of the hyperpolarizing step in B represents I_T.

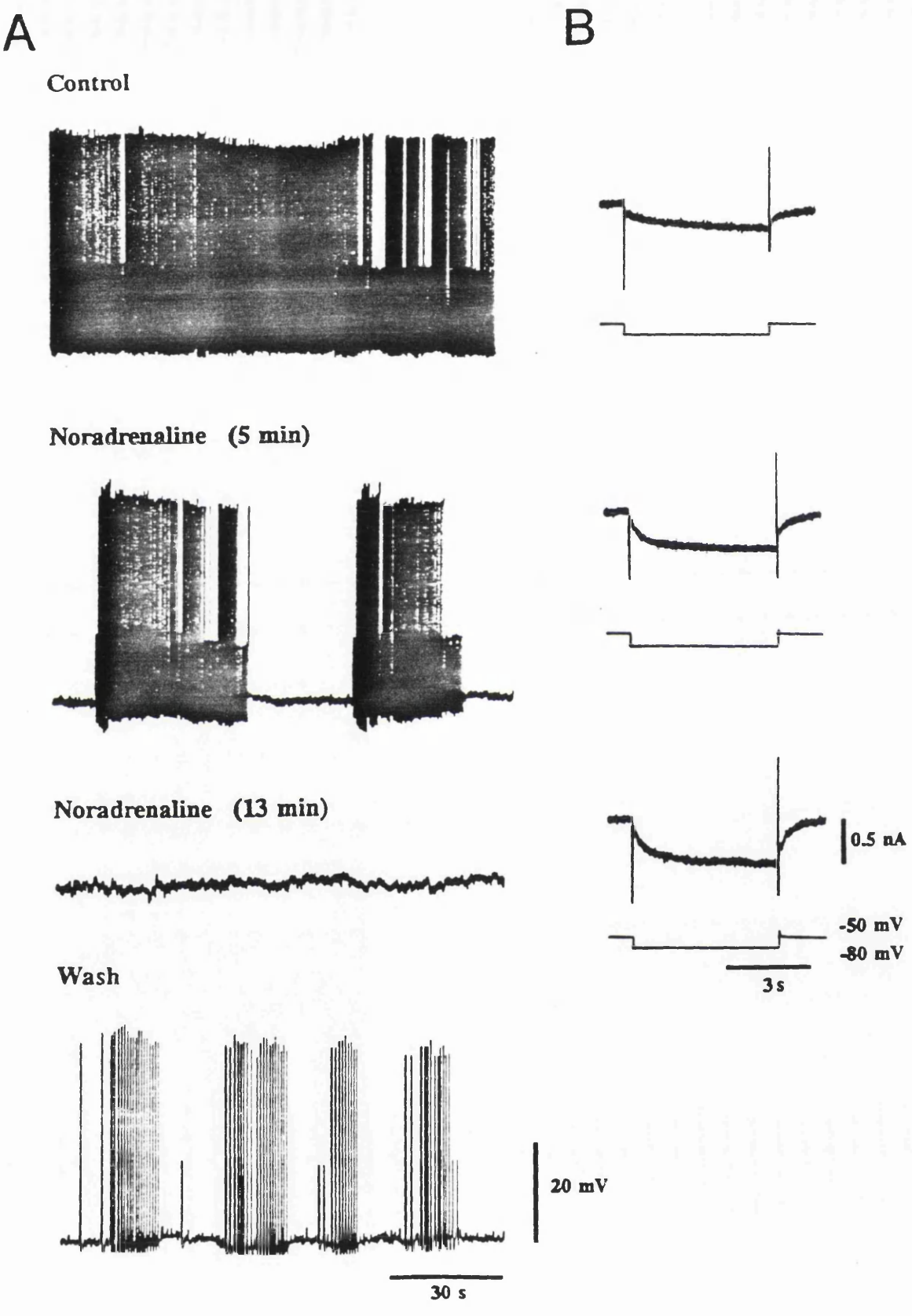
A
B
Control
Noradrenaline (5 min)
Noradrenaline (13 min)
Wash
0.5 nA
-50 mV
-80 mV
3 s
20 mV
30 s

Fig. 4.10. Effect of isoprenaline on the "pacemaker" oscillations. A, intracellular records show the effect of 20 μM isoprenaline on a TC cell displaying "pacemaker" oscillations. 8 mins after the introduction of isoprenaline the "pacemaker" oscillations were blocked, although, as the bottom record shows, the cell was still capable of displaying some LTCPs when hyperpolarized from -55 to -70 mV. B shows voltage clamp records from the same cell demonstrating the concomitant increase in the amplitude of I_h following selective activation of β-adrenoreceptors by isoprenaline and were recorded 10-30 s after the corresponding current clamp record in A.

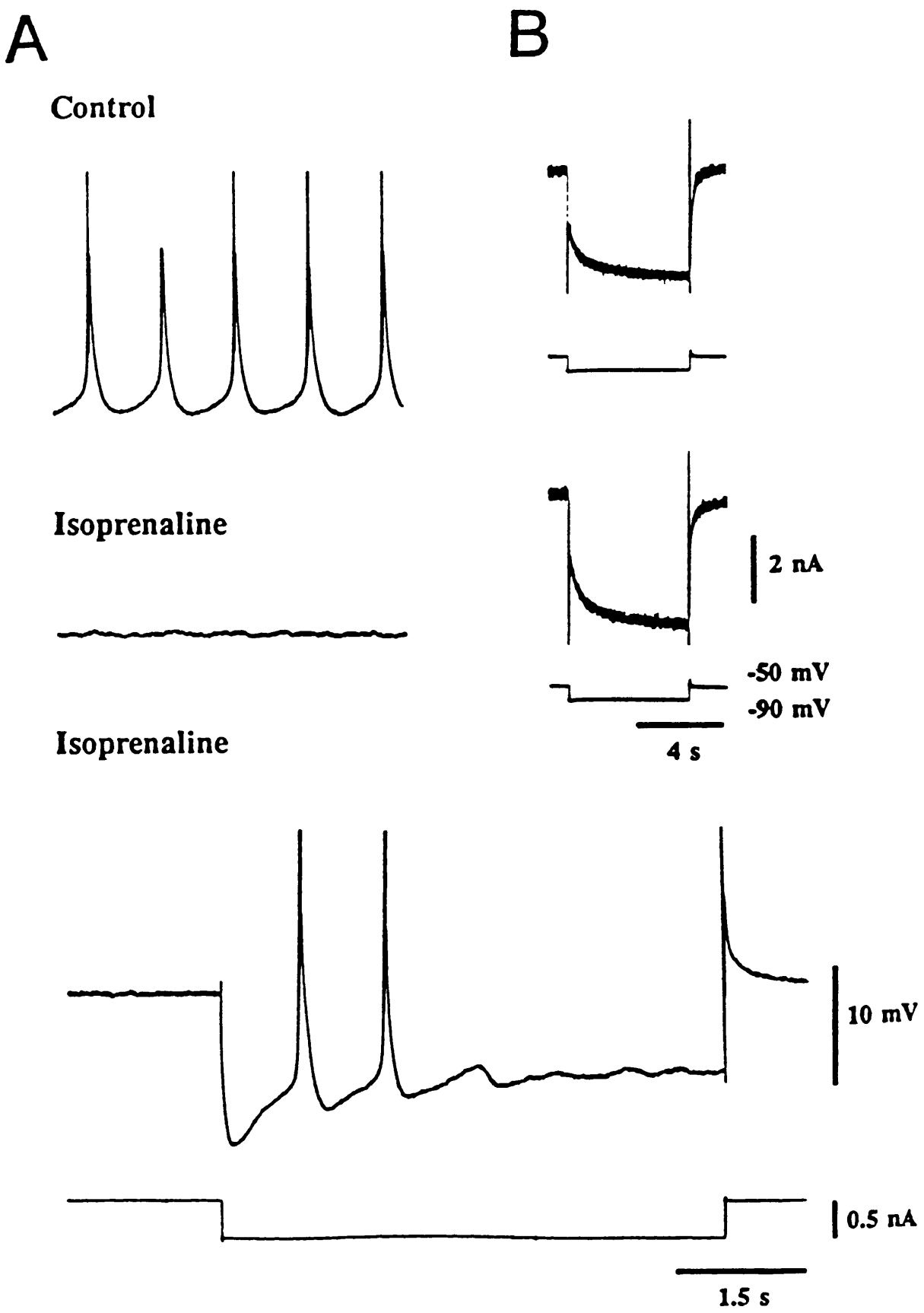
A
B
Control
Isoprenaline
Isoprenaline
2 nA
-50 mV
-90 mV
4 s
10 mV
0.5 nA
1.5 s

Fig. 4.11. The effects of Cs^+ on a cell not showing spontaneous "pacemaker" oscillations. A, intracellular voltage records show the effect of 2 mM Cs^+ on a non-oscillating cell. 4 mins after the introduction of Cs^+ the cell started to show "spindle-like" oscillations. After an additional 4 mins the "spindle-like" oscillations were transformed into the "pacemaker" oscillations (1.2 Hz) that persisted for about 6 mins before all activity ceased.

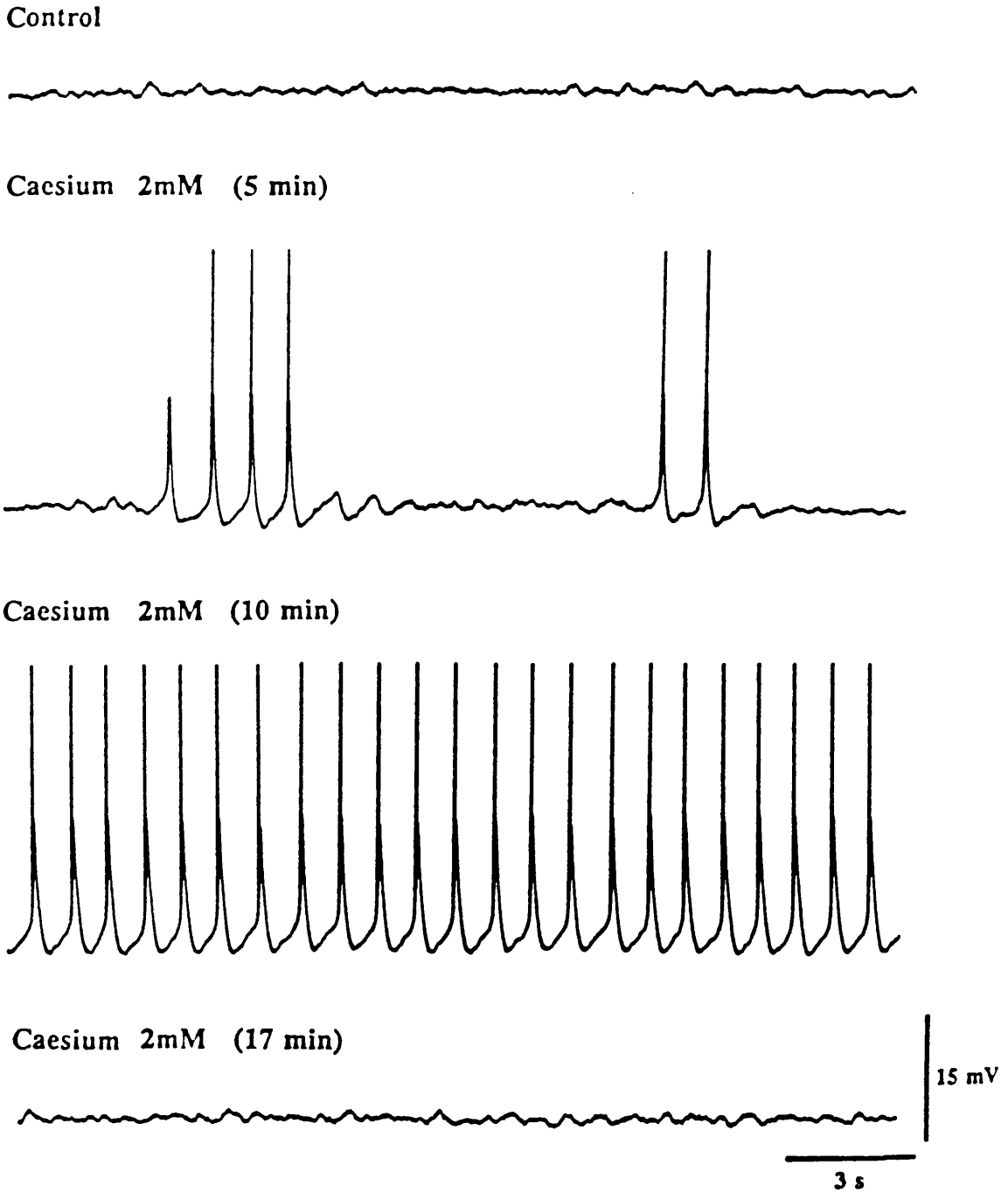
Control
Caesium 2mM (5 min)
Caesium 2mM (10 min)
Caesium 2mM (17 min)
15 mV
3 s

Fig. 4.12. Time course of current development at the peak of the hyperpolarization of the "pacemaker" oscillations. A, at the most hyperpolarized potential (-75 mV) of the fifth cycle of the "pacemaker" oscillations (top trace) the preamplifier was switched from current into voltage clamp to measure the total current developing (bottom trace). B, the bottom trace shows the size of I_h, generated in the same cell, by a voltage step (top trace) from a holding potential of -55 mV (where all I_h channels are inactivated) to -75 mV, the most hyperpolarized potential reached during the "pacemaker" oscillations. C, shows the digital subtraction of the current trace in B from the current trace in A.

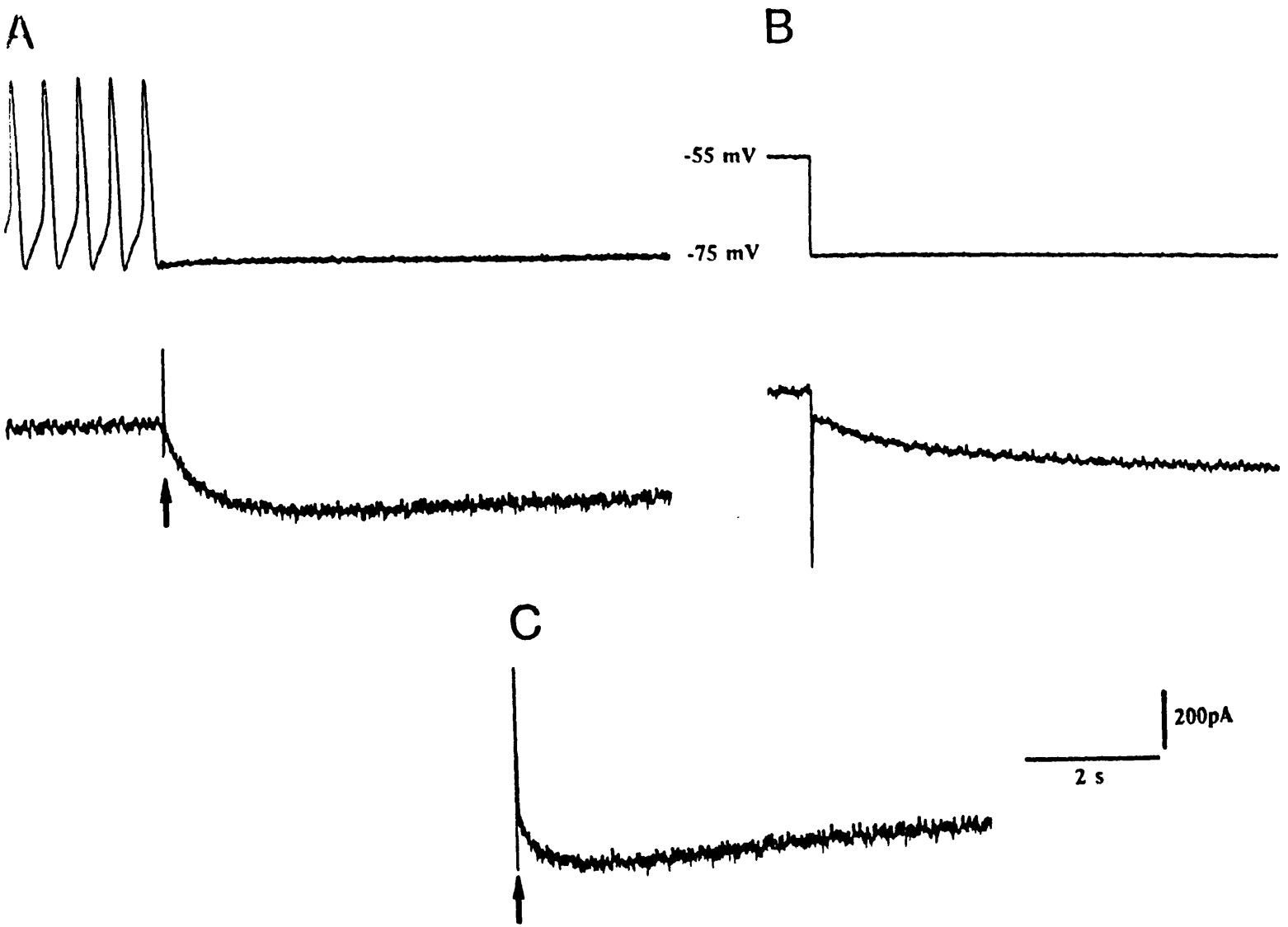
A
B
-55 mV
-75 mV
C
200pA
2 s

CHAPTER FIVE

DISCUSSION

5.1. Origin of I_T and I_h

All cells had the ability to generate I_T and/or I_h, depending on the contents of the experimental medium being used. Since previous studies have shown that morphologically and physiologically identified interneurones in the LGN and other thalamic nuclei of the cat do not generate LTCPs and lack a prominent "sag" in their hyperpolarizing electrotonic potentials (Deschenes et al., 1984; McCormick and Pape, 1988), this clearly identifies the recorded neurones as TC cells.

Although the precise cellular location of I_h is unknown, two lines of evidence suggest that I_T is of somatic and/or proximal dendritic origin. Firstly in cat thalamic cells in vivo, Deschenes et al. (1984) found that low-threshold Ca^{2+} potentials could be evoked by the initial segment component of antidromically activated action potentials, even in the absence of the soma-dendritic component. Secondly, a low-threshold Ca^{2+} current has been described in freshly isolated thalamic cells that lack a significant dendritic arborization (Kay and Wong, 1986; Coulter et al., 1989; Hernandez-Cruz and Pape, 1989; Suzuki and Rogawski, 1989).

5.2. The Ca^{2+} current underlying the LTCP

There are several lines of evidence indicating that I_T is responsible for generating LTCPs :-

a) both the LTCP and I_T are carried by Ca^{2+} ions;

b) Both the LTCP and I_T are transient phenomena whose amplitude

decays follow similar time courses;

c) Both the LTCP and I_T deinactivate at hyperpolarized potentials and are activated upon depolarization to the same voltage region.

5.2.1. Properties of I_T

Evidence that I_T is a T-type Ca^{2+} current is provided by its inhibition when external Mg^{2+} ions are substituted for Ca^{2+} ions, and its similarity in voltage dependence, relative sensitivity to Ni^{2+} and Cd^{2+} and dihydropyridine insensitivity to the transient T-type current described by Fox et al. (1987a) in cultered sensory ganglion cells.

The electrical properties of I_T, found in this study, are very similar to those found in more recent studies by other groups (Coulter et al., 1989; Hernandez-Cruz and Pape, 1989; Suzuki and Rogawski, 1989), and can be summarized as follows:-

a) the activation threshold of I_T lies at -65 to -70 mV;

b) I_T decay follows a single exponential time course with a time constant which is voltage sensitive and ranges from 20 to 100 ms;

c) I_T inactivation occurs positive to -65 mV but this is removed at more hyperpolarized potentials in a time and voltage dependent manner.

Assuming that high voltage activated Ca^{2+} currents, possibly similar to those of the L- or N-type (Fox et al., 1987a), exist in LGN cells (Coulter et al., 1989; Hernandez-Cruz and Pape, 1989) it is unlikely that they make any contribution to I_T. Their activation thresholds are relatively depolarized (-20

to -10 mV) and their comparitively slow inactivation rates would have resulted in a current which had more than one time constant of decay (Fox et al., 1987a).

The properties of I_T closely resemble some of the features characterizing low-threshold Ca^{2+} currents in a variety of cells (e.g. Carbone and Lux, 1984a, b; Armstrong and Matteson, 1985; Bean, 1985; Fedulova et al., 1985; Bossu et al., 1985; Docherty and Brown, 1986; Narahasi et al., 1987), particularly the T-type Ca^{2+} current of cultered sensory ganglion cells described by Fox et al. (1987a).

However, while the inactivation curve for I_T at 25°C is similar to that for the T-current of sensory ganglion cells (V_0 = -78 mV, k = 5 mV) (Fox et al. 1987a), the activation curve for I_T is steeper and lies around 10 mV more hyperpolarized than that for the T-current (V_0 = -51 mV, k = 6.5) (Fox et al. 1987a). The difference in V_0 of the activation curves may reflect the difference in the external Ca^{2+} concentration between this study (1-1.5 mM) and that of Fox et al. (1987a) (10 mM), since there is evidence that higher levels of external Ca^{2+} shift the voltage dependence of Ca^{2+} current activation to more depolarized potentials (Fedulova et al., 1985). However, it is likely that I_T activation curves in TC cells show a real difference in the steepness of activation compared with those in other cell types (maintained in culture), since a very steep activation curve is necessary to produce the rapid depolarizing phase of LTCPs.

The extreme voltage dependence of I_T activation will mean that once threshold is achieved, activation can be regarded as regenerative. Small depolarizations beyond the threshold activate a small percentage of the total

available channels, which leads to further depolarization and activation of more channels at a faster rate. This process then continues to produce the LTCP. However, very slow depolarizations (<30 mV/s) will not activate I_T, even if they do cross the threshold, since by the time threshold voltage has been reached, all inactivation removal has been reversed and no current is available for activation.

Since the activation process is essentially automatic the precise size of LTCPs will be controlled by the extent of the removal of I_T inactivation. This is voltage and time dependent, imposing an upper limit on the frequency with which they can occur and also controlling whether or not the depolarization is powerful enough to result in a burst of action potentials.

5.2.2. Pharmacology of I_T

Although the absolute sensitivity of I_T to Cd^{2+} and Ni^{2+} is less than that of the T-current of Fox et al. (1987a, b) (5 mM Ni^{2+} was required to abolish their low-voltage-activated Ca^{2+} current), the relative potency of the two ions and the ineffectiveness of nifedipine support the classification of I_T as a T-type current on pharmacological grounds.

As outlined in chapter 1.5.3., of the various compounds reported to block potently and selectively the low voltage-activated, transient (T-type) calcium current, amiloride and 1-octanol have appeared promising (Tsien et al, 1988; Kostyuk, 1989). As a result, they have been used as pharmacological "tools" to help identify T-type calcium currents (Thompson and Wong, 1989; Scott et al., 1990).

However, as shown in chapter 3.4., amiloride, even at concentrations as high as 1 mM, reduces I_T by only 30%. This is supported by results from Suzuki and Rogowski (1989), who found that amiloride (0.25-5 mM) failed to block I_T in dissociated guinea pig LGN cells. In mouse neuroblastoma cells and in embryonic limb motoneurones amiloride inhibits T-type calcium currents by 80 to 100% at concentrations of 500 µM and 1 mM, respectively (Tang et al., 1988; McCobb et al., 1989) suggesting that the potency of amiloride against this current depends on the cell type. However, at concentrations lower than those required to block the T-type calcium current in the latter cell types, amiloride has been shown to have additional effects: in mouse neuroblastoma cells, for instance, 200 µM amiloride abolishes Na^+/H^+ exchange (Moolenaar et al., 1981), a result similar to the one found in rat brain synaptosomes (Jean et al., 1985). These properties of amiloride, together with its lack of selectivity between the T- and N-type calcium current in hippocampal cells (Takahashi et al., 1989), cast strong doubts on its use as a pharmacological agent to investigate voltage activated calcium currents and their contribution to different physiological and pathological processes both in vitro and in vivo (Kamiya, 1989; Seabrook and Adams, 1989; Sinton et al., 1989).

Another finding of the present study is that 1-octanol fully and dose-dependently blocks I_T in TC cells with an IC_{50} of 430 µM. This concentration is higher than the one previously reported for a similar block of I_T (50 µM, cf. Fig 2 of Llinas et al., 1989), a discrepancy that might be due to the use of different conditions/protocols (the maximum amplitude of I_T, for instance, is ten times smaller and is activated at more depolarized

potentials following removal of inactivation at -75 mV in Llinas et al, 1989). Indeed, other differences in the pharmacological sensitivity of I_T also exist between studies using different experimental conditions/preparations: 50 μM Ni^{2+}, for instance, abolishes I_T in acutely dissociated TC cells (Hernandez-Cruz and Pape, 1989) while, as shown in chapter 3.4., the same effect requires a concentration of 500 μM Ni^{2+} in slices perfused with a medium containing a lower Ca^{2+}/Mg^{2+} ratio.

In other cell types, such as rat dorsal root ganglion cells (Scott et al., 1990) and inferior olivary cells (Llinas, 1988; Llinas et al., 1989), 1-octanol is undoubtedly more potent against T-type calcium currents (1 μM and 20-50 μM required for a full block, respectively) than in TC cells, supporting the suggestion that not all low-voltage activated, T-type Ca^{2+} currents are pharmacologically alike (Llinas et al., 1989; Takahashi et al., 1989). Indeed, while in dorsal root ganglion cells and inferior olivary cells 1-octanol is selective for the T-type calcium current (Llinas and Yarom, 1986; Llinas et al., 1989; Scott et al., 1990), in hippocampal pyramidal cells it also inhibits the N- and L-type currents (Takahashi et al., 1989).

Another effect of 1-octanol observed in this study is the marked increase in the "leak" current, and hence the decrease in cell input resistance, that occurred at the concentrations even lower than those required to inhibit I_T. Whatever the precise mechanism of this effect, this finding makes 1-octanol far from ideal as an agent to investigate the contribution of the thalamic I_T to physiological and pathological processes.

More recent studies have also indicated that the potency as well as the selectivity with which amiloride and 1-octanol block T-type calcium currents

vary greatly in different cell types (Akaike et al., 1989; Takahashi et al., 1989).

5.2.3. Contribution of I_T to oscillatory activities

The LTCPs generated by I_T closely resemble the large depolarizations seen when the cells display "pacemaker" and "spindle-like" oscillations in vitro. Also the voltage region where these oscillations are observed (Leresche et al., 1990) coincide with the voltage activation and inactivation properties of I_T, suggesting that it plays a role in these activities. Although the voltage steps used when studying the basic properties of I_T don't match those seen during "physiological" activities, the experiments using "ramp" depolarizations (see chapter 3.5.1.) indicate that it can be activated by the depolarizations that occur during spontaneous membrane potential oscillations.

The involvement of I_T is also supported by the Ni^{2+} inhibition of "pacemaker" oscillations, at a concentration shown to block I_T.

5.2.4. Postnatal development of I_T

The results in chapter 3.6. show that the amplitude of I_T increases during postnatal development and is approximately two and a half times larger in the adult than in a 13-day-old kitten. However, the voltage dependence of activation and inactivation, the latency to peak and the time dependence of inactivation removal are similar in the newborn and the adult.

Since the total current (I) follows the relationship I = Nip (where N is

the number of channels, p the probability of opening and i the single channel current), the increase in I_T with age is due to an increase in either the the number of channels, the single channel current and\or the probability of channel opening. Anatomical studies have shown up a two-fold increase in the cross-sectional soma area of cat LGN neurons from seven to ninety days of age (Elgeti et al., 1976; Garey et al., 1973; Hickey, 1980; Kalil, 1978; Mason, 1983).Thus, the simplest explanation might be that this increase in soma size, without a change in channel density, is sufficient to produce the observed increase in the amplitude of I_T, a suggestion supported by the lack of any other major change observed in the properties of I_T during postnatal development. However it is only an investigation at the single channel level that will completely clarify this problem.

As mentioned in chapter 1.5.4. I_T decreases or even disappears during embryogenesis or the first weeks of postnatal life in a variety of neurones and in skeletal muscle. As shown in chapter 1.5. in TC cells the situation is markedly different, since I_T maintains most of its characteristic properties and increases in its maximum amplitude. This increase in amplitude of I_T with age, however, does not correspond to an increase in the amplitude of low threshold Ca^{2+} potentials.

Thus, in a neuronal cell type where I_T is present and plays an important role in adulthood, its properties are remarkably similar to those in the newborn. Since, as shown in chapter 3.5. I_T is one of the dominant membrane currents involved in membrane potential oscillations, it is possible that this current is required by all developing neuronal cell types in order to produce oscillatory activities that appear to play a key role during neuronal

development (Walton and Llinas, 1986; Llinas, 1988). Later, at maturity, some neurones (i.e. in the thalamus, inferior olive etc.), which still require these oscillatory behaviours, will retain I_T with unaltered properties, while in others (i.e. hippocampus, dorsal root ganglia, etc.) I_T is gradually lost because its developmental oscillatory-producing role is no longer required.

5.3. The inward rectifier current

5.3.1. Properties of I_h

As well as possessing a T-type Ca^{2+} current cat TC cells possess, as shown in chapter 4, a slowly developing, non-inactivating, mixed Na^+/K^+ inward rectifier current.

It has been shown that mixed Na^+/K^+ inward rectifier currents are altered in size when the external Na^+ or K^+ ion concentration is changed (Mayer and Westbrook, 1983; Pape and McCormick, 1989), but this isn't direct evidence that both ion species contribute to the current. For example, an increase in the external Na^+ concentration increases the single channel conductance of the inward rectifier in tunicate egg cell membranes (Fukushima, 1982), although it is a pure K^+ conductance. The results in chapter 4.3.2. show that the reversal potential of G_h follows changes in the external Na^+ and K^+ concentrations, which clearly demonstrates that this current is indeed carried by these two ion species.

I_h is activated when cat TC cells are hyperpolarized negative to -60 mV, and its properties resemble those of mixed Na^+/K^+, inward rectifier currents

found in other excitable cells, variously named I_h (Mayer and Westbrook, 1983; Crepel and Penit-Soria, 1986; Lacey and North, 1988), I_f (Brown et al., 1979; Brown and DiFrancesco, 1980), I_Q (Halliwell and Adams, 1982), I_{AR} (Spain et al., 1987) and i (Benham et al., 1987).

Properties of this current that seem to vary between cell types include :-

(a) its reversal potential which probably represents a difference in the ratio of contribution to the conductance by Na^+ and K^+ between the cell types. The similar mV/decade values for Na^+ and K^+ obtained in this study indicate that in TC cells these two ions contribute approximately equally to g_h.

(b) its time course of activation which is much slower and more voltage dependent in TC neurones than in hippocampal pyramidal cells (Halliwell and Adams, 1982), cerebral cortical pyramidal cells (Spain et al., 1987) and cerebellar Purkinje cells (Crepel and Penit-Soria, 1986). These characteristics make I_h similar to inward rectifier conductances found in sensory sympathetic ganglia (Mayer and Westbrook, 1983) and heart cells (DiFrancesco, 1985).

5.3.2. Pharmacology of I_h

The pharmacology of I_h was also similar to that of other mixed Na^+/K^+ currents. Indeed, it was insensitive to TTX, TEA and, unlike pure K^+ inward rectifier currents (Standen and Stanfield, 1978; Hagiwara et al, 1978), to Ba^{2+}, and it was blocked by Cs^+. It was also confirmed that selective activation of β-adrenoreceptors (by NA in the presence of α antagonists, or by isoprenaline) increases the amplitude of I_h in TC cells (Pape and McCormick, 1989).

5.3.3. Contribution of I_h to the resting membrane potential

In TC cells I_h begins to activate negative to -60 mV and is fully activated at a level of around -95 mV, a range similar to the one found in other neurones (Spain et al., 1987; Lacey and North, 1988). Thus, I_h is partially activated at the resting membrane potentials of TC cells in vitro (-65 mV, Steriade and Llinas, 1988; Llinas, 1988) and presumably plays a role in maintaining the resting membrane potential, a function that has already been suggested for similar currents in other cell types (Edman et al., 1987; Spain et al., 1987). Indeed, this is in agreement with the findings that TC cells hyperpolarize when I_h is blocked by Cs^+, and depolarize when I_h is enhanced by β-adrenoceptor stimulation (see chapter 4.5.).

Since, as stated in chapter 1.4.3., the value of membrane potential critically determines the excitability and pattern of action potentials of TC neurones, I_h may contribute to establishing either burst activity, associated

with the burst-firing mode, or the generation of single spikes, associated with the relay mode.

5.3.4. Contribution of I_h to "pacemaker" oscillations

An involvement of I_h in the in vitro "pacemaker" and the "spindle-like" oscillations is indicated by the fact that membrane potentials reached during these oscillations are within the activation range of I_h. In addition, as shown in chapter 4.5., both Cs^+ and β-adrenoreceptor stimulation abolish "pacemaker" oscillations, although Cs^+ is also capable of inducing pacemaker oscillations in otherwise silent cells. All these experiments, but in particular the blockade by Cs^+, indicate a contribution of I_h to the mechanism responsible for the "pacemaker" and the "spindle-like" oscillations. A tentative mechanism for, and the contribution of I_h to, "pacemaker" oscillations might, therefore, be as follows. Starting from the most hyperpolarized level of an oscillation cycle, I_h activation will depolarize the cell until the voltage threshold of activation of I_T is reached. Since the hyperpolarization had provided the requirements in terms of time and voltage to de-inactivate I_T, a LTCP is generated. The transient nature of I_T alone, or with the contribution of other currents, will then terminate the depolarization and hyperpolarize the cell. Since the depolarization associated with a LTCP will partly de-activate I_h, at the end of a LTCP there will be less I_h activated (i.e. less inward current) than at its beginning (see chapter 4.5.1.) and, as a consequence, the membrane potential will hyperpolarize to a potential more negative than the threshold voltage at which I_T had been evoked. The cell

will thus reach the peak of the hyperpolarization, and, since the preceding depolarization has provided the time and voltage requirements necessary for partial de-activation of the I_h channels, I_h could be re-activated and the cycle restarts again. It is important to note that, because of its slow time constant of activation (2 sec at -75 mV), I_h does not have time to fully activate during the hyperpolarizing phase (150-500 msec) of the "pacemaker" oscillations. Likewise, since depolarizations of about 1 sec are required for its full de-activation, I_h is not fully de-activated during the depolarizaing phase (80-350 msec) of the "pacemaker" oscillations, and a certain amount of I_h, therefore, is continuously activated during "pacemaker" oscillations.

In those TC cells that did not show oscillations before Cs^+ application, I_h might have been too large (or too large with respect to other voltage activated currents) for the cells to oscillate, possibly by decreasing the cell input resistance over the voltage region where oscillations would otherwise have occurred. By reducing I_h with Cs^+, non-oscillating cells were then able to show the "pacemaker" oscillations, until, in the continuous presence of Cs^+, I_h was reduced to such an extent that the oscillations were again blocked. Support for this interpretation comes from the finding that in cells where I_h was increased by activation of β-adrenoreceptors the "pacemaker" oscillations were blocked. Thus, the "pacemaker" oscillations are blocked by an I_h that is either too large or too small.

5.3.4. Contribution of I_h to "spindle-like" oscillations

The finding that the "spindle-like" oscillations were observed before the "pacemaker" oscillations when progressively decreasing I_h with Cs^+ and following the "pacemaker" oscillations when progressively increasing I_h with β-adrenoreceptor stimulation suggests that the "spindle-like" oscillations are due to the interplay of I_T with, in this case, an I_h that is relatively larger than the one required for the "pacemaker" oscillations. This may be because during each oscillation cycle, the relatively larger I_h will not have sufficient time to de-activate as much as is required to reach the equilibrium achieved during the "pacemaker" oscillations. Thus, following a certain number of oscillations, the amount of I_h evoked by the repetitive oscillations will progressively and steadily increase, with the consequence of slowly depolarizing the cell and not providing a hyperpolarization sufficient for the subsequent de-inactivation of I_T. This, and the concomitant decrease in input resistance associated with the increased I_h, will reduce the ability of the cell to oscillate. Then, between each oscillation cycle, a portion of I_h slowly inactivates, the membrane potential slowly hyperpolarizes and the input resistance of the cell increases, so that a new oscillation cycle can begin. This interpretation of the "spindle-like" oscillations simply regards them as a peculiar stage of the "pacemaker" oscillations where, however, a new equilibrium is achieved between I_T and I_h.

Apart from their action on I_h, Cs^+ and selective activation of β-adrenoreceptors might be having other effects on TC cells, some of which cannot be completely ruled out at present. However, this is unlikely for

extracellular Cs^+ since it is probably selective for inward rectifier currents (at the concentrations used in this study), and, unlike intracellular Cs^+, has no effect on outward K^+ currents (Hagiwara et al., 1976; Gay and Stanfield, 1977; Adleman and French, 1978; Storm, 1989). As far as NA is concerned, no study has investigated the effect of this monoamine on I_T in TC cells and evidence from other neurones points to an action of NA on the high threshold Ca^{2+} current(s) (i.e. N- and L- types) (Gray and Johnston, 1987). An effect of β-adrenoreceptor stimulation by NA observed in other neurones is the reduction of Ca^{2+} activated K^+ conductance(s) (Madison and Nicoll, 1986), a current that might contribute to the hyperpolarizing phase of an oscillation cycle. Although no analysis of the type(s) and properties of Ca^{2+} activated K^+ currents in TC cells has been carried out, current clamp experiments have shown the presence of a Ca^{2+} and K^+ sensitive after-hyperpolarization following mainly Na^+ action potentials and high threshold but not low threshold Ca^{2+} potentials (Jahnsen and Llinas, 1984a, b). In addition, the slow after-hyperpolarization present in TC cells of some thalamic nuclei is reduced by NA (McCormick and Prince, 1988) but no pharmacological analysis of this effect has been carried out.

The different time courses of the inward relaxation developing from the most hyperpolarized potential of an oscillation cycle and of the development of I_h (see chapter 4.5.2.) indicate that the "pacemaker" oscillations cannot be accounted for only by the two inward currents, I_h and I_T, acting independently. Indeed, in the absence of I_h, I_T decay is complete after 200 msec (see chapter 3.3.3.), and, in the absence of I_T, I_h does not de-activate.

Thus, either these two currents are affecting each other in such a way as to modify markedly their time course and voltage ranges of activation/inactivation or there are other current(s) involved in the pacemaker oscillations. In this respect, obvious possible membrane currents include, for instance, high threshold Ca^{2+} current(s), Ca^{2+} activated K^+ current(s), I_A, delayed rectifier and non-inactivating Na^+ current whose voltage ranges of activation/inactivation (Llinas, 1988) are reached during the low frequency oscillations (Leresche et al., 1990).

5.4. I_T and I_h contributions to in vivo oscillations

The question arises as to the relevence of in vitro spontaneous membrane potential oscillations, and thus the relevance of I_T and I_h involvement, in the TC cell activity associated with the burst-firing mode.

It is possible that the "pacemaker" oscillations represent the basic pattern of electrical activity of in vivo TC cells when the membrane potential is negative to -65 mV and synaptic inputs are diminished. Neurotransmitters, via transmitter-gated conductances and transmitter-modulated voltage-dependent conductances may then modify the rhythm and frequency of the "pacemaker" oscillations to generate the full repertoire of low frequency oscillations observed in vivo, such as during stages of synchronized sleep (Llinas, 1988; Steriade and Llinas, 1988; McCormick, 1989; Crunelli and Leresche, 1991), when the membrane potential of TC cells (Hirsch et al., 1983) is within the voltage region where, for instance, I_T and I_h can be activated. Indeed, the finding that "pacemaker" oscillations can be changed to

a "spindle-like" activity by modulating I_h suggest that this might be an important transmitter-modulated voltage-dependent conductance involved in the generation and modulation of the low frequency oscillatory activities observed in TC cells in vivo during normal (Steriade and Llinas, 1988) and pathological conditions (Gloor and Fariello, 1988; Buzsaki et al., 1990). In addition, when considering oscillatory rhythm and frequency changes, it should be noted that the rhythmic activity of one cell type may lead to activities of different frequencies in other cell types with different membrane properties, through a resonance-like process (Llinas, 1988).

During REM sleep and during the relay-mode of wakefullness, instead, extra-thalamic synaptic inputs will depolarize the cells towards membrane potentials where the voltage activated conductances responsible for the "pacemaker" oscillations (and other types of low frequency oscillatory activities involving I_T and I_h) can no longer be operational (Hirsch et al., 1983; Steriade and Llinas, 1988; McCormick, 1989; Crunelli and Leresche, 1991). Indeed, the NA mediated increase of I_h and subsquent blockade of "pacemaker" oscillations represents one such possible mechanism by which brain stem activation could lead to an inhibition of the burst-firing mode. As outlined in chapter 1.2.2. the brain stem projects to the thalamus, and it has been suggested that its serotonergic, cholinergic and noradrenergic connections are involved in switching the thalamus from a relay to a burst-firing mode (Singer, 1977; Sillito et al., 1983; Hobson and Steriade, 1986). The mechanism of the NA mediated blockade of "pacemaker" oscillations thus provides an interesting way by which this might be achieved. By increasing I_h, not only is a cell depolarized to a level less favourable for the

generation of oscillations, but also, even at more hyperpolarized potentials the increase in I_h is responsible for a dampening of its spontaneous activity.

When considering pathological conditions, the 3 Hz spike-wave discharge present in the EEG during petit mal epileptic seizures is a possible in vivo comparison with the "pacemaker" or "spindle-like" oscillations. As outlined in chapter 1.3.2.2., experiments in a well-studied animal model of petit mal epilepsy suggest the TC neurones play a critical role in its generation (Gloor and Fariello, 1988), a conclusion supported by EEG recordings from human thalamus in patients with petit mal epilepsy (Williams, 1953). Recently, the involvement of I_T in the generation of this condition has been indicated by the finding that specific petit mal anticonvulsants reduce this current in thalamic neurones, at therapeutic concentrations (Coulter et al., 1989).

REFERENCES

REFERENCES

ADELMAN, W.J. and FRENCH, R.J. (1978). Blocking of the squid axon potassium channel by external caesium ions. J. Physiol. **276**, 13-25.

ADRIAN, E.D. (1941). Afferent discharges to the cerebral cortex from periferal sense organs. J. Physiol. **100**, 159-191.

ADRIAN, R.H. (1969). Rectifiction in muscle membrane. Prog. Biophys. Mol. Biol. **19**, 340-369.

ADRIAN, R.H., CHANDLER, W.K. and HODGKIN, A.L. (1970). Slow changes in potassium permeability in skeletal muscle. J. Physiol. **208**, 645-668.

ADRIAN, R.H. and FREYGANG, W.H. (1962). The potassium and chloride conductance of frog muscle membrane. J. Physiol. **163**, 115-137.

AKAIKE, N., KANAIDE, H., KUGA, T., NAKAMURA, M., SADOSHIMA, J-I. and TOMOIKE, H. (1989). Low-voltage-activated calcium current in rat aorta smooth muscle cells in primary culture. J. Physiol. **416**, 141-160.

ALMERS, W. (1972). The decline of potassium permeability during extreme hyperpolarization in frog skeletal muscle. J. Physiol. **225**, 57-83.

ANDERSEN, P. and ANDERSSON, S.A. (1968). Physiological basis of the alpha rhythm, Appleton-Century-Crofts, N.Y..

ANDERSEN, P., ECCLES, J.C. and SEARS, T.A. (1964). The ventrobasal complex of the thalamus: types of cells, their responses and their functional organisation. J. Physiol. **174**, 370-399.

ANDERSEN, P. and SEARS, T.A. (1964). The role of inhibition in the phasing of spontaneous thalamocortical discharge. J. Physiol. **173**, 459-480.

ANDERSSON, T.A., HOLMGREN, E. and MANSON, J.R. (1971). Localised thalamic rhythmicity induced by spinal and cortical lesions. Electroenceph. Clin. Neurophysiol. **31**, 21-34.

ARMSTRONG, C.M. and MATTESON, D.R. (1985). Two distinct populations of calcium channels in a clonal line of pituitary cells. Science **227**, 65-67.

BADER, C.R. and BERTRAND, D. (1984). Effects of changes in intra- and extracellular sodium on the inward (anomalous) rectification in salamander photoreceptors. J. Physiol. **347**, 611-631.

BADER, C.R., BERTRAND, D. and SCHWARTZ, E.A. (1982). Voltage-activated and calcium-activated current studied in solitary rod inner segments from the salamander retina. J. Physiol. **331**, 253-284.

BEAM, K.G. and KNUDSON, C.M. (1988). Effect of postnatal development on calcium currents and slow charge movement in mammalian skeletal muscle. J. Gen. Physiol. **91**, 799-815.

BEAN, B.P. (1985). Two kinds of calcium channels in canine atrial cells. J. Gen. Physiol. **86**, 1-30.

BELL, G.H. (1973). Solubilities of normal aliphatic acids, alcohols and alkanes in water. Chemistry and Physics of Lipids **10**, 1-10.

BENHAM, C.D., BOLTON, T.B., DENBIGH, J.S. and LANG, R.J. (1987). Inward rectification in freshly isolated single smooth muscle cells of the rabbit jejunum. J. Physiol. **383**, 461-476.

BENOIT, O. and CHATEIGNIER, C. (1973). Patterns of spontaneous unitary discharges in thalamic ventrobasal complex during wakefulness and sleep. Exp. Brain Res. **17**, 348-363.

BLOOMFIELD, S.A., HAMOS, J.E. and SHERMAN, M.S. (1987). Passive cable properties and morphological correlates of neurones in the lateral geniculate nucleus of the cat. J. Physiol., **383**, 653-692.

BOSSU, J.L., FELTZ, A. and THOMANN, J.M. (1985). Depolarization elicits distinct calcium currents in vertebrate sensory neurones. Pflug. Arch. **403**, 360-368.

BREMER, F. (1938). Effets de la deafferentation complete d'une region de l'ecorce cerebrale sur son activite electrique spontanee. C. R. Soc. Biol. Paris **127**, 355-359.

BROWN, H.F., DENYER, J.C. and KIMURA, J. (1989). Manganese-induced increase of hyperpolarization-activated current, I_f, in rabbit sino-atrial node multicellular preparations and isolated cells. J. Physiol. **416**, 45P.

BROWN, H.F. and DIFRANCESCO, D. (1980). Voltage-clamp investigation of membrane currents underlying pacemaker activity in rabbit sinoatrial node. J. Physiol. **308**, 331- 351.

BROWN, H.F, DIFRANCESCO, D., KIMURA, J. and NOBLE, S.J. (1981). Caesium: a useful tool for investigating sino-atrial (SA) node pacemaking. J.Physiol. **317**, 54P.

BROWN, H.F., DIFRANCESCO, D. and NOBLE, S.J. (1979a). How does adrenaline accelerate the heart? Nature **280**, 235-236.

BROWN, H.F., DIFRANCESCO, D. and NOBLE, S.J. (1979b). Cardiac pacemaker oscillation and its modulation by autonomic transmitters. J. Exper. Biol. **81**, 175-204.

BROWN, H.F., KIMURA, J., NOBLE, D., NOBLE, S.J. and TAUPIGNON, A. (1984). The ionic currents underlying pacemaker activity in rabbit sino-atrial node: experimental results and computer simulations. Proc. R. Soc. Lond. **222**, 329-347.

BURLHIS, T.M. and AGHAJANIAN, G.K. (1988). Pacemaker potentials of seroternigic dorsal raphe neurons: contribution of a low-threshold Ca^{2+} conductance. Synapse **1**, 582-588.

BUSER, P. (1987). Thalamocortical mechanisms underlying synchronized EEG activity. In: A Textbook of Clinical Neurophysiology. Edited by A.M. Halliday, S.R. Butler and R. Paul. John Wiley and Sons Ltd. 595-621.

BUZSAKI., G., SMITH, A., BERGER, S., FISHER, L.J. and GAGE, F.H. (1990). Petit mal epilepsy and parkinsonian tremour: hypothesis of a common pacemaker. Neuroscience **36**, 1-14.

CAFFREY, J.M., BROWN, A.M. and SCHNEIDER, M.D. (1987). Mitogens and oncogenes can block the induction of specific voltage-gated ion channels. Science, **236**, 570-573.

CARBONE, E. and LUX, H.D. (1984a). A low voltage-activated, fully inactivating Ca channel in vertebrate sensory neurones. Nature **310**, 501-501.

CARBONE, E. and LUX, H.D. (1984b). A low voltage-activated calcium conductance in embryonic chick sensory neurones. Biophys. J. **46**, 413-418.

CARBONE, E. and LUX, H.D. (1987a). Kinetics and selectivity of a low-voltage-activated calcium currents in chick and rat sensory neurones. J. Physiol. **386**, 547-570.

CARBONE, E. and LUX, H.D. (1987b). Single low-voltage-activated calcium channels in chick and rat sensory neurones. J. Physiol. **386**, 571-601.

CHESNOY-MARCHAIS, D. (1982). A Cl^- conductance activated by hyperpolarization in aplysia neurones. Nature **299**, 357-361.

CHESNOY-MARCHAIS, D. (1983). Characterization of a chloride conductance activated by hyperpolarization in aplysia neurones. J. Physiol. **342**, 277-308.

CONSTANTI, A. and GALVAN, M (1983). Fast inward-rectifying current accounts for anomalous rectification in olfactory cortex neurones. J. Physiol. **335**, 153-178.

COULTER, D.A., HUGUENARD, J.R. and PRINCE, D.A. (1989). Calcium currents in rat thalamocortical relay neurones: kinetic properties of the transient, low-threshold current. J. Physiol. **414**, 587-604.

COULTER, D.A., HUGUENARD, J.R. and PRINCE, D.A. (1989). Specific petit mal anticonvulsants reduce calcium currents in thalamic neurons. Neurosci. Lett. **98**, 74-78.

CREPEL, F. and PENIT-SORIA, J. (1986). Inward rectification and low threshold calcium conductance in rat cerebellar Purkinje cells. An in vitro study. J. Physiol. **372**, 1-23.

CROPPER, E.C., EISENMAN, J.S., AZMITIA, E.C. (1984). An immunocytochemical study of serotonergic innervation of the thalamus of the rat. J. Comp. Neurol. **224**, 38-50.

CRUNELLI, V., HABY, M., JASSIK-GERSCHENFELD, D. and LERESCHE, N. (1987a). Two types of ipsps recorded in projection cells of the rat lateral geniculate nucleus in vitro. J. Physiol., **390**, 33P.

CRUNELLI, V., HABY, M., JASSIK-GERSCHENFELD, D., LERESCHE, N., and PIRCHIO, M. (1988). Cl^-- and K^+-dependent inhibitory postsynaptic potentials evoked by interneurones of the rat lateral geniculate nucleus. J. Physiol. **399**, 153-176.

CRUNELLI, V., KELLY, J.S., LERESCHE, N. and PIRCHIO, M. (1987b). On the excitatory post-synaptic potential evoked by stimulation of the optic tract in the rat lateral geniculate nucleus. J. Physiol. **384**, 603-618.

CRUNELLI, V., KELLY, J.S., LERESCHE, N. and PIRCHIO, M. (1987c). The ventral and dorsal lateral geniculate nucleus of the rat: intracellular recordings in vitro. J. Physiol. **384**, 587-601.

CRUNELLI, V., and LERESCHE, N. (1990). A role for $GABA_B$ receptors in excitation and inhibition of thalamocortical cells. Trends Neurosci. **14**, 16-21.

CRUNELLI, V., LERESCHE, N. and PARNAVELAS, J.G. (1987d). Membrane properties of morphologically identified X and Y cells in the lateral geniculate nucleus of the cat in vitro. J. Physiol. **390**, 243-256.

DEITMER, J.W. (1984). Evidence for two voltage-dependent calcium currents in the membrane of the ciliate stylonychia. J. Physiol. **355**, 137-159.

DEMPSEY, E.W. and MORISON, R.S. (1942). The interaction of spontaneous and induced cortical potentials. Amer. J. Physiol. **135**, 301-308.

DESCHENES, M.A., MADARIAGA-DOMICH, A and STERIADE, M. (1986). Dendrodendritic synapses in the cat reticularis thalami nucleus: a structural basis for thalamic spindle synchronization. Brain Res. **334**, 165-168.

DESCHENES, M., PARADIS, M., ROY, J.P. and STERIADE, M. (1984). Electrophysiology of neurones of lateral thalamic nuclei in cat: Resting properties and burst discharges. J. Neurophysiol. **51**, 1196-1219.

DESIRAJU, T. and PURPURA, D.P. (1970). Organization of specific-nonspecific thalamic internuclear synaptic pathways. Brain Res. **21**, 169-182.

DIFRANCESCO, D. (1981a). A new interpretation of the pacemaker current in calf Purkinje fibres. J. Physiol. **314**, 359-376.

DIFRANCESCO, D. (1981b). A study of the ionic nature of the pace-maker current in calf purkinje fibres. J. Physiol. **314**, 377-393.

DIFRANCESCO, D. (1981c). Voltage dependence of Cs effects on the pacemaker current in Purkinje fibres. J. Physiol. **320**, 31P.

DIFRANCESCO, D. (1985). The cardiac hyperpolarizing-activated current, I_f. Origins and developments. Prog. Biophys. Molec. Biol. **46**, 163-183.

DIFRANCESCO, D. and OJEDA, C. (1980). Properties of the current I_f in the sino-atrial node of the rabbit compared with those of the current iK2 in Purkinje fibres. J. Physiol. **308**, 353-367.

DINGLEDINE, R. (1984). Brain Slices. Plenum Press, N.Y.

DOCHERTY, R.J. and BROWN, D.A. (1986). Interaction of 1,4-dihydropyridines with somatic Ca currents in hippocampal CA1 neurones of the guinea-pig in vitro. Neurosci. Lett. **70**, 110-115.

EDMAN, A., GESTRELIUS, S. and GRAMPP, W. (1987). Current activation by hyperpolarization in the slowly adapting lobster stretch receptor neurone. J. Physiol. **384**, 671-690.

EDWARDS, F.R., HIRST, G.D.S. and SILVERBERG, G.D. (1988). Inward rectification in rat cerebral arterioles; involvment of potassium ions in autoregulation. J.Physiol. **404**, 455-466.

ELGETI, H., ELGETI, R. and FLEISCHHAUER, K. (1976). Postnatal growth of the dorsal lateral geniculate nucleus in the cat. Anat. Embryol. **149**, 1-13.

EYSEL, U.T. (1976). Quantitative studies of intracellular postsynaptic potentials in the lateral geniculate nucleus of the cat with respect to optic tract stimulation. Exp. Brain Res. **25**, 469-486.

FAMIGLIETTI, E.V. and PETERS, A. (1972). The synaptic glomerulus and the intrinsic neuron in the dorsal lateral geniculate nucleus of the cat. J. Comp. Neurol. **144**, 285-334.

FEDULOVA, S.A., KOSTYUK, P.G. and VESELOVSKY, N.S. (1985). Two types of calcium channels in the somatic membrane of new-born rat dorsal root ganglion neurones. J. Physiol. **359**, 431-446.

FENWICK, E.W., MARTY, A. and NEHER, E. (1982). Sodium and calcium channels of cultured sensory and sympathetic neurons of chick. J. Physiol. **331**, 599-635.

FINDLEY, L.J. and CAPILDEO, R. (1984). Movement disorders: Tremour. Oxford University Press, N.Y..

FINDLEY, L.J. and GRESTY, M.A. (1981). Tremour. Br. J. Hosp. Med. **26**, 16-32.

FINKEL, A.S. and REDMAN, S. (1984). Theory and operation of a single micro-electrode voltage clamp. J. Neurosci. Meth. **11**, 101-127.

FOURMENT, A., HIRSCH, J.C. and MARC, M.E. (1985). Oscillations of the spontaneous slow-wave sleep rhythm in lateral geniculate nucleus relay neurones of behaving cats. Neuroscience **14**, 1061-1075.

FOX, A.P, NOWYCKY, M.C and TSIEN, R.W. (1987a). Kinetic and pharmacological properties distinguishing three types of calcium currents in chick sensory neurones. J. Physiol. **394**, 149-172.

FOX, A.P, NOWYCKY, M.C and TSIEN, R.W. (1987b). Single channel recordings of three types of calcium currents in chick sensory neurones. J. Physiol. **394**, 173-200.

FRIEDLANDER, M.J., LIN, C.-S., STANFORD, L.R. and SHERMAN, S.M. (1981). Morphology of functionally identified neurons in the lateral geniculate nucleus of the cat. J. Neurophysiol. **46**, 80-129

FUKUSHIMA, Y. (1982). Blocking kinetics of the anomalous potassium rectifier of tunicate eggs studied by single channel recording. J. Physiol. **331**, 311-331.

GABBOT, P.L.A., SOMOGYI, J., STEWART, M.G. and HAMORI, J. (1985). GABA-immunoreactive neurons in the rat dorsal lateral geniculate nucleus: light microscopic observations. Brain Res. **346**, 171-175.

GABBOT, P.L.A., SOMOGYI, J., STEWART, M.G. and HAMORI, J. (1986). GABA-immunoreactive neurons in the dorsal lateral geniculate nucleus of the rat: characterisation by combined Golgi-impregnation and immunocytochemistry. Exp.Brain Res. **61**, 311-322.

GARCIA, J. and STEFANI, E. (1987). Appropriate conditions to record activation of fast Ca^{2+} channels in frog skeletal muscle (Rana pipiens). Pflug. Arch. **408**, 646-648.

GAREY, L.J., FISKEN, R.A. and POWEL, T.P.S. (1973). Observations on the growth of cells in the lateral geniculate nucleus of the cat. Brain Res. **52**, 359-362.

GAY, L.A. and STANFIELD, P.R. (1977). Cs^+ causes a voltage-dependent block of inward K currents in resting skeletal muscle fibres. Nature **267**, 169-170.

GLOOR, P. (1979). Generalized epilepsy with spike-and-wave discharge: a reinterpretation of its electrographic and clinical manifestations. Epilepsia **20**, 571-588.

GLOOR, P. and FARIELLO, R.G. (1988). Generalized epilepsy: some of its cellular mechanisms differ from those of focal epilepsy. Trends Neurosci. **11**, 63-68.

GONOI, T. and HASEGAWA, S. (1988). Post-natal disappearance of transient calcium channels in mouse skeletal muscle: effects of denervation and culture. J. Physiol. **401**, 617- 637.

GRAY, R. and JOHNSTON, D. (1987). Noradrenaline and β-adrenoceptor agonists increase activity of voltage-dependent calcium channels in hippocampal neurons. Nature **327**, 620-622.

GUILLERY, R.W. (1966). A study of golgi preparations from the dorsal lateral geniculate neurons of the cat. J. Comp. Neurol. **128**, 21-50.

HAAS, H.L., SCHAERER, B. and VOSMANSKY, M. (1979). A simple perfusion chamber for the study of nervous tissue slices in vitro. J. Neurosci. Meth. **1**, 323-325.

HAGIWARA, N., IRISAWA, H. and KAMEYAMA, M. (1988). Contribution of two types of calcium currents to the pacemaker potentials of rabbit sino-atrial node cells. J. Physiol. **395**, 233-253.

HAGIWARA, S. and JAFFE, L.A. (1979). Electrical properties of egg cell membranes. Annu. Rev. Biophys. Bioeng. **8**, 385-416.

HAGIWARA, S., MIYAZAKI, S., MOODY, W. and PATLAK, J. (1978). Blocking effects of barium and hydrogen ions on the potassium current during anomalous rectification in the starfish egg. J. Physiol. **279**, 167-185.

HAGIWARA, S., MIYAZAKI, S. and ROSENTHAL, N.P. (1976). Potassium current and the effect of cesium on this current during anomalous rectification of the egg cell membrane of a starfish. J. Gen. Physiol. **67**, 621-638.

HAGIWARA, S., OZAWA, S. and SAND, O. (1975). Voltage clamp analysis of two inward current mechanisms in the egg cell membrane of a starfish. J. Gen. Physiol. **65**, 617-644.

HAGIWARA, S. and TAKAHASHI, K. (1974). The anamalous rectification and cation selectivity of the membrane of a starfish egg cell. J. Memb. Biol. **18**, 61-80.

HAGIWARA, S. and YOSHII, M. (1979). Effects of internal potassium and sodium on the anomolous rectification of the starfish egg as examined by internal perfusion. J. Physiol. **292**, 251-265.

HALLIWELL, J.V. and ADAMS, P.R. (1982). Voltage-clamp analysis of muscarinic excitation in hippocampal neurons. Brain Res. **250**, 71-92.

HANBERY, J. and JASPER, H. (1953). Independence of diffuse thalamocortical projection system shown by specific nuclear destructions. J. Neurophysiol. **16**, 252-271.

HARDING, B.N. and POWELL, T.P.S. (1977). An electron microscopic study of the centre median and ventrolateral nuclei of the thalamus in the monkey. Proc. R. Soc. Lond.B. Biol. Sci. **279**, 357-412.

HAUSWIRTH, O., NOBLE, D., and TSIEN, R.W. (1968). Adrenaline: mechanism of action on the pacemaker potential in cardiac Purkinje fibres. Science **162**, 916-917.

HENDRICKSON, A.E., OGREN, M.P., VAUGHN, J.E., BARBER, R.P. and WU, J.Y. (1983). Light and electron microscopic immunocytochemical localization of glutamic acid decarboxylase in monkey geniculate complex: evidence for GABAergic neurons and synapses. J. Neurosci. **3**, 1245- 1262.

HERNANDEZ-CRUZ, A. and PAPE, H-C., (1989). Identification of two calcium currents in acutely dissociated neurons from the rat lateral geniculate nucleus. J. Neurophysiol. **61**, 1270-1283.

HESS, P., LANSMAN, J.B. and TSIEN, R.W. (1984). Mechanism of ion permeation through calcium channels. Nature **309**, 453-456.

HESTRIN, S. (1981). The interaction of potassium with the activation of anomalous rectification in frog muscle membrane. J. Physiol. **317**, 497-508.

HICKEY, T.L. (1980). Development of the dorsal lateral geniculate nucleus in normal and visually deprived cats. J. Comp. Neurol. **189**, 467-481.

HILLE, B. (1984). Potassium channels and chloride channels. In Ionic Channels of Excitable Membranes. Sunderland, M.A., U.S.A.: Sinauer Associates Inc.

HILLE, B. and SCHWARZ, W. (1978). K channels in excitable cells as multi-ion pores. Brain Res. Bull. 4, 159-162.

HIRNING, L.D., FOX, A.P., McCLESKEY, E.W., OLIVERA, B.M., THAYER, S.A., MILLER, R.J. and TSIEN, R.W. (1988). Dominant role of N-type Ca^{2+} channels evoked release of norepinephrine from sympathetic neurons. Science **239**, 57-61.

HIRSCH, J.C. and BURNOD, Y. (1987). A synaptically evoked late hyperpolarization in the rat dorsolateral geniculate nucleus in vitro. Neuroscience **23**, 457-469.

HIRSCH, J.C., FOURMENT, A. and MARC, M.E (1983). Sleep-related variations of membrane potential in the lateral geniculate body relay neurons of the cat. Brain Res. **259**, 308-312.

HOBSON, J.A. and STERIADE, M. (1986). Neuronal basis of behavioural state control. In: Fields H.W., et al., eds. Handbook of physiology - The nervous system IV, Chapter 14. Washington, D.C.. Am. Phys. Soc. 701-823.

HOSHI, T. and SMITH, S. (1987). Large depolarization induces long openings of voltage-dependent calcium channels in adrenal chromaffin cells. J. Neurosci. **7**, 571-580.

HOUSER, C.R., VAUGHN, J.E., BARBER, R.P. and ROBERTS, E. (1980). GABA neurons are the major cell type of the nucleus reticularis thalami. Brain Res. **200**, 341-354.

HOBSON, J.A. and STERIADE, M. (1986). Neuronal basis of behavioural state control. In: Fields H.W., et al., eds. Handbook of Physiology - The nervous system IV, Chapter 14. Washington, D.C. Am. Phys. Soc., 701-823.

HU, B., STERIADE, M. and DESCHENES, M. (1989a). The effects of brainstem peribrachial stimulation on reticular thalamic neurons: The blockage of spindle waves. Neuroscience **31**, 1-12.

HU, B., STERIADE, M. and DESCHENES, M. (1989b). The cellular mechanism of the pontogeniculo-occipital waves. Neuroscience **31**, 25-35.

HUBBARD, J.F., LLINAS, R. and QUASTEL, D.M.J. (1969). Measurement of cell electrical properties. In: Electrophysiological Analysis of Synaptic Transmission. Edited by H. Davson, A.D.M. Greenfield, R. Whittam and G.S. Brindley. Edward Arnold Ltd. (London). 94-100.

IDE, L.S. (1982). The fine structure of the perigeniculate nucleus in the cat. J. Comp. Neurol. **210**, 317-334.

INOUE, M., NAKAJIMA, S. and NAKAJIMA, Y. (1988). Somatostatin induces an inward rectification in rat locus coeruleus neurones through a pertussis toxin-sensitive mechanism. J. Physiol. **407**, 177-198.

JACOBSON, S.J. and TROJANOWSKI, J.Q. (1975). Corticothalamic neurons and thalamocortical terminal fields: an investigation in rat, using horseradish peroxidase and autradiography. Brain Res. **85**, 385-401.

JAHNSEN, H and LLINAS, R. (1984a). Electrophysiological properties of guinea-pig thalamic neurones: an in vitro study. J. Physiol. **349**, 205-226.

JAHNSEN, H. and LLINAS, R. (1984b). Ionic basis for electroresponsiveness and oscillatory properties of guinea-pig thalamic neurones in vitro. J. Physiol. **349**, 227-247.

JASPER, H.H. (1954). Functional properties of the thalamic reticular system. In: Brain Mechanisms and Conciousness. Edited by F. Delafreysnaye. Blackwell, Oxford. 374-401.

JASPER, H.H. (1960). Unspecific thalamocortical relations. In: Handbook of Physiology. Neurophysiology. Washington, D.C.: Am. Physiol. Soc., sect. 1, vol. II, Chapt. 53, 1307-1321.

JASPER, H.H. (1981). Problems of relating cellular or modular specificity to cognitive functions: importance of state-dependent reaction. In: The organization of the cerebral cortex. Edited by F.O. Schmitt, F.G. Worden, G. Adelman and S.G. Dennis. M.A.: M.I.T. Press. 375-393.

JASPER, H.H., NAQUET, R. and KING, E.E. (1955). Thalamo-cortical recruiting responses in sensory recieving areas in the cat. Electroenceph. Clin. Neurophysiol. **7**, 99-114.

JEAN, T., FRELIN, C., VIGNE, P., BARBRY, P. and LAZDUNSKI, M. (1985). Biochemical properties of the Na^+/H^+ exchange system in rat brain synaptosomes. J. Biol. Chem. **260**, 9678-9684.

JOFFROY, A.J. and LAMARRE, Y. (1974). Single cell activity in the ventral lateral thalamus of the unanaesthetised monkey. Exp. Neurol. **42**, 1-16.

JONES, E.G. (1975). Some aspects of the organization of the thalamic reticular complex. J. Comp. Neurol. **162**, 285-308.

JONES, E.G. (1985). The thalamus. New York: Plenum press. 227-244.

KALIL, R. (1978). Development of the dorsal lateral geniculate nucleus in the cat. J. Comp. Neurol. **182**, 265-292.

KAMIYA, H. (1989). Amiloride suppresses the induction of long-term potentiation in the mossy fiber pathway but not in the commissural/association pathway of the hippocampal CA3 region. Synapse **3**, 286-287.

KATZ, B. (1949). Les constantes electriques de la membrane du muscle. Arch. Sci. Physiol. **2**, 285-299.

KAY, A.R and WONG, R.K.S. (1986). Variation of calcium channel properties in neurones from different brain regions. Soc. Neurosci. Abstr. **12**, 368.6.

KELLAWAY, P. (1985). Sleep and epilepsy. Epilepsia **26**, S15-S30.

KELLAWAY, P., GOL, A. and PROLER, M. (1966). Electrical activity of the isolated cerebral hemisphere and isolated thalamus. Exp. Neurol. **14**, 281-304.

KELLY, J.S, GODFRAIND, J.M. and MARUYAMA, S. (1979). The presence and nature of inhibition in small slices of dorsal lateral geniculate nucleus of rat and cat incubated in vitro. Brain Res. **168**, 388-392.

KEMP, J.A and SILLITO, A.N. (1982). The nature of the excitatory transmitter mediating X and Y cell inputs to the cat dorsal lateral geniculate nucleus. J. Physiol. **323**, 377-391.

KERKUT, G.A. and WHEAL, H.W. (1981). Electrophysiology of isolated mammalian CNS preparations. Academic Press, London.

KOSTOPOULOS, G., GLOOR, P., PELLEGRINI, A. and GOTMAN, J. (1981). A study of the transition from spindles to spike wave discharge in feline generalized penicillin epilepsy: microphysiological features. Expl. Neurol. **73**, 55-77.

KOSTYUK, P.G. (1989). Diversity of calcium ion channels in cellular membranes. Neuroscience **28**, 253-261.

KOSTYUK, P.G., FEDULOVA, S.A. and VESELOVSKII, N.S. (1986). Changes in the ionic mechanisms of the electrical excitability of rat sensory neuronal somatic membrane during ontogenesis. Distribution of ionic channels carrying inward currents. Neurophysiol. (Kiev) **18**, 813-820.

KREITNER, D. (1981). Existence of two distinct kind of pacemaker cells in isolated pieces of the rabbit sinus node. J. Physiol. **312**, 37P.

LACEY, M.G. and NORTH, R.A. (1988). An inward current activated by hyperpolarization (I_h) in rat substantia nigra zona compacta neurones in vitro. J. Physiol. **406**, 18P.

LEECH, C.A. and STANFIELD, P.R. (1981). Inward rectification in frog skeletal muscle fibres and its dependence on membrane potential and external potassium. J. Physiol. **319**, 295-309.

LERESCHE, N., JASSIK-GERSCHENFELD, D., HABY, M., SOLTESZ, I. and CRUNELLI, V. (1990). Pacemaker-like and other types of spontaneous membrane potential oscillations in thalamocortical cells. Neurosci. Lett. **113**, 72-77.

LERESCHE, N., LIGHTOWLER, S., SOLTESZ, I. JASSIK-GERSCHENFELD, D. and CRUNELLI, V. (1991). Low frequency oscillatory activities intrinsic to thalamocortical cells. J.Physiol. 441, 155-174.

LEVAY, S. and FERSTER, D. (1979). Proportions of interneurons in the cat's lateral geniculate neurons. Brain Res. **164**, 304-308.

LEVENTHAL, A.G. (1979). Evidence that the different classes of relay cells ot the cat's lateral geniculate nucleus terminate in different layers of the striate cortex. Exp. Brain Res. **37**, 349-372.

LLINAS, R.R. (1988). The intrinsic electrophysiological properties of mammalian neurons: insights into central nervous system function. Science **242**, 1654-1664.

LLINAS, R.R and GEIJO-BARRIENOS (1988). In vitro studies of mammalian thalamic and nucleus reticularis thalami neurons. In: Cellular Thalamic Mechanisms. Edited by M. Bentivoglio and R. Spreafico. Amsterdam: Elsevier Science Publishers, 23-37.

LLINAS, R.R., SUGIMORI, M. and CHERKSEY, B. (1989a). Voltage-dependent calcium conductances in mammalian neurons. Ann. N.Y. Acad. Sci. **560**, 103-111.

LLINAS, R., SUGIMORI, M., LIN, J-W., and CHERKSEY, B. (1989b). Blocking and isolation of a calcium channel from neurons in mammals and cephalopods utilizing a toxin fraction (FTX) from funnel-web spider poison. Proc. Natl. Acad. Sci. U.S.A. **86**, 1689-1693.

LLINAS, R.R. and YAROM, Y. (1986). Specific blockade of the low threshold calcium channel by high molecular weight alcohols. Amer. Neurosci. Abst. **12**, 49.3.

MADISON, D.V., MALENKA, R.C. and NICOLL, R.A. (1986). Phorbol esters block a voltage-sensitive chloride current in hippocampal pyramidal cells. Nature **321**, 695-697.

MADISON, D.V. and NICOLL, R.A. (1986). Actions of noradrenaline recorded intracellularly in rat hippocampal CA1 pyramidal neurones, in vitro. J. Physiol. **372**, 221-244.

MARCHETTI, C., CARBONE, E. and LUX, H.D. (1986). Effects of dopamine and noradrenaline on Ca channels of cultured sensory and sympathetic neurons of chick. Pflug. Arch. **406**, 104-111.

MASON, C.A. (1983). Postnatal maturation of neurons in the cat's lateral geniculate nucleus. J. Comp. Neurol. **217**, 458-469.

MAYER, M and WESTBROOK, G.L. (1983). A voltage-clamp analysis of inward (anomalous) rectification in mouse spinal sensory ganglion neurones. J. Physiol. **340**, 19-45.

McCLESKEY, E.W., FOX, A.P, FELDMAN, D.H., CRUZ, L.J., OLIVERA,B.M. and TSIEN, R.W. (1987). ω-Conotoxin: Direct and persistant blockade of specific types of calcium channels in neurons but not muscle. Proc. Natl. Acad. Sci. U.S.A. **84**, 4327-4331

McCOBB, D.P., BEST, P.M. BEAM, K.G. (1989). Development alters the expression of calcium currents in chick limb motoneurons. Neuron **2**, 1633-1643.

McCORMICK, D.A. (1989). Cholinergic and noradrenergic modulation of thalamocortical processing. Trends Neurosci. **12**, 215-221.

McCORMICK, D.A. and PAPE, H-C. (1988). Acetylcholine inhibits identified interneurons in the cat lateral geniculate nucleus. Nature **334**, 246-248.

McCORMICK, D.A. and PRINCE, D.A. (1988). Noradrenergic modulation of firing pattern in guinea-pig and cat thalamic neurons in vitro. J. Neurophysiol. **59**, 978-996.

MESULAM, M-M., MUFSOM, E.G., WAINER, B.H., LEVEY, A.I. (1983). Central cholinergic pathways in the rat: an overview based on an alternative nomenclature. Neuroscience **10**, 1185-1201.

MITRA, R. and MORAD, M. (1986). Two types of calcium channels in guinea-pig ventricular myocytes. Proc. Natl. Acad. Sci. U.S.A. **83**, 5340-5344.

MONTERO, V.M. and SCOTT, G.L. (1981). Synaptic terminals in the dorsal lateral geniculate neurons of the thalamic reticular nucleus: a light and electron microscope autoradiographic study. Neuroscience **6**, 2561-2577.

MONTERO, V.M. and SINGER, W. (1984). Ultrastructure and synaptic relations of neural elements containing glutamic acid decarboxylase (GAD) in the perigeniculate nucleus of the cat. Exp. Brain Res. **56**, 115-125.

MONTERO, V.M. and SINGER, W. (1985). Ultrastructure identification of somata and neural processes immunoreactive to antibodies against glutamic acid decarboxylase (GAD) in the dorsal lateral geniculate nucleus of the cat. Exp. Brain Res. **59**, 151-165.

MOOLENAAR, W.H., BOONSTRA, J., VAN DER SAAG, P.T. and DE LAAT, S.W. (1981). Sodium/proton exchange in mouse neuroblastoma cells. J. Biol. Chem. **256**, 12883-12887

MOREST, D.K. (1971). Dendrodendritic synapses of cells that have axons: the fine structure of the Golgi type II cell in the medial geniculate body of the cat. Z. Anat. Entwicklungsgesch. **133**, 216-246.

MOREST, D.K. (1975). Synaptic relationships of Golgi Type II cells in the medial geniculate body of the cat. J. Comp. Neurol. **162**, 157-194.

MORISON, R.S. and BASSET, D.L. (1945). Electrical activity of the thalamus and basal ganglia in decorticate cats. J. Neurophysiol. **8**, 309-314.

MORISON, R.S. FINCHLEY, K.H. and LONTHROP, G.N. (1943). Spontaneous electrical activity of the thalamus and other forebrain structures. J. Neurophysiol. **6**, 243-254.

MULLE, C., MADARIAGA, A. and DESCHENES, M. (1986). Morphology and electrophysiological properties of reticularis thalamic neurons in cat: in vivo study of a thalamic pacemaker. J. Neurosci. **6**, 2134-2145.

MYSLOBODSKY, M. (1976). Petit Mal Epilepsy. Academic Press, N.Y.

NAKAMURA Y., NAKAJIMA, S. and GRUNDFEST, H. (1965). Analysis of spike electrogenesis and depolarizing K inactivation in electroplaques of Electrophorus electricus L. J. Physiol. **49**, 321-349.

NARAHASHI, T., TSUNOO, A. and YOSHII, M. (1987). Characterization of two types of calcium channels in mouse neuroblastoma cells. J. Physiol. **383**, 231-249.

NOWYCKY, M.C., FOX, A.P. and TSIEN, R.W. (1985). Three types of neuronal calcium channel with different calcium agonist sensitivity. Nature **316**, 440-443.

OHARA, P.T. and LIEBERMAN, A.R. (1985). The thalamic reticular nucleus of the adult rat: experimental anatomical studies. J. Neurocytol. **14**, 365-411.

OHARA, P.T., LIEBERMAN, A.R., HUNT, S.P. and WU, J.Y. (1983). Neural elements containing glutamic acid decarboxylase (GAD) in the dorsal lateral geniculate nucleus of the rat: immunohistochemical studies by light and electron microscopy. Neuroscience **8**, 189-211.

OHARA, P.T., SEFTON, A.J. and LIEBERMAN, A.R. (1980). Mode of termination of afferents from the thalamic reticular nucleus in the dorsal lateral geniculate nucleus of the rat. Brain Res. **197**, 503-506.

OHMORI, H. (1978). Inactivation kinetics and steady-state current noise in the anomalous rectifier of tunicate egg cell membranes. J. Physiol. **281**, 77-99.

OSMANOVIC, S.S. and SHEFNER, S.A. (1987). Anomalous rectification in rat locus coeruleus neurons. Brain Res. **417**, 161-166.

OTTERSEN, O.P. and STORM-MATHISEN, J. (1984). Glutamate- and GABA-containing neurons in the mouse and rat brain, as demonstrated with a new immunocytochemical technique. J. Comp. Neurol. **229**, 374-392.

OVERWEG, J., BINNIE, C.D., MEIJER, J.W.A., MEINARDI, H., NULJTEN, S.T.M. and WAUQUIER, A. (1984). Double-blind placebo-controlled trial of flunarizine as add-on therapy in epilepsy. Epilepsia **25**, 217-222.

PAPE, H-C. and McCORMICK, D.A. (1989). Norepinephrine and serotonin selectively modulate thalamic burst firing by enhancing a hyperpolarization-activated cation current. Nature **340**, 715-718.

PENNY, G.R., FITZPATRICK, D., SCHMECHEL, D. and DIAMOND, I.T. (1983). Glutamic acid decarboxylase immunoreactive neurons of the ventral psterior nucleus of the cat and Galago Senegalis. J. Neurosci. **3**, 1868-1887.

PENNY, G.R, ITOH, R.K. and DIAMOND, I.T. (1982). Cells of different sizes in the ventral nuclei project to different layers of the somatic cortex in the cat. Brain Res. **242**, 55-65.

POGGIO, G.F. and MOUNTCASTLE, V.B. (1963). The functional properties of ventobasal thalamic neurons studied in unanaesthetised monkeys. J. Neurophysiol. **26**, 775-806.

PRINCE, D. and FARELL, D. (1969). "Centrencephalic" spike-wave discharges following parental penicillin injection in the cat. Neurology **19**, 309-310.

PURPURA, D.P. (1970). Operations and processes in thalamic and synaptically related neuronal subsystems. In: The Neurosciences - Second Study Program, edited by F.O. Schmitt. N.Y.: Rockefeller Univ. Press, 458-470.

RALSTON, H.J. (1971). Evidence for presynaptic dendrites and a proposal for their mechanism of action. Nature **230**, 585-587.

RAUSELL, E. and AVENDANO, C. (1985). Thalamocortical neurons projecting to superficial and deep layers in parietal, frontal and prefrontal regions in the cat. Brain Res. **347**, 159-165.

ROY, J.P., CLERQ, M., STERIADE, M. and DESCHENES, M. (1984). Electrophysiology of neurones of lateral thalamic nuclei in the cat: mechanism of long lasting hyperpolarization. J. Neurophysiol. **51**, 1220-1235.

SALT, T.E. (1986). Mediation of thalamic sensory input by both NMDA and non-NMDA receptors. Nature **322**, 263-265.

SANDBERG, M. and LINDSTROM, S. (1983). Amino acids in the dorsal lateral geniculate nucleus of the cat: collection in vivo. J. Neurosci. Meth. **9**, 65-74.

SCHEIBEL, M.E. and SCHEIBEL, A.B. (1966). The organisation of the nucleus reticularis thalami: a Golgi study. Brain Res. **1**, 43-62.

SCHEIBEL, M.E. and SCHEIBEL, A.B. (1972). Specialized organisational patterns within the nucleus reticularis thalami of the cat. Exp. Neurol. **34**, 316-322.

SCHEIBEL, M.E, DAVIES, T.L. and SCHEIBEL, A.B. (1973). On thalamic substrates of cortical synchrony. Neurology **23**, 300-304.

SCOTT, R.H., WOOTTON, J.F. and DOLPHIN, A.C. (1990). Modulation of neuronal T-type calcium channel currents by photoactivation of intracellular guanosine 5'-O(3-thio)triphosphate. Neuroscience **38**, 285-294.

SEABROOK, G.R. and ADAMS, D.J. (1989). Inhibition of neurally-evoked transmitter release by calcium channel antagonists in rat parasympathetic ganglia. Br. J. Pharmacol. **97**, 1125-1136.

SELYANKO, A.A. (1984). Cd^{2+} suppresses a time-dependent Cl^- current in rat sympathetic neurone. J. Physiol. **350**, 49P.

SHERMAN, S.M. and KOCH, C. (1986). The control of retinogeniculate transmission in the mammalian lateral geniculate nucleus. Exp. Brain. Res. **63**, 1-20.

SILLITO, A.M., KEMP, J.A. and BARARDI, N. (1983). The cholinergic influence on the function of the cat dorsal lateral geniculate nucleus (dLGN). Brain Res. **280**, 299-308.

SINGER, W. (1977). Control of thalamic transmission by corticofugal and ascending reticular pathways in the visual system. Physiol. Rev. **57**, 386-420.

SINTON, C.M., KROSSER, B.I., WALTON, K.D. and LLINAS, R.R. (1989). The effectiveness of different isomers of octanol as blockers of harmaline-induced tremour. Pflug. Arch. **414**, 31-36.

SOLTESZ, I., HABY, M., LERESCHE, N. and CRUNELLI, V. (1988). The $GABA_B$ antagonist phaclofen inhibits the late K^+-dependent IPSP in cat and rat thalamic and hippocampal neurones. Brain Res. **448**, 351-354.

SOLTESZ, I., LIGHTOWLER, S., LERESCHE, N. and CRUNELLI, V. (1989a). Optic tract stimulation evokes $GABA_A$ but not $GABA_B$ inhibitory postsynaptic potentials in the rat ventral lateral geniculate nucleus. Brain Res. **479**, 49-55.

SOLTESZ, I., LIGHTOWLER, S., LERESCHE, N. and CRUNELLI, V. (1989b). On the properties and origin of the $GABA_B$ inhibitory postsynaptic potential recorded in morphologically identified projection cells of the cat dorsal lateral geniculate nucleus. Neuroscience **33**, 23-33.

SPAIN, W.P., SCHWINDT, P.C. and CRILL, W.E. (1987). Anomalous rectification in neurones from cat sensorimotor cortex in vitro (Betz cells). J. Neurophysiol. **57**, 1555-1576.

SPREAFICO, R, SCHMECHEL, D.E., ELLIS, L.C. and RUSTIONI, A. (1983). Cortical relay neurons and interneurons in the n. ventralis posterolateralis of cats: a horseradish peroxidase, electron-microscopic, Golgi and immunocytochemical study. Neuroscience **9**, 491-509.

STANDEN, N.B. and STANFIELD, P.R. (1978). A potential- and time-dependent blockade of inward rectification in frog skeletal muscle fibres by barium and strontium ions. J. Physiol. **280**, 169-191.

STANDEN, N.B. and STANFIELD, P.R. (1979). Potassium depletion and sodium block of potassium currents under hyperpolarization in frog sartorius muscle. J. Physiol. **294**, 497-520.

STANDEN, N.B. and STANFIELD, P.R. (1980). Rubidium block and rubidium permeability of the inward rectifier of frog skeletal muscle fibres. J. Physiol. **304**, 415-435.

STANFORD, L.E., FRIEDLANDER, M.J. and SHERMAN, S.M. (1981). Morphology of physiologically identified W-cells in the C laminae of the cats lateral geniculate nucleus. J. Neurosci. **1**, 578-584.

STERIADE, M. (1990). Spindling, incremental thalamocortical processes, and spike and wave epilepsy. In: Generalized Epilepsy. Edited by M. Avoli, P.Gloor, G. Kostopoulos and R. Naquet. Birkhauser, Boston.

STERIADE, M. and DESCHENES, M. (1984). The thalamus as a neuronal oscillator. Brain Res. **8**, 1-63.

STERIADE, M., DOMICH, L. and OAKSEN, G. (1986). Reticularis thalami neurons revisited: activity changes during shifts in states of vigilance. J. Neurosci. **6**, 68-81.

STERIADE, M., DOMICH, L., OAKSON, G. and DESCHENES, M. (1987). The deafferented reticular thalamic nucleus generates spindle rhythmicity. J. Neurophysiol. **57**, 260-273.

STERIADE, M. and HOBSON, J.A. (1976). Neuronal activity during the sleep-waking cycle. Progr. Neurobiol. Oxf. 6: 155-376.

STERIADE, M., PARENT, A. and HADA, J. (1984b). Thalamic projections of nucleus reticularis thalami of cat: a study using retrograde transport of horseradish peroxidase and double fluorescent tracers. J. Comp. Neurol. **229**, 531-547.

STERIADE, M. and LLINAS, R.R. (1988). The functional states of the thalamus and the associated neuronal interplay. Physiol. Rev. **68**, 649-742.

STORM, J.F. (1989). After-hyperpolarization of medium duration in rat hippocampal pyramidal cells. J. Physiol. **409**, 171-190.

SUZUKI, S. and ROGAWSKI, M.A. (1989). T-type calcium channels mediate the transition between tonic and phasic firing in thalamic neurons. Proc. Natl. Aca. Sci. **86**, 7228-7232.

SWANSON, L.N. and HARTMAN, B.K. (1975). The central adrenergic system: an immunofluorescence study of the location of cell bodies and their efferent connections in the rat utilizing dopamine-beta-hydroxylase as a marker. J. Comp. Neurol. **163**, 467-506.

SZENTAGOTHAI, J. (1963). The structure of the synapse in the lateral geniculate body. Acta Anat. **55**, 166-185.

SZENTAGOTHAI, J., HAMORI, J. and TOMBOL, T. (1966). Degeneration and electron microscope analysis of the synaptic glomeruli in the lateral geniculate body. Brain Res. **2**, 283-301.

TAKAHASHI, K., WAKAMORI, M. and AKAIKE, N. (1989). Hippocampal CA1 pyramidal cells of rats have four voltage-dependent calcium conductances. Neurosci. Lett. **104**, 229-234.

TANG, C-H., PRESSER, F. and MORAD, M. (1988). Amiloride selectively blocks the low threshold (T) calcium channel. Science **240**, 213-215.

THOMPSON, S.M. and WONG, R.K.S. (1989). Low threshold, transient calcium current is present in young, but not adult, isolated rat hippocampal pyramidal cells. Am. Neurosci. Abstr. **15**, 264.11.

TOMBOL, T. (1966). Short neurons and their synaptic relations in the specific thalamic nuclei. Brain Res. **3**, 307-326.

TRIGGLE, D.J. (1981). New Perspectives on calcium antagonists. Edited by G.B. Weiss. Am. Phys. Soc., Betheseda, 1-18.

TSENG, G.F. and ROYCE, G.J. (1986). A Golgi and ultrastructural analysis of the centromedian nucleus of the cat. J. Comp. Neurol. **245**, 359-378.

TSIEN, R.W., LIPSCOMBE, D., MADISON, D.V., BLEY, K.R. and FOX, A.P. (1988). Multiple types of neuronal calcium channels and their selective modulation. Trends Neurosci. **11**, 43.

VILLABLANCA, J. (1974). Role of the thalamus in sleep control: sleep-wakefulness studies in chronic diecephalic and athalamic cats. In: Basic Sleep Mechanisms, edited by O. Petre-Quadens and J. Schlag. N.Y.: Academic, 51-58.

WALTON, K. and LLINAS, R. (1986). Calcium-dependent low threshold rebound potentials and oscillatory potentials in neonatal rat spinal motoneurons in vitro. Soc. Neurosci. Abstr. **12**, 386.

WEIDMAN, S. (1951). Effect of current flow on the membrane potential of cardiac muscle. J. Physiol. **115**, 227-236.

WHITE, M.W. and MILLER, C. (1979). A voltage-gated anion channel from the electric organ of Torpedo californica. J. Biol. Chem. **254**, 10161-10166.

WILLIAMS, D. (1953). A study of thalamic and cortical rhythms in petit mal. Brain **76**, 50-69.

YAMAMOTO, C. and McILAIN, H. (1966). Electrical activities in thin slices from the mammalian brain maintained in chemically defined media in vitro. Brain Res. **152**, 591-596.

YANAGIHARA, K. and IRISAWA, H. (1980). Inward current activated during hyperpolarization in the rabbit sinoatrial node cell. Pflugers Arch. **385**, 11-19.

YEN, C.T., CONLEY, M., HENDRY, S.H.C. and JONES E.G. (1985a). The morphology of physiologically identified GABAergic neurons in the somatic sensory part of the thalamic reticular nucleus on the cat. J. Neurosci. **5**, 2254-2268.

YEN, C.T., CONLEY, M. and JONES, E.G. (1985b). Morphological and functional types of neurons in cat ventral posterior thalamic nucleus. J. Neurosci. **5**, 1316-1338.

REFERENCES THAT THIS WORK HAS CONTRIBUTED TOWARDS

CRUNELLI, V., LIGHTOWLER, S. and POLLARD, C.E (1989). A T-type Ca^{2+} current underlies low-threshold Ca^{2+} potentials in cells of the cat and rat lateral geniculate nucleus. J. Physiol. **399**, 153-176.

LIGHTOWLER, S., HYND, J.W., POLLARD, C.E and CRUNELLI, V. (1989). Inward rectification of projection cells in the rat and cat lateral geniculate nucleus. Soc. Neurosci. Abstr. **15**, 516.17.

LIGHTOWLER, S., POLLARD, C.E., CRUNELLI, V. (1990). The slow Na^+/K^+ inward rectifier current of cat thalamocortical cells in vitro. J. Physiol. **426**, 46P.

LIGHTOWLER, S., POLLARD, C.E., CRUNELLI, V. (1990). The effects of amiloride and 1-octanol on I_T, the T-type calcium current of thalamocortical cells. Br. J. Pharmacol. Submitted.

PIRCHIO, M., LIGHTOWLER, S., CRUNELLI, V. (1990). Postnatal development of the T calcium current in cat thalamocortical cells. Neuroscience **38**, 39-45.

SOLTESZ, I., LIGHTOWLER, S., LERESCHE, N., JASSIK-GERSCHENFELD, D., POLLARD, C.E., CRUNELLI, V. (1990). Two inward currents and the transformation of low frequency oscillations of thalamocortical cells. J. Physiol. 441, 175-197.